

Dissertation zur Erlangung des Doktorgrades der
Fakultät für Chemie und Pharmazie der
Ludwig-Maximilians-Universität München

Multi-omics studies of tissue-specific molecular alterations in insulin- deficient pigs and their offspring

Bachuki Shashikadze

aus

Khelvachauri, Georgia

2024

Erklärung

Diese Dissertation wurde im Sinne von § 7 der Promotionsordnung vom 28. November 2011 von Herrn Prof. Dr. Eckhard Wolf betreut und von Herrn Prof. Dr. Klaus Förstemann von der Fakultät für Chemie und Pharmazie vertreten.

Eidesstattliche Versicherung

Diese Dissertation wurde eigenständig und ohne unerlaubte Hilfe erarbeitet.

01.03.2024

München, -----

.....
Bachuki Shashikadze

Dissertation eingereicht am 01.03.2024

1. Gutachter: Prof. Dr. Klaus Förstemann
2. Gutachter: Prof. Dr. Eckhard Wolf

Mündliche Prüfung am 10.04.2024

This work is dedicated to Mom, Dad and Esma

ეს ნაშრომი ეძღვნება დედას, მამას და ესმას

Table of Contents

SUMMARY	1
LIST OF PUBLICATIONS.....	4
1. INTRODUCTION.....	7
1.1. MASS SPECTROMETRY-BASED OMICS	7
1.1.2. <i>Proteomics</i>	8
1.1.3. <i>Metabolomics</i>	9
1.1.1. <i>Muti-omics approaches to study diseases: focus on proteomics and metabolomics</i> .	10
1.2. DIABETES MELLITUS: A GLOBAL HEALTH PROBLEM	10
1.3. THE PIG AS AN ANIMAL MODEL FOR HUMAN DISEASE.....	11
1.3.1. <i>General considerations</i>	11
1.3.2. <i>Pig genome project</i>	12
1.3.3. <i>Genetic engineering of pigs</i>	13
1.4. INSULIN DEFICIENT DIABETES OF YOUTH	13
1.4.1. <i>Insulin biosynthesis</i>	13
1.4.2. <i>Insulin misfolding</i>	14
1.4.3. <i>Munich MIDY pig model</i>	15
1.5. AIM OF THE THESIS.....	16
2. SECTION A: INVESTIGATION OF THE EFFECT OF MATERNAL HYPERGLYCAEMIA ON NEONATAL OFFSPRING LIVER METABOLISM	17
2.1. LITERATURE REVIEW	17
2.1.1. <i>Article 1</i>	17
2.1.2. <i>Previous studies on effects of maternal hyperglycemia on offspring using transgenic animal models</i>	45
2.2. ARTICLE 2	47
3. SECTION B: INVESTIGATION OF THE EFFECT OF HYPERGLYCAEMIA ON LUNG	66
3.1. LITERATURE REVIEW	66
3.1.1. <i>Physiology and anatomy of lung – susceptibility to diabetes</i>	66
3.1.2. <i>Pig lung – relevance to study human disease</i>	67
3.2. ARTICLE 3	68

4. APPENDIX	112
4.1. PRESENTATIONS, AND CONFERENCE CONTRIBUTIONS	112
5. ACKNOWLEDGEMENTS	113
6. REFERENCES.....	114

Summary

Diabetes mellitus is a global health problem whose prevalence is increasing worldwide. Central metabolic pathways such as glycolysis, gluconeogenesis, glycogenesis, and glycogenolysis are responsible for regulating blood glucose levels and therefore are highly relevant in the context of diabetes. Although these pathways are known for a long time, the molecular consequences of diabetes on different organs are not fully understood. The broad majority of metabolic disorders including diabetes are associated with alterations in the complex network of biological pathways. Understanding these alterations is crucial for developing effective prevention and treatment strategies. Since no *in vitro* system can fully mimic human whole-body pathophysiology, and due to ethical reasons only samples with minimal or non-invasive ways are available from humans, pathomolecular characterization of various organs is mostly feasible using animal models. To ensure animal-to-human translational success, clinically relevant animal models with high physiological similarities with humans are essential. Due to the pathophysiological resemblance with humans, the availability of genetic modification toolkits and good ethical acceptance, the pig has become an attractive animal model to study various diseases including diabetes.

Omics technologies, especially multi-omics, further combined with relevant histological examinations can significantly contribute to the understanding of diseases and disorders. The proteome and metabolome are the downstream products of gene transcription and therefore resemble a substantial part of the phenotype of the biological system. In this thesis, shotgun proteomics and targeted metabolomics in tandem with histological investigations were used to study (i) the molecular effects of maternal diabetes on offspring liver and (ii) the molecular effects of diabetes on lung. In the case of proteomics, a data-independent acquisition-based (DIA) approach was employed which provided high analytic depth and data completeness, as well as quantitative accuracy. As part of the DIA method, high-quality DIA libraries of the lung and liver tissues were generated which contain relevant physical-chemical characteristics of thousands of peptides that can be used in future studies and therefore were deposited in a public database (Liver, PXD040305; Lung, PXD038014). When appropriate, a highly sensitive peptide-level quantification strategy was used,

which allowed the detection of quantitative changes, otherwise not detectable with traditional statistical methods. Furthermore, an R package with a wide range of functionalities, allowing convenient proteomics data analysis, was developed. The package is freely available on a GitHub page: <https://github.com/bshashikadze/pepquantify>.

In the first part of this thesis, the effect of maternal diabetes on the offspring's liver is described. Maternal diabetes is known to predispose offspring to a future metabolic disorder, thus exploring associated molecular alterations in the key metabolic tissue – the liver – is essential for the development of effective prevention and treatment strategies. Prior to this investigation, we reviewed systematically the published literature. This revealed a clear lack of knowledge about molecular alterations in offspring liver induced by maternal diabetes. To address this, we performed molecular and histological profiling of liver and serum samples from offspring born to a genetically engineered diabetic pig model for mutant INS gene-induced diabetes of youth (MIDY) (PHG) and from offspring born to WT littermate controls (PNG). In PHG, we observed stimulated gluconeogenesis and increased hepatic lipid content independent of *de novo* lipogenesis (DNL). Latter is in line with the observation that DNL capacity is limited in fetuses and drivers of fat accumulation are provided transplacentally. Similarly, although phosphatidylcholines (PC) were increased, key enzymes involved in its synthesis were downregulated. Conversely, enzymes involved in PC breakdown and translocation were elevated. Shifting the balance of lipid metabolism away from *de novo* synthesis to favor lipid breakdown potentially represents counter-regulatory mechanisms to maternally elevated lipid levels.

In the second part, molecular effects of hyperglycemia on lung tissue are described. The rich vascularization makes the lung prone to deleterious effects of hyperglycemia, similar to other organs affected by diabetic microvascular complications. However, the molecular mechanisms of diabetes-associated pulmonary damage have not yet been investigated comprehensively. This is a highly relevant topic, as increased susceptibility to respiratory infections is frequently observed in the context of diabetes. Using a combined proteomics and lipidomics approach we found alterations of key biomolecules involved in inflammatory and immune system-related pathways. Specifically, polyunsaturated fatty acid lipoyxygenase (ALOX15) involved in eicosanoid metabolism was strongly decreased. As ALOX15 products are well-known to be

involved in inflammation resolution, its downregulation provides molecular insights into the impoverished ability of inflammation resolution as a hallmark of diabetes lung disease.

List of publications

This thesis is based on the following publications and manuscripts, reprinted in Sections A (1, 2) and B (3)

1. **Shashikadze, B.**, F. Flenkenthaler, J.B. Stockl, L. Valla, S. Renner, E. Kemter, E. Wolf, and T. Frohlich, *Developmental Effects of (Pre-)Gestational Diabetes on Offspring: Systematic Screening Using Omics Approaches*. Genes (Basel), 2021. **12**(12).
2. **Shashikadze, B.**, L. Valla, S.D. Lombardo, C. Prehn, M. Haid, F. Riols, J.B. Stockl, R. Elkhateib, S. Renner, B. Rathkolb, J. Menche, M. Hrabe de Angelis, E. Wolf, E. Kemter, and T. Frohlich, Maternal hyperglycemia induces alterations in hepatic amino acid, glucose and lipid metabolism of neonatal offspring: Multi-omics insights from a diabetic pig model. Mol Metab, 2023. 75: p. 101768.
3. **Shashikadze, B.**, F. Flenkenthaler, E. Kemter, S. Franzmeier, J.B. Stöckl, M. Haid, F. Riols, M. Rothe, L. Pichl, S. Renner, A. Blutke, E. Wolf, T. Fröhlich *Multi-omics analysis of diabetic pig lungs reveals molecular derangements underlying pulmonary complications of diabetes mellitus*
Manuscript submitted

Additional publications and manuscripts with contributions by Bachuki Shashikadze during the preparation of this thesis:

4. **Shashikadze, B.**, S. Franzmeier, I. Hofmann, M. Kraetzl, F. Flenkenthaler, A. Blutke, T. Frohlich, E. Wolf, and A. Hinrichs, Structural and proteomic repercussions of growth hormone receptor deficiency on the pituitary gland: Lessons from a translational pig model. J Neuroendocrinol, 2023: p. e13277.
5. Stirm, M., **B. Shashikadze**, A. Blutke, E. Kemter, A. Lange, J.B. Stockl, F. Jaudas, L. Laane, M. Kurome, B. Kessler, V. Zakhartchenko, A. Bahr, N. Klymiuk, H. Nagashima, M.C. Walter, W. Wurst, C. Kupatt, T. Frohlich, and E. Wolf, Systemic deletion of DMD exon 51 rescues clinically severe Duchenne muscular dystrophy in a pig model lacking DMD exon 52. Proc Natl Acad Sci U S A, 2023. 120(29): p. e2301250120.
6. Horánszky, A., **B. Shashikadze**, R. Elkhateib, S.D. Lombardo, F. Lamberto, M. Zana, J. Menche, T. Fröhlich, and A. Dinnyés, Proteomics and disease network associations evaluation of environmentally relevant Bisphenol A concentrations

- in a human 3D neural stem cell model. *Front Cell Dev Biol*, 2023. 11: p. 1236243.
7. Lamberto, F., **B. Shashikadze**, R. Elkhateib, S.D. Lombardo, A. Horánszky, A. Balogh, K. Kistamás, M. Zana, J. Menche, T. Fröhlich, and A. Dinnyés, Low-dose Bisphenol A exposure alters the functionality and cellular environment in a human cardiomyocyte model. *Environmental Pollution*, 2023. 335: p. 122359.
 8. Jaudas F., Bartenschlager F., **Shashikadze B.**, Santamaria G., Schnell A., Gräber S., Bähr A., Cambra-Bort M., Krebs S., Schulz C., Zawada D., Janda2, Ignacio Caballero-Posadas M., Kunzelmann K., Morretti A., Laugwitz K.L., Kupatt C., Saalmüller A., Fröhlich T., Wolf E., Mall M., Mundhenk L., Gerner W., Klymiuk N., Increased pulmonary infiltration and attenuated phagocytosis defines perinatal dysfunction of innate immunity in Cystic Fibrosis
Manuscript submitted
 9. Sen, P., **B. Shashikadze**, T. Sittig, J. Hamers, S. Bierschenk, L. Zandbergen, H. Zhang, N. Hesse, V. Pauly, S. Clauss, T. Fröhlich, and D. Merkus, *Mitochondrial and contractile dysfunction in a swine model of early chronic kidney disease*. *European Heart Journal*, 2023. **44**.
 10. Zandbergen, L., C. Dijk, P. Sen, O. Sorop, R. van Drie, **B. Shashikadze**, T. Fröhlich, M. Verhaar, C. Cheng, D. Duncker, and D. Merkus, *Impaired cardiac BCAA catabolism associated with impaired myocardial efficiency during exercise in a porcine model with multiple risk factors*. *European Heart Journal*, 2023. **44**.
 11. Sarala Raj Murthi, A. Petry, **B. Shashikadze**, M. Schmid, G. Santamaria, K. Klingel, D. Kračun, X. Chen, Y. Qin, J. P. Schmitt, J. B. Stöckl, F. Flenkenthaler, J. M. Gorham, C. Toepfer, D. Potěšil, P. Hruška, Z. Zdráhal, S. Bauer, M. Klop, L. Lehmann, Z. Mayer, L. Papanakli, N. Spielmann, A. Moretti, T. Fröhlich, P. Ewert, S. Holdenrieder, J. Seidman, C. E. Seidman, A. Görlach, C. M. Wolf
Hypoxia-Inducible Factor 1a signaling contributes to disease pathogenesis in sarcomeric hypertrophic cardiomyopathy
Manuscript submitted
 12. Baehr A., P. Hoppmann, T. Bozoglu, M. Stirn, I. Luksch, T. Ziegler, N. Hornaschewitz, S. Shresta, **B. Shashikadze**, J. Stöckl, N. Raad, H. Blum, S. Krebs, T. Fröhlich, C. Baumgartner, M. N. Imialek, M. Walter, C. Weber, S.

Engelhardt, A. Moretti, N. Klymiuk, W. Wurst, K. L. Laugwitz, R. Hajjar, E. Wolf, and C. Kupatt

Gene Therapy for Cardiomyopathy associated with Duchenne Muscular Dystrophy in a Pig Model

Manuscript submitted

13. Sen, P., **B. Shashikadze**, F. Flenkenthaler, E. Van de Kamp, S. Tian, C. Meng, M. Gigl, T. Fröhlich, and D. Merkus, Proteomics- and Metabolomics-Based Analysis of Metabolic Changes in a Swine Model of Pulmonary Hypertension. *International Journal of Molecular Sciences*, 2023. 24(5): p. 4870.
14. Flenkenthaler, F., E. Landstrom, **B. Shashikadze**, M. Backman, A. Blutke, J. Philippou-Massier, S. Renner, M. Hrabe de Angelis, R. Wanke, H. Blum, G.J. Arnold, E. Wolf, and T. Frohlich, Differential Effects of Insulin-Deficient Diabetes Mellitus on Visceral vs. Subcutaneous Adipose Tissue-Multi-omics Insights From the Munich MIDY Pig Model. *Front Med (Lausanne)*, 2021. 8: p. 751277.
15. Stirm, M., L.M. Fonteyne, **B. Shashikadze**, M. Lindner, M. Chirivi, A. Lange, C. Kaufhold, C. Mayer, I. Medugorac, B. Kessler, M. Kurome, V. Zakhartchenko, A. Hinrichs, E. Kemter, S. Krause, R. Wanke, G.J. Arnold, G. Wess, H. iNagashima, M. Hrabe de Angelis, F. Flenkenthaler, L.A. Kobelke, C. Bearzi, R. Rizzi, A. Bahr, S. Reese, K. Matiasek, M.C. Walter, C. Kupatt, S. Ziegler, P. Bartenstein, T. Frohlich, N. Klymiuk, A. Blutke, and E. Wolf, A scalable, clinically severe pig model for Duchenne muscular dystrophy. *Dis Model Mech*, 2021. 14(12).
16. Stirm, M., L.M. Fonteyne, **B. Shashikadze**, J.B. Stockl, M. Kurome, B. Kessler, V. Zakhartchenko, E. Kemter, H. Blum, G.J. Arnold, K. Matiasek, R. Wanke, W. Wurst, H. Nagashima, F. Knieling, M.C. Walter, C. Kupatt, T. Frohlich, N. Klymiuk, A. Blutke, and E. Wolf, Pig models for Duchenne muscular dystrophy - from disease mechanisms to validation of new diagnostic and therapeutic concepts. *Neuromuscul Disord*, 2022. 32(7): p. 543-556.

1. Introduction

1.1. Mass spectrometry-based omics

1.1.1. General aspects

Mass spectrometry (MS) is a sophisticated analytical technique that is used to identify and quantify molecules [1], and provides a rapid and sensitive assessment of biomolecules such as proteins, peptides, metabolites, or even DNA and RNA. Furthermore, the signal measured by MS can additionally provide quantitative information [2]. Before entering the mass spectrometer, analytes are often separated with liquid chromatography (LC). During LC separation, the sample with the liquid mobile phase will pass through the column packed with a stationary phase. The separation of analytes is driven by the chemical or physical interactions of the sample with the mobile and stationary phases [3]. After LC separation, analytes are desolvated into the gas phase, ionized and are then analysed by the mass spectrometer.

MS-based omics can be performed in a targeted or untargeted way. In the case of targeted omics, preselected analytes, e.g., peptides or lipids, are analysed in a hypothesis-driven manner. In turn, the untargeted strategy, which is also referred to as shotgun approach, provides a comprehensive analysis of all detectable analytes. Untargeted proteomics or metabolomics can be performed using data-dependent (DDA) or data-independent acquisition (DIA). In the case of DDA, a tandem mass spectrometer is programmed to select the most intense ions in the first stage of tandem mass spectrometry (MS1, precursor ion selection), followed by fragmentation and analysis of a fixed number of most abundant ions in a second stage of tandem mass spectrometry (MS2, precursor fragmentation). Already fragmented precursors are excluded from fragmentation for a fixed time to avoid redundancy. Due to the complexity of biological samples this process leads to “run to run” variabilities since a given biomolecule may not always be selected for fragmentation in each sample. Conversely, in DIA mode [4], during each cycle, the MS focuses on a wide mass window of precursors and acquires MS/MS data from all precursors detected within that window. DIA avoids precursor-based selection and yields higher coverage at the expense of more complex MS2 spectra. Recent implementations of machine learning and deep learning methods in omics data analysis have greatly advanced analysis of complex DIA datasets [5].

1.1.2. Proteomics

Recent developments in next-generation DNA sequencing technologies (NGS) have revolutionized our understanding of the biological state of health and disease. Although genes are the basic units of heredity, the most fundamental level at which the genotype gives rise to the phenotype is when genes are translated to proteins. The first ground-breaking demonstration of the importance of proteins was the characterization of the “molecular disease” by Linus Pauling in 1949 in which a change in a single protein (hemoglobin) was identified as the cause of a devastating human disease: sickle cell. Transcript levels have been frequently assumed as the main contributors to the protein abundances and thus were used as proxies for the concentrations and activities of the corresponding proteins [6]. However, studies quantifying transcripts and proteins revealed that beyond transcript concentration, multiple other processes determine protein abundance and therefore transcript levels alone are not sufficient to predict protein levels (reviewed in [7]). The proteome is the complete set of proteins present in biofluids, cells and tissues and reflects the functional state of the biological system. Proteomics can address challenges that cannot be approached by the analysis at the DNA/RNA level, specifically, post-translational modifications, compartmentalization and turnover, as well as protein interactions [8].

One of the early attempts to analyse protein sequences was Edman degradation, sequentially removing one residue at a time from the amino terminus of a peptide. Because of its sensitivity and speed, mass spectrometry (MS)-based techniques, in which biomolecule masses are measured after ionization replaced laborious Edman degradation during the 1990s. In the last few decades, further technological improvements such as introduction of high precision, fast scanning mass spectrometers have established MS not only as the definitive tool to study the structure of proteins but also as a central technology for the analysis of protein abundance, modifications, and interactions in biological and clinical investigation. One of the most used approaches is bottom-up proteomics where complex mixtures of proteins are digested into smaller peptide sequences. The resulting peptide mixtures are separated based on their hydrophobicity via nano-flow reversed-phase liquid chromatography (nano-LC). Eluted peptides are then ionized and introduced into a mass spectrometer. In the mass spectrometer, peptide ions generally encounter three fundamental stages:

(i) precursor selection, (ii) fragmentation, and (iii) detection. Post-analysis data processing allows protein inference from peptide-specific precursor and/or fragment ions.

1.1.3. Metabolomics

According to the central dogma of molecular biology, the genetic information is encoded in the DNA and is transcribed into RNAs, which are then translated to functional proteins. Proteins then affect the abundance of their substrates, which are integrated into complex metabolic pathways. Metabolomics is the systematic study of a wide range of small molecules, typically in the context of stimuli or disease states. Genetic and epigenetic regulation affects cellular homeostasis and subsequently metabolic output, thus the metabolome closely reflects environment–gene interactions and is a sensitive indicator of an organism’s physiological state [9]. Metabolomics measurements fall into two distinct categories. Untargeted metabolomics aims to comprehensively assess all measurable analytes in a sample including chemical unknowns. In turn, targeted metabolomics measures preselected annotated metabolites. While an untargeted approach provides an unbiased survey of molecules and can sometimes lead to novel unexpected findings, many of the detected analytes remain unannotated. Conversely, a targeted approach is performed in hypothesis-driven studies and yields an accurate quantification of a wide class of metabolites [10]. Mass spectrometry and nuclear magnetic resonance spectroscopy (NMR) are the two most commonly used approaches in the field of metabolomics. During the past few years, great progress has been made in the metabolomics field. Specifically, improving instrument performance, experimental design and sample preparation, facilitated broader analytical capabilities. Moreover, progress in bioinformatics tools greatly advanced data acquisition and analysis. These allowed sensitive and accurate assessment of metabolites in various samples to reveal biomarkers that are reflective of various pathophysiological states [10].

1.1.1. Multi-omics approaches to study diseases: focus on proteomics and metabolomics

Genome analysis answers what can be performed, transcriptome analysis answers what is currently performing while proteomics can say what was done. Finally, metabolome profile confirms what was and is going on [11]. Even if the information from DNA is transcribed to mRNA properly, the synthesis of proteins can be altered or specific enzymes may be present in an inactive form. Moreover, specific metabolites might not be synthesized [11]. Many diseases are associated with disturbances in the complex network of biological molecules essential to accomplish a particular biological function. Understanding the interplay between the genes, their products (RNAs, proteins, and metabolites) and many environmental factors that influence their functioning is essential to empower more effective investigation and complete understanding of biological systems [12]. The recent advances in so-called systems biology techniques enable the characterization of these integrative pathways. Multi-omics data analysis is complex since a huge amount of data is generated and proper statistical evaluation is critical [13]. However, with a carefully planned study design and sample handling followed by suitable data analysis, multi-omics represents a powerful approach to decipher the molecular basis of various diseases.

1.2. Diabetes mellitus: a global health problem

Diabetes mellitus (DM) along with its associated complications is a global health problem with rapidly expanding prevalence. According to the International Diabetes Federation, 537 million people had DM in 2021. DM is a heterogeneous metabolic disorder characterized by the presence of hyperglycemia due to impaired insulin secretion, defective insulin action, or both. The disease can be classified into the following general categories [14]: I. type 1 diabetes mellitus (T1DM) (autoimmune-mediated pancreatic beta-cell loss, leading to absolute insulin deficiency); II. type 2 diabetes mellitus (T2DM) (combination of insulin resistance and dysfunctional pancreatic β -cells failing to provide adequate compensatory insulin secretion); III. gestational DM (a glucose intolerance which manifests in the second or third trimester of pregnancy); IV. other specific types of DM include a broad range of causes e.g., drug- or chemical-induced diabetes, diseases of the exocrine pancreas, monogenic

diabetes syndromes, permanent neonatal diabetes, etc. Despite several approved treatment options, there is still no cure for any form of diabetes mellitus. Due to the high heterogeneity of diabetes, a renewed classification was proposed to individualize treatment regimens. Ahlqvist et al. identified five clusters of patients with diabetes, which had significantly different patient characteristics and risk of diabetic complications: (1) severe autoimmune diabetes (SAID), (2) severe insulin-deficient diabetes (SIDD), (3) severe insulin-resistant diabetes (SIRD), (4) mild obesity-related diabetes (MOD) and (5) mild age-related diabetes (MARD) [15].

1.3. The pig as an animal model for human disease

1.3.1. General considerations

In biomedical research, the patient situation is frequently not mimicked well enough to reliably predict the efficacy and side effects of a novel drug or device. Therefore, despite increased scientific discoveries and financial investments, many biomarkers proposed from basic research do not enter the market (also known as the “pipeline problem” [16]). Human samples can usually only be collected by non- or minimally invasive procedures. Additionally, there are no *in vitro* systems that can fully mimic human whole-body pathophysiology, thus biomedical research still relies on animal models [17]. Animal models are essential to understand the onset and progression of diseases and to discover and validate therapeutic drugs as well as their side effects. Due to ethical reasons, work with laboratory animals must be carefully controlled, and researchers have a duty to ‘replace, reduce and refine’ their application whenever possible [17]. In other words, the potential benefits of the research project to society must outweigh and justify the costs to the animals. Therefore, to derive high-quality data from research, the use of animal models should ideally be restricted to investigating specific and well-defined characteristics that both resemble and are predictive of the disease in humans [18]. Mice and other small rodents are dominant animal models in biomedical research, and provided insights into the molecular basis of many human diseases and enabled proof-of-principle studies. Their dominance is due to the fact that they are convenient and cheap to maintain, have good ethical acceptance, rapid reproduction and methods for their genetic modification are well established [19]. However, mice considerably differ from humans in size, physiology

and lifespan which reduces their translational value [20]. Additionally, differences exist between rodents and humans in the regulatory networks controlling the metabolic functions, activity of the immune system, and responses to stress [21]. There has been a growing recognition of the limitations of some animal models since in many cases they poorly reflect human physiology [22]. The need to check the translational relevance of hypotheses developed in non-mammalian organisms and rodents, under conditions more similar to human biology, has greatly increased demands for large animal models which are better mimicking human physiology [23]. Non-human primate models are phylogenetically very close to humans but have clear drawbacks due to low ethical acceptance. Additionally, they have long generation intervals and are mostly uniparous [20]. Dogs and cats have also been used, however, unless they present spontaneous cases of disease, they also raise ethical concerns due to their use as companion animals [24]. Pigs are one of the most common domestic animals in the world with a rapid growth rate, short generation intervals, large litter sizes, and standardized breeding techniques [25]. Moreover, pigs share several key similarities with humans in terms of their body size, anatomical features, physiological and pathophysiological responses [26]. These practical factors, combined with the possibility of dietary and surgical interventions, efficient and specific genetic modifications and ethical acceptance, make the pig an excellent model to overcome gaps between proof-of-concept studies and clinical trials [23]. Importantly, major limitations of the pig models have been tackled by the advancement in the genetic toolbox for gene-editing [17, 27] and by the publication of the pig genome [28]. These developments have significantly pushed the importance of the porcine model in biomedical research, and are discussed below.

1.3.2. Pig genome project

As a member of the artiodactyls (cloven-hoofed mammal), pig is evolutionarily distinct from the primates and rodents, which last shared a common ancestor with humans between 79 and 97 million years ago. The release of its genome sequence has provided a critical component for the development and broad acceptance of the pig as a clinically relevant biomedical model [24]. Sequencing of the porcine genome was initiated with the establishment of the Swine Genome Sequencing Consortium in September 2003 [29]. However, the pig genome project greatly benefited from early attempts like European PiGMap project which stretches back to early 1990s and

USDA Pig genome coordinated activities in the US. A high-quality draft genome sequence for the porcine was published in Nature in 2012 [28] and described the sequencing, analysis, and annotation of the draft genome sequence. The provided knowledge further underlined the genome-level similarity between pigs and humans. Specifically, the pig and human genomes have similar size, complexity and chromosomal organization [29].

1.3.3. Genetic engineering of pigs

Transgenic pigs were first described in the 1980s with the creation of pigs expressing various hormones, including human growth hormone [30]. Since then, pigs were genetically modified to replicate the genetic and/or functional basis of various human diseases [27]. Current approaches for genetic modification of pigs include DNA microinjection into the pronuclei of fertilized oocytes (DNA-MI), sperm-mediated gene transfer (SMGT), lentiviral transgenesis (LV-TG) and somatic cell nuclear transfer using genetically modified nuclear donor cells (SCNT) [17, 31]. Although DNA-MI is straightforward, it is quite inefficient in terms of the proportion of transgenic animals produced. The efficiency of SMGT which transfers genes based on the ability of sperm cells to spontaneously bind to and internalize exogenous DNA and transport it into an oocyte during fertilization to produce genetically modified animals is also low [32]. Gene targeting using adeno-associated viral vectors has also been established in pigs. For example, lentiviral gene transfer was adapted to pigs and resulted in high proportions of transgenic offspring [27]. During SCNT, the nucleus of a somatic donor cell is transferred to an enucleated egg whose nuclear DNA has been removed. The reconstructed SCNT oocytes are then artificially activated by the host cell to progressively develop into blastocysts. Resulted embryos can be transferred to a recipient, enabling development to term. SCNT produces embryos or animals that are genetically identical to the donor cells [33].

1.4. Insulin deficient diabetes of youth

1.4.1. Insulin biosynthesis

Despite having a net weight in humans of only about 2 grams, pancreatic islets and their secreted peptide hormones are crucial for normal body metabolism [34]. Insulin is a master hormone that regulates and maintains metabolic homeostasis in the body

whose structure is fairly conserved across species. In pancreatic beta-cells, the insulin biosynthetic pathway starts when the *INS* gene product is translated as preproinsulin [34] which consists of the signal peptide, the insulin B domain, the C domain flanked by dibasic cleavage sites, and the insulin A domain [34]. Newly synthesized preproinsulin undergoes co- and post-translational translocation across the membrane of the endoplasmic reticulum (ER), where it is cleaved by signal peptidase to form proinsulin [35]. Nascent proinsulin must fold properly including the formation of three evolutionary conserved disulphide bonds (B7-A7, B19-A20 and A6-A11) [36] which stabilizes its structure. Correct disulphide pairing appears to be one of the most important events in determining whether proinsulin molecules can achieve their native folded structure [35]. Noncovalently-associated homodimers of proinsulin undergo intracellular transport from the ER to the Golgi complex and into secretory granules, during which it forms hexamers and is proteolytically processed to C-peptide and mature bioactive insulin that is stored in granules. Upon stimulation, insulin granule exocytosis quickly secretes the insulin to the bloodstream to lower blood glucose levels [35].

1.4.2. Insulin misfolding

One-third of all newly synthesized proteins may not achieve proper folding and this has to be addressed by cell machinery via protein refolding or elimination [34]. Loss of intermolecular disulphide bond due to insulin mutations results in the formation of non-native intermolecular disulphide bonds with other mutant and wild-type proinsulin molecules [34]. As a result, high molecular weight complexes are formed and they entrap mutant and WT proinsulin, hindering the exit of insulin from the ER. Entrapment of insulin in ER subsequently reduces circulating insulin levels which in turn upregulates proinsulin biosynthesis. This results in ER stress and leads to beta-cell failure [37]. Misfolded proinsulin molecules can either be refolded to their native structure or degraded through ER-associated degradation (ERAD) and autophagy [38]. Furthermore, even in the absence of any mutation, a defective ER folding environment can provide a “first hit” to beta cells, affecting the folding of wild-type proinsulin and leading to an increase of proinsulin misfolding [35]. Accumulating evidence indicates that the underlying mechanism initiating insulin-deficient diabetes

in *Akita* mice and mutant insulin deficient diabetes of youth (MIDY) patients is an impairment of the ER export of wild-type proinsulin due to blockade by co-expressed mutant proinsulin [34].

1.4.3. Munich MIDY pig model

Pig models for (pre)diabetes can be generated using one of the following strategies: (1) partial or complete surgical removal of the pancreas; (2) chemical treatment (e.g. streptozotocin or alloxan) causing selective beta cell destruction; (3) by dietary intervention (e.g., high-energy, high-fat, high-sugar diet); or (4) by genetic modification [39]. Advantages and disadvantages of these methods are reviewed in [39]. Dietary interventions alone rarely cause substantial hyperglycemia in the pig [39]. A transgenic pig model is superior to surgically and chemically induced diabetes models as it is less invasive, the exocrine pancreas stays intact and phenotypic inter-individual variance is minor [20]. Two different pig models for permanent neonatal diabetes were established - transgenic pigs expressing the mutant insulin C94Y [40] or C93S [41] based on the analogous mutations in humans and rodents. C93S had a lower level of mutant *INS* transgene expression compared to C94Y line and consequently, the phenotype was less severe. A comprehensive biobank of body fluids and tissues was established from long-term diabetic *INS*^{C94Y} transgenic pigs (MIDY) [42]. The review from Renner et al. summarises results from studies showing diabetes-related complications in various tissues of MIDY pigs including myocardium [43], retina [44] and liver [45]. Additionally, a recent study showed significant changes in proliferative response, CD4⁺ T cell proteomes and the metabolic phenotypes in MIDY pigs [45]. Furthermore, Flenkenthaler et al. used transcriptomics and proteomics for molecular profiling of visceral and mesenteric adipose tissue of MIDY and WT pigs and identified depot-specific alteration of key metabolic processes [46].

1.5. Aim of the thesis

The goal of this thesis was two-fold:

- (i) Investigation of the effect of maternal hyperglycaemia on neonatal offspring liver metabolism (**Section A**)

Little is known about early determinants of liver disorders in offspring born to diabetic mothers since associated molecular drivers were not yet explored in a high-throughput manner. To address this, the hepatic proteome, lipidome, metabolome as well as clinical parameters of serum from 3-day-old wild-type (WT) piglets born to hyperglycemic mothers were compared to the profiles of WT controls born to normoglycemic mothers. To complement the molecular findings, a further histomorphological examination of the liver was performed. Additionally, protein-protein interaction network analysis was used to reveal highly interacting proteins that participate in the same molecular mechanisms and to relate these mechanisms with human pathology.

- (ii) Investigation of the effect of hyperglycaemia on lung (**Section B**)

Increased susceptibility to respiratory infections is frequently observed in the context of diabetes. So far, the research focus was mainly on epidemiological associations between diabetes and impaired lung function and at the molecular level diabetes-associated pulmonary damage was not addressed. To systematically study pulmonary changes in response to chronic insulin deficiency and hyperglycemia data-independent acquisition-based proteomics and targeted analysis of relevant lipid molecules were performed on lung tissue samples from the Munich MIDY pig biobank. To localize differentially abundant key molecules in their pathophysiological context, further immunohistochemical and quantitative morphological analyses were carried out.

2. Section A: Investigation of the effect of maternal hyperglycaemia on neonatal offspring liver metabolism

2.1. Literature review

2.1.1. Article 1

This chapter contains a review article published in MDPI Genes (2021) with the title:

Developmental Effects of (Pre-)Gestational Diabetes on Offspring: Systematic Screening Using Omics Approaches





Bachuki Shashikadze, Florian Flenkenthaler, Jan B. Stöckl, Libera Valla, Simone Renner, Elisabeth Kemter, Eckhard Wolf and Thomas Fröhlich

Author contributions:

Conceptualization, B.S.; writing—original draft preparation, B.S.; Review and editing, J.B.S., L.V., F.F., E.K., S.R., T.F. and E.W.; Supervision T.F. and E.W. All authors have read and agreed to the published version of the manuscript.

Review

Developmental Effects of (Pre-)Gestational Diabetes on Offspring: Systematic Screening Using Omics Approaches

Bachuki Shashikadze ¹, Florian Flenkenthaler ¹, Jan B. Stöckl ¹ , Libera Valla ², Simone Renner ^{2,3,4}, Elisabeth Kemter ^{2,3,4} , Eckhard Wolf ^{1,2,3,4,*}  and Thomas Fröhlich ^{1,*} 

¹ Laboratory for Functional Genome Analysis (LAFUGA), Gene Center, LMU Munich, 81377 Munich, Germany; shashikadze@genzentrum.lmu.de (B.S.); flenkenthaler@genzentrum.lmu.de (F.F.); stoekli@genzentrum.lmu.de (J.B.S.)

² Chair for Molecular Animal Breeding and Biotechnology, Gene Center and Department of Veterinary Sciences, LMU Munich, 81377 Munich, Germany; Libera.Valla@gen.vetmed.uni-muenchen.de (L.V.); Simone.Renner@lmu.de (S.R.); Kemter@genzentrum.lmu.de (E.K.)

³ Center for Innovative Medical Models (CiMM), LMU Munich, 85764 Oberschleißheim, Germany

⁴ German Center for Diabetes Research (DZD), 85764 Neuherberg, Germany

* Correspondence: ewolf@genzentrum.lmu.de (E.W.); froehlich@genzentrum.lmu.de (T.F.)

Abstract: Worldwide, gestational diabetes affects 2–25% of pregnancies. Due to related disturbances of the maternal metabolism during the periconceptional period and pregnancy, children bear an increased risk for future diseases. It is well known that an aberrant intrauterine environment caused by elevated maternal glucose levels is related to elevated risks for increased birth weights and metabolic disorders in later life, such as obesity or type 2 diabetes. The complexity of disturbances induced by maternal diabetes, with multiple underlying mechanisms, makes early diagnosis or prevention a challenging task. Omics technologies allowing holistic quantification of several classes of molecules from biological fluids, cells, or tissues are powerful tools to systematically investigate the effects of maternal diabetes on the offspring in an unbiased manner. Differentially abundant molecules or distinct molecular profiles may serve as diagnostic biomarkers, which may also support the development of preventive and therapeutic strategies. In this review, we summarize key findings from state-of-the-art Omics studies addressing the impact of maternal diabetes on offspring health.

Keywords: DOHaD (developmental origins of health and disease); gestational diabetes mellitus (GDM); pregestational diabetes mellitus (PGDM); Omics



Citation: Shashikadze, B.; Flenkenthaler, F.; Stöckl, J.B.; Valla, L.; Renner, S.; Kemter, E.; Wolf, E.; Fröhlich, T. Developmental Effects of (Pre-)Gestational Diabetes on Offspring: Systematic Screening Using Omics Approaches. *Genes* **2021**, *12*, 1991. <https://doi.org/10.3390/genes12121991>

Academic Editor: Martine De Rycke

Received: 29 October 2021

Accepted: 10 December 2021

Published: 15 December 2021

Publisher's Note: MDPI stays neutral with regard to jurisdictional claims in published maps and institutional affiliations.



Copyright: © 2021 by the authors. Licensee MDPI, Basel, Switzerland. This article is an open access article distributed under the terms and conditions of the Creative Commons Attribution (CC BY) license (<https://creativecommons.org/licenses/by/4.0/>).

1. (Pre-)Gestational Diabetes Mellitus and Omics: A Brief Introduction

Pregnancy is a dynamic state associated with major metabolic adaptations [1,2], being crucial for fetal development [3], delivery, and breastfeeding [4]. The primary source of energy for the fetus is maternal glucose [5]. An increased rate of hepatic glucose production [6], combined with insulin resistance (IR), are important mechanisms adopted by the mother to meet the high demand for glucose. The development of IR, which has diabetogenic effects during pregnancy [7], is an evolutionary mechanism to minimize maternal glucose utilization and to ensure an adequate supply for the growing fetus [8]. In addition, during normal pregnancy, as a response to elevated glucose production and decreased insulin sensitivity (equivalent to IR), β cells need to undergo changes to further elevate insulin synthesis and to maintain a normoglycemic state [9]. Furthermore, insulin in concert with placenta-derived hormones [10] reprograms the metabolism of lipids [11], leading to the accumulation of maternal fat in early and mid-pregnancy and promoting fat utilization at a later stage.

The inability to compensate for the increased demand for insulin during pregnancy underlies the pathophysiological mechanisms of gestational diabetes mellitus (GDM) [12]. GDM is one of the most common complications of pregnancy, with a prevalence rang-

ing from 2% to 25% depending on the used diagnostic criteria and the studied population [13–16]. GDM is defined as glucose intolerance, firstly diagnosed during pregnancy [17]. Obesity, a family history of diabetes, and previous GDM pregnancies are among the major risk factors for developing GDM [18]. In the case of GDM, maternal glucose tolerance usually normalizes shortly after pregnancy but leads to a substantially increased risk of developing type 2 diabetes in later life [19]. Apart from GDM, pre-existing, poorly controlled diabetes can also lead to maternal hyperglycemia. Elevated maternal glucose can penetrate through the placenta and reach the fetus, while insulin cannot [20]. The arising hyperglycemia can lead to insulin overproduction (hyperinsulinemia) in the fetus. This phenomenon was first described by Jorgen Pedersen and is known as Pedersen’s hypothesis [21]. Such an aberrant intrauterine environment induced by maternal diabetes is related to an increased risk for complications both for the mother and the offspring (Table 1).

Table 1. Maternal and fetal/offspring risks associated with maternal diabetes [19,22–28].

Maternal	Fetal/Offspring
Pre-eclampsia	Intrauterine death
Cesarean section	Congenital malformations
Labor complications	Macrosomia
Pre-term delivery	Polycythemia and hyperbilirubinemia
Postpartum hemorrhage	Respiratory distress syndrome
Recurrent GDM	Insulin resistance Metabolic syndrome
Type 2 diabetes	Type 2 diabetes
Complications of type 2 diabetes (cardiovascular disease, nephropathy, neuropathy, retinopathy)	Complications of type 2 diabetes (cardiovascular disease, nephropathy, neuropathy, retinopathy)
weight gain/obesity	Weight gain/obesity

The broad majority of diseases and metabolic disorders are associated with imbalances in the complex network of biological molecules necessary to accomplish a particular biological function. High-throughput Omics technologies analyzing complex mixtures of biological molecules, in combination with advanced data mining and rigorous statistical tools, have reshaped biomedical research. In the last few decades, the application of Omics studies on different molecular levels (e.g., genomics, epigenomics, transcriptomics, proteomics, and metabolomics) successfully deciphered the complex nature of various diseases [29]. Omics research in maternal diabetes and associated offspring health is still in an exploratory phase (i.e., screening for novel biomarkers, revealing dysregulated biological pathways). The screening and diagnostic methods for GDM are mainly based on glucose metabolism (e.g., fasting plasma glucose (FPG), oral glucose tolerance test (OGTT), glycated hemoglobin, etc.). However, currently, there is no broad consensus on appropriate screening/diagnostic tests for GDM (discussed in [30]). Additionally, there are no effective strategies to prevent health complications to offspring due to the lack of systematic insight into maternal diabetes-associated molecular derangements.

With the “central dogma of molecular biology” in mind that the genetic information of a biological system is encoded in the DNA and is transcribed to RNAs, which are translated to functional proteins, controlling an organism’s metabolism (Figure 1), this review is focused on recent findings of (epi-)genomics, transcriptomics, proteomics, and metabolomics studies, addressing molecular changes in offspring after exposure to (pre-)gestational diabetes. Furthermore, studies from other growing Omics fields, such as microbiomics and nutriomics, will be discussed. In this review, we mainly focus on studies

reflecting molecular changes observed at birth (i.e., cord blood studies, fetal-side placenta, and tissues from different animal models) and in later life.

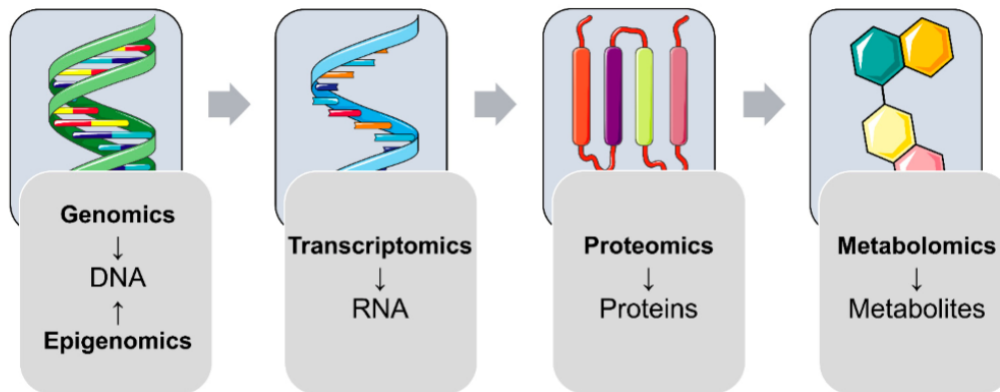


Figure 1. Overview of Omics fields addressing different classes of molecules. Interactions of the different classes of molecules can be addressed using more than one Omics technique in a so-called multi-Omics approach.

2. Animal Models Are Valuable for Studying Effects of Maternal Diabetes on Offspring

Studies on the negative effects of maternal diabetes on the health of human offspring show several limitations due to the number of co-occurring factors, such as the person's lifestyle and medical history. For example, most of the human studies include cases of maternal diabetes accompanied by other metabolic disorders, which makes it difficult to differentiate the consequences of diabetes from those of comorbidities. Therefore, animal models living under tightly controlled laboratory environments with the option of standardized tissue sampling [31] are necessary. So far, a variety of animal models have been generated to study GDM [32]. For instance, rodent models for GDM, generated by the usage of chemicals leading to β cell loss, are widely used. However, rodent models frequently lack clinical relevance due to fundamental physiological differences from humans. Clinically more relevant, large animal models have the potential to bridge the gap between proof-of-concept studies and clinical trials (Figure 2). Non-human primate models have been used to study the developmental programming of diabetes and obesity [33]. Pigs are also attractive animal models due to their similarities with humans in anatomy and metabolism [34]. For diabetes, specific characteristics are particularly relevant (e.g., size and distribution of β cells, similarity in insulin structure) that make the pig a valuable model for human glucose metabolism [35,36]. Importantly, despite structural differences between porcine and the human placenta (epitheliochorial vs. hemochorial), the transfer of glucose, amino acids, and partially fatty acids towards the fetus take place in both species [37].

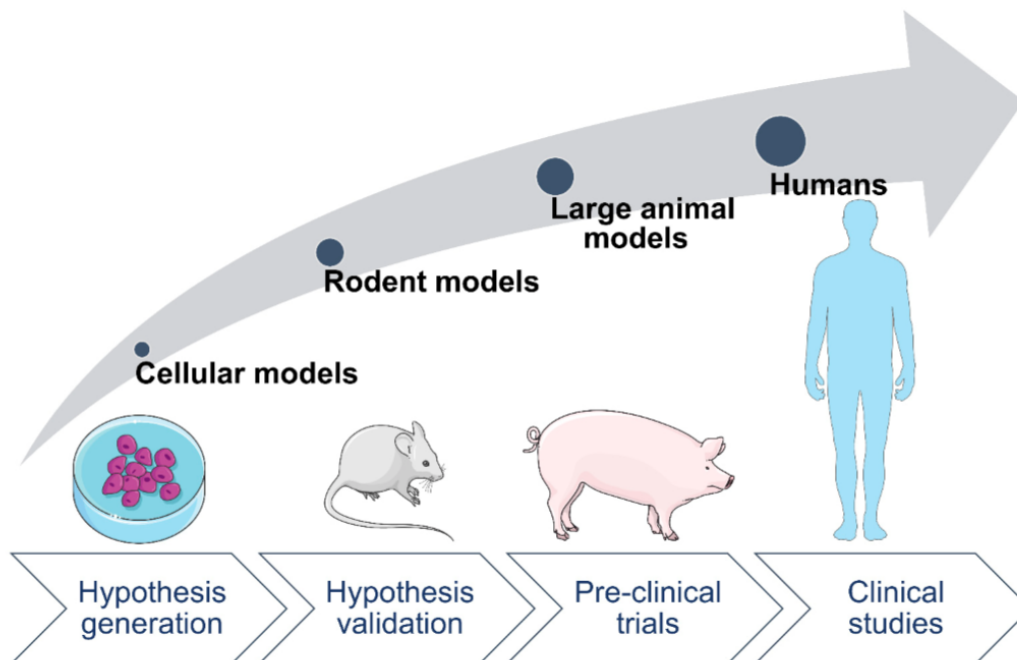


Figure 2. Overview of the different model systems used for translational research. Easy to handle and reproducible cellular models are useful for deciphering molecular disease mechanisms, which can be validated in animal models. Large animal models better mimicking human diseases are valuable to fill the gap between proof-of-concept studies and clinical trials.

3. Common Tissues and Biofluids for Studying Effects of Maternal Diabetes on Offspring

The use of Omics technologies on human samples and samples from clinically relevant animal models, which enable the detection of molecular changes in pathological conditions, represents a promising strategy to study the effects of maternal diabetes on offspring future health at a mechanistic level. Depending on the experimental aim, biological samples can be collected from the mother (plasma, urine, vaginal fluids, milk, placenta, and hair) or the fetus/newborn (amniotic fluid, umbilical cord blood, plasma, urine, meconium, and saliva, etc.) [38]. Due to ethical reasons, human samples can only be collected by non or minimally invasive procedures. Therefore, cord blood is frequently used to explore diabetes-induced molecular changes in human neonates. Longitudinal studies exploring the postpartum effect of maternal diabetes often use the offspring's peripheral blood. These studies will be extensively discussed in this review. Furthermore, molecular changes in the placenta might be reflective of disorders during fetal development. However, as the placenta is only available at birth, it is unclear to what extent alterations observed at delivery resemble those in utero during fetal development [39]. Furthermore, not every study specifies if the maternal or the fetal side of the placenta was analyzed. Therefore, this review focuses on those studies that specifically analyzed the fetal side of the placenta (also reviewed in [40,41]). To verify whether the findings from cord blood or placenta studies reflect molecular derangements of different organs, animal models, which facilitate the molecular profiling of various tissues, are necessary. Therefore, studies from human offspring and animal models will be discussed side-by-side in this review.

4. (Epi)Genetic Factors Affecting Offspring Outcomes after Exposure to Maternal Diabetes

An organism's complete set of DNA is referred to as a genome. Genomics, which is the oldest and most established of the Omics disciplines, uses various methods, including DNA sequencing combined with bioinformatics, to study the structure and function of genomes [42]. Genome-wide association studies (GWAS) are powerful approaches to associate genetic variation with traits such as particular disease states [43].

In extensive population-based studies, elevated maternal glucose levels were associated with "large for gestational age" (LGA) fetuses, which is particularly relevant since high birth weight is among the risk factors of future metabolic disorders, including obesity [44,45] (Figure 3). In the context of GDM, insulin and glucose, together with several adipokines (leptin, adiponectin, and others), are thought to be involved in imbalanced fetal growth [46]. Interestingly, Hughes et al. reported that not only maternal glucose but also the fetal genotype has an effect on birth weight. The authors generated a fetal genetic score using birth weight-associated single nucleotide polymorphisms (SNPs) and investigated their associations with the offspring birth weights at varying levels of maternal fasting plasma glucose (FPG). For FPG levels, data from "The Exeter Family Study of Childhood Health" (EFSOCH) [47] and "The Hyperglycemia and Adverse Pregnancy Outcome" (HAPO) [48] study were used. Interestingly, no association between the fetal genetic score and cord blood insulin or C-peptide was found. The fetal genetic score influenced birth weight independently of maternal FPG and impacted growth at all levels of maternal glycemia. The authors concluded that fetal genetics has a major impact on fetal growth and mainly acts through mechanisms independent of FPG levels [49].

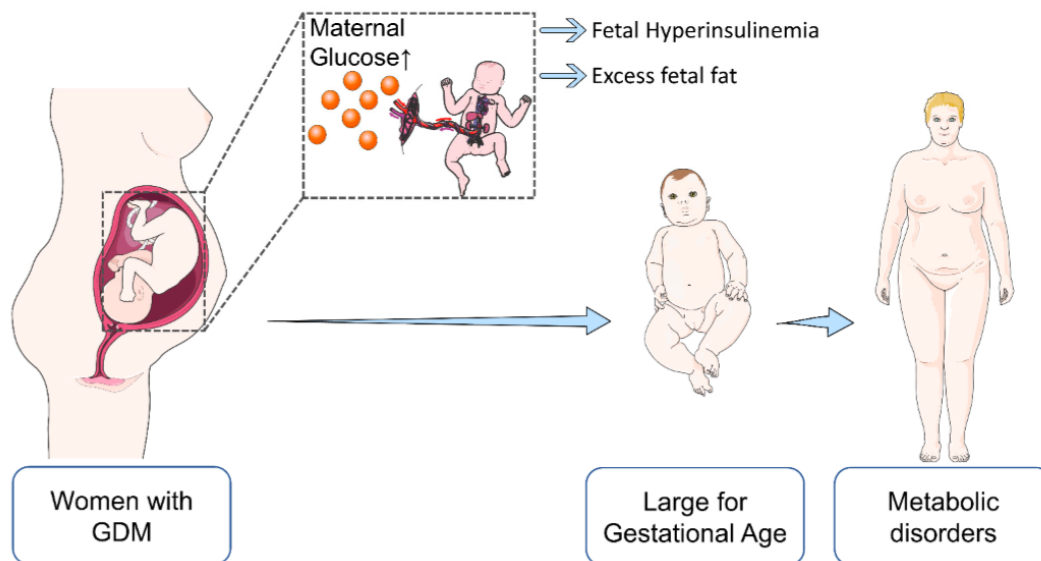


Figure 3. Maternal diabetes predisposes offspring to future metabolic disorders. In response to elevated maternal glucose supply, the fetus increases insulin secretion, resulting in hyperinsulinemia, increased body fat, and subsequently higher birth weight (LGA). The latter is a risk factor for future metabolic syndrome, type 2 diabetes and obesity.

Apart from mutations or genetic variations, covalent modifications of DNA and histones are major regulators of gene transcription and are therefore determinants of cell fate [50]. These modifications, without accompanying changes of the nucleotide sequence, are collectively referred to as an epigenome and are the focus of the epigenomics field. The most extensively studied epigenetic modification is DNA methylation, which is known to be responsive to environmental stimuli [51]. DNA methylation is not limited to but is generally associated with repression of gene expression (gene silencing) [52,53]. Genome-wide DNA methylation variations induced by GDM are supposed to have an important role in metabolic disease programming in offspring [54].

Epigenomic changes in offspring induced by maternal diabetes have been the focus of multiple research projects (Table 2) and are discussed in various review articles [22,55–59]. Therefore, only major findings from selected studies will be discussed here. Although a variety of these studies were performed with small sample sizes and limited statistical power, several of the obtained results suggest that elevated maternal glucose during pregnancy is associated with DNA methylation at the cytosine–guanine (CpG) dinucleotide sites in genes related to metabolic functions within the offspring's genome. These epigenetic alterations are further supposed to result in a predisposition for metabolic, neurodevelopmental, and immune-related disorders.

For example, a significant influence of elevated maternal glucose on the epigenetic pattern of the offspring's leptin (*LEP*) gene was demonstrated. While Lesseur et al. found a 2.5 % increased methylation level of *LEP* in the fetal placenta portion in GDM subjects [60], other studies revealed lower methylation levels of *LEP* in the fetal-side placenta [61] and in the cord blood [62], which was associated with increased cord blood leptin levels. In a study by Côté et al., more differentially methylated genes were found in the fetal-side placenta from hyperglycemic pregnancies. Interestingly, altered methylation of the peroxisome proliferator-activated receptor- γ co-activator 1 α (*PPARGC1A*) gene mediated the association between maternal hyperglycemia and the cord blood leptin levels [63]. A key function of leptin is to regulate energy balance [64,65], and in the "Project Viva" prospective cohort study, leptin levels in the cord blood were associated with elevated adiposity rates at the age of 3 years [66]. Therefore, altered DNA methylation at the *LEP* locus might contribute to the increased risk of obesity in offspring born to hyperglycemic mothers.

Epigenetic variation in the context of maternal diabetes was also detected at other adipokine loci. For instance, Bouchard et al. found that elevated maternal glucose levels during the second trimester of pregnancy were correlated with lower methylation levels of the adiponectin (*ADIPOQ*) gene promoter in the fetal placenta portion. The authors hypothesized that this could be one of the mechanisms involved in the fetal programming of metabolic disorders [67]. Houde et al. found reduced methylation of both *LEP* and *ADIPOQ* in the fetal-side placenta with increased maternal blood glucose concentrations. The authors concluded that maternal hyperglycemia has similar effects on both genes [68]. Taken together, it is conceivable that maternal diabetes influences epigenetic marks of adipokine genes, which predisposes offspring to future metabolic disorders.

In line with the role of the placenta in fetal–maternal communication and nutrient transfer, several studies investigated epigenetic changes of genes encoding transporter proteins. Houde et al. found in GDM pregnancies a reduced methylation level of the lipoprotein lipase (*LPL*) gene in the fetal part of the placenta. *LPL* plays a role in the transfer of fatty acids to the fetus. Furthermore, epivariation of *LPL* was associated with cord blood lipid levels. The authors concluded that the methylation level at a specific *LPL* CpG locus might influence placental lipid flux and lipid metabolism in the offspring [69]. Another study showed that epivariation near the *LPL* locus in the fetal-side placenta correlates with anthropometric characteristics (i.e., birth weight, mid-childhood weight, fat mass) of children at the age of 5 years [70].

In addition to altered methylation of the genes coding for lipid transporters, reduced methylation of the serotonin transporter (*SLC6A4*) gene was found in the fetal side of the

placenta from GDM pregnancies [71]. Serotonin is a multifunctional signaling molecule associated with mental health conditions, including autism spectrum disorder [72]. Interestingly, a recent meta-analysis suggests a possible association of maternal GDM with an autism spectrum disorder in offspring [73].

Multiple studies investigated epigenetic changes in cord blood in the context of maternal diabetes. For instance, Howe et al. [13] analyzed the association between maternal GDM and cord blood DNA methylation in the pregnancy and childhood epigenetics (PACE) consortium [74] and identified two hypomethylated regions; one in the gene body of *CYP2E1* and another one in the *OR2L13* promoter. These genes are associated with type 1/2 diabetes and with an autism spectrum disorder, respectively [13]. As a potential mechanism for maternal diabetes-induced autism spectrum disorder, Wang et al. found that maternal hyperglycemia suppressed superoxide dismutase 2 (*Sod2*) expression in the amygdala of rat offspring, resulting in autism-like behavior. The authors further found that the *Sod2* suppression may result from oxidative stress-mediated histone methylation and the subsequent dissociation of the transcription factor early growth response 1 (EGR1) from the *Sod2* promoter in neurons [75].

A genome-wide comparative methylome analysis of cord blood samples from offspring of GDM and normal pregnancies detected differential methylation patterns of genes mainly involved in pathways related to type 1 diabetes mellitus, immune system/major histocompatibility complex (MHC), and neuron development [76].

Furthermore, epigenetic dysregulation of the mesoderm specific transcript (*MEST*) gene was suggested as a possible risk factor for obesity in offspring. El Hajj et al. observed reduced DNA methylation levels of *MEST* in the cord blood of GDM subjects. In addition, the authors detected significantly lower DNA methylation of *MEST* in the blood of morbidly obese adults [77].

Various studies focused on epigenomic programming effects being present years after birth in offspring born to diabetic mothers. For instance, Shiau et al. investigated the association between prenatal GDM exposure and offspring DNA methylation at ages 3–10 years postpartum and found signs of accelerated epigenetic aging associated with cardiometabolic risk factors [78]. The association between the exposure to maternal diabetes in utero and the risk of cardiometabolic disorders in children (aged 8–12 years) was confirmed by another study performing genome-wide methylation analyses of peripheral blood mononuclear cells. Several genes, known to be associated with cardiometabolic traits, were found to be differentially methylated [79]. Yang et al. [80] performed DNA methylation analyses of blood samples from the Exploring Perinatal Outcomes among Children (EPOCH) cohort [81] (average age of investigated subjects: 10.5 years) and found in offspring exposed to GDM several differentially methylated regions, including loci linked to adiposity. In particular, methylation of the *SH3PXD2A* gene was significantly associated with multiple adiposity-related outcomes, including body mass index (BMI), waist circumference, as well as blood leptin levels [80]. Hjort et al. determined DNA methylation profiles in the peripheral blood of GDM-exposed and unexposed children aged between 9–16 years and validated potentially GDM-associated, differentially methylated CpGs in a larger replication cohort. Ingenuity pathway analysis (IPA) analysis showed enrichment of various functional networks, with lipid metabolism ranking highest. The authors further discussed the association of the identified differentially methylated genes with type 2 diabetes, obesity, diabetic nephropathy, or coronary heart disease, as found in previous reports [82].

Table 2. Summary of selected human studies linking maternal diabetes with the (epi-)genome profiles of offspring.

Maternal Characteristics	Bio-Specimen	Major Findings in Offspring	Reference
GDM	Fetal-side placenta	Reduced methylation level of <i>LEP</i> , contributing to cord blood leptin level regulation	[61]
GDM	Fetal-side placenta	Increased <i>LEP</i> methylation	[60]
GDM	Fetal-side placenta	Altered methylation of <i>PPARGC1A</i> mediating the association between maternal hyperglycemia and cord blood leptin levels	[63]
GDM	Fetal-side placenta	DNA methylation profile of <i>ADIPOQ</i> was associated with maternal glucose status	[67]
GDM	Fetal-side placenta	Reduced <i>LPL</i> methylation	[69]
GDM	Fetal-side placenta	Epivariation near the <i>LPL</i> locus correlated with anthropometric parameters (birth weight, mid-childhood weight, fat mass) of children at age 5 years	[70]
GDM	Fetal-side placenta	Reduced <i>SLC6A4</i> DNA methylation	[71]
GDM	Cord blood and chorionic villi	Decreased <i>MEST</i> methylation	[77]
GDM	Cord blood	Altered methylation of the <i>OR2L13</i> promoter (a gene associated with autism spectrum disorder) and of the gene body of <i>CYP2E1</i> (which is upregulated in type 1 and type 2 diabetes)	[13]
GDM	Cord blood	Differentially methylated genes associated with type 1 diabetes mellitus, immune MHC, and neuron development	[76]
GDM	Cord blood	Decreased <i>LEP</i> methylation; association with increased cord blood leptin levels	[62]
GDM	Peripheral blood	Differentially methylated genes associated with type 2 diabetes, obesity, diabetic nephropathy or coronary heart disease	[82]
GDM	Peripheral blood mononuclear cells	Differential methylation of several genes known to be associated with cardiometabolic traits;	[79]
GDM	Peripheral blood	Accelerated epigenetic aging associated with cardiometabolic risk factors	[78]
GDM	Peripheral blood	Methylation of <i>SH3PXD2A</i> was associated with multiple adiposity-related outcomes, including BMI, waist circumference, and circulating leptin levels	[80]

5. Transcriptomic Changes in Offspring after Exposure to Maternal Diabetes

Ribonucleic acid (RNA) transcripts can have various biological functions, such as carrying genetic information from the genome as well as regulating gene expression, both essential for an organism's survival [83]. The entirety of all coding and non-coding RNA transcripts of a cell or tissue at a given timepoint is referred to as a transcriptome [84]. Transcriptomics technologies can be used to study an organism's transcriptome qualitatively (e.g., checking the presence of a transcript and spotting new splice variants) and quantitatively (determination of levels of given RNA species) [50]. Unlike DNA, which is generally static, RNA levels are sensitive to epigenetic regulation as well as to environmental stimuli (e.g., diseases) [85]. Two widely used techniques in the field of transcriptomics are DNA microarrays and the more powerful RNA sequencing (RNA-seq). While the

former quantifies a set of predetermined sequences by hybridization with probes spotted on a solid support, RNA-seq mostly uses next-generation sequencing (NGS) and is able to capture whole transcriptomes [86] in a highly effective and sensitive way. Since gene expression is mediated by messenger RNAs (mRNAs), high-throughput transcriptome studies mostly focus on this type of transcript.

The impact of maternal diabetes on offspring gene expression was the focus of several studies (Table 3). To study the effects of chronic hyperglycemia on the fetal vascular cell transcriptome, Ambra et al. used Affymetrix microarrays to analyze human umbilical vein endothelial cells (HUVEC) obtained from GDM women at delivery. Several genes coding for growth factors linked to insulin sensing and to the extracellular matrix were upregulated in GDM-HUVEC cells [87]. Furthermore, Koskinen et al. used microarrays to determine gene expression profiles in umbilical cord tissues from neonates born to type 1 diabetic mothers, compared to neonates born to a healthy control group. The authors found that maternal diabetes had a major effect on the expression of genes involved in vascular development, vessel wall integrity, and vascular function. Additionally, the authors hypothesized that the observed alterations in cords might similarly occur in the developmental regulation of various tissues in the offspring of diabetic mothers [88].

Other studies used animal models to reveal the effects of maternal diabetes on transcriptome profiles in the offspring's pancreas and liver, two major organs controlling blood sugar levels. Casanovas et al. utilized an infusion model for localized fetal hyperglycemia in rats. Using a vascular catheter, glucose delivery was targeted to fetuses residing in the left uterine horn, allowing the use of fetuses in the right uterine horn as genetically similar controls with normal glucose levels. RNA-seq of pancreatic islets from gestational day 22 (GD22) fetuses detected 87 differentially expressed genes (DEGs) in hyperglycemia-exposed offspring, which were associated with diabetes mellitus as well as inflammation and cell-death pathways [89]. In a further study, Inoguchi et al. investigated the liver gene expression profiles of offspring of poorly controlled diabetic female mice generated by streptozotocin (STZ) administration. Pathway enrichment analysis showed "FOXO signaling pathway" and "PPAR signaling pathway" to be enriched in the set of DEGs of male offspring, while genes related to "AMPK signaling pathway" and "Fatty acid metabolism pathway" as well as "PPAR signaling pathway" were overrepresented in the set of DEGs from the female offspring. A key finding of this study was an increased activation of the forkhead box protein O1 (*Foxo1*) gene in the liver of the male offspring, associated with increased FOXO1 protein levels and a decreased phosphorylation at Ser256, inhibiting its activity. Moreover, in male but not female offspring, the transcript levels of two gluconeogenic genes, glucose 6-phosphatase catalytic subunit (*G6pc*) and phosphoenolpyruvate carboxykinase 1 (*Pck1*), were upregulated. The authors suggested that dysregulation of FOXO1 target genes in the liver may contribute to increased gluconeogenesis in male offspring. However, these changes were not pronounced in female offspring [90]. Interestingly, decreased phosphorylation levels of FOXO1 but an increased total of FOXO1 protein levels with increased abundance of PCK1 and other gluconeogenic enzymes were also detected in the livers of female transgenic pigs expressing mutant insulin C94Y, a model of insulin-deficient diabetes mellitus. Using transcriptomics, proteomics, and metabolomics analysis, the authors were able to support the hypothesis that increased gluconeogenesis in insulin deficiency is associated with elevated levels of retinol dehydrogenase 16 (RDH16) and its metabolic product all-trans retinoic acid that stimulates the expression of *PCK1* [91].

Several studies indicated that, apart from the pancreas and liver, other human organs, such as the brain, are affected by maternal diabetes. For example, an increased risk of future weight gain or obesity in children exposed to maternal diabetes was associated with hypothalamic transcriptome alterations [92]. Moreover, the brain is particularly relevant since maternal diabetes is supposed to predispose offspring to neurodevelopmental and cognitive disorders. The association between maternal diabetes and cognitive impairments in infants is underpinned by the systematic review from Robles et al. [93]. Addressing the effects of GDM on the brain transcriptome, Aviel-Shekler et al. investigated a mouse model

of diabetes based on STZ administration to pregnant mice. RNA-seq analysis of brains from male offspring detected a dysregulation of only nine genes in the frontal cortex, which were related to forebrain development. While no significant change of gene expression was observed in striatum, weighted correlation network analysis (WGCNA) revealed dysregulation of neurodevelopment- and immune-related genes [94]. Furthermore, Money et al. investigated in mice the impact of diet-induced maternal diabetes alone or in combination with maternal immune activation (MIA) on the developing brain of offspring. Interestingly, each condition alone resulted in altered expression profiles of genes related to inflammatory and neurodevelopmental processes, which was even worsened in the combination of GDM and MIA. Interestingly, GDM increased the expression of vascular endothelial growth factor A (*Vegfa*) mRNA, which is known to be associated with hypoxic conditions. The authors suggested that the altered hypoxia-related signature might be a consequence of an increased oxygen requirement due to an elevated metabolic demand associated with maternal hyperglycemia [95]. The main regulator of responses to a hypoxic environment is hypoxia-inducible factor 1 (HIF1) [96]. In line with this, Cerychova et al. investigated in a mouse model combinatorial effects of maternal diabetes and haploinsufficiency of *Hif1a* on the heart's left ventricles (LV) of offspring. The authors found that the combination of maternal diabetes and *Hif1a* haploinsufficiency results in significant metabolic, structural, and functional changes in the LV myocardium. Additionally, RNA-seq analysis revealed alterations of transcripts associated with metabolic processes, including two genes that are known to be HIF1A targets: *Cd36* and lactate dehydrogenase A (*Ldha*). The authors concluded that HIF1A deficiency and maternal diabetes exposure increase the predisposition to cardiac dysfunction in offspring [97]. These findings obtained in a mouse model may be of translational importance because a predisposition for cardiovascular disorders (CVD) was demonstrated in a recent population-based human cohort study with 40 years of follow-up. The authors demonstrated that children born to a mother with diabetes have increased rates of early-onset CVD [98]. In also addressing the impact of maternal diabetes on the heart transcriptome in offspring, Preston et al. used microarray gene expression profiling of heart samples from newborn offspring of diabetic rats, rats exposed to a high-fat diet, or the combination of both. Diabetes in female rats was induced via the administration of STZ during pregnancy. While the combination of diabetes and a high-fat diet resulted in more pronounced changes, diabetes alone induced only a few changes. Among the differentially abundant transcripts were α hemoglobin stabilizing protein (*Ahsp*) and Kell metallo-endopeptidase (*Kel*), both encoding proteins highly expressed in red blood cells. The authors assumed that the higher levels of *Ahsp* and *Kel* mRNA were due to a higher number of residual red cells in the myocardial vasculature, and they put this into the context of neonatal polycythemia, which is a common complication of maternal diabetes [99].

Table 3. Summary of selected studies linking maternal diabetes with the transcriptome profiles of offspring.

Species	Maternal Characteristics	Bio-Specimen	Major Findings in Offspring	Reference
Human	GDM	HUVEC	Increased mRNA levels of genes coding for growth factors linked to insulin sensing and to the extracellular matrix	[87]
Human	Type 1 diabetes	Umbilical cord	Altered expression of genes involved in vascular development, vessel wall integrity, and vascular function	[88]
Rat	STZ-induced diabetes	Heart	Altered expression of <i>Ahsp</i> and <i>Kel</i> ; possible relation to polycythemia	[99]
Mouse	STZ-induced diabetes	Heart	Altered expression of <i>Cd36</i> and <i>Ldha</i> induced by maternal diabetes plus haploinsufficiency of <i>Hif1a</i>	[97]
Mouse	STZ-induced diabetes	Brain	Dysregulation of genes in frontal cortex related to forebrain development; dysregulation of neurodevelopment and immune-related genes in the striatum	[94]
Mouse	Diet-induced diabetes	Brain	Altered expression of genes related to inflammatory and neurodevelopmental processes	[95]
Rat	Infusion model of localized hyperglycemia	Islets	Dysregulation of genes associated to diabetes mellitus, inflammation and cell-death pathways	[89]
Mouse	STZ-induced diabetes	Liver	Differential expression of genes related to “FOXO signaling pathway” and “PPAR signaling pathway” in male offspring, and of genes related to “AMPK signaling pathway”, “fatty acid metabolism pathway”, and “PPAR signaling pathway” in female offspring	[90]

6. Proteomic Changes in Offspring after Exposure to Maternal Diabetes

The proteome is the complete set of proteins expressed by a cell, tissue, or organism at a given state. Proteins are the primary functional actors of the cell, performing diverse functions, such as catalyzing chemical reactions, facilitating cellular transport, mediating signaling and many other tasks necessary for living organisms. The systematic large-scale identification and quantification of proteins and the analysis of their post-translational modification are called proteomics. Even though NGS-based transcriptomics is a very powerful technique with outstanding analytical depth, comparisons between transcriptomic and proteomic data indicate that only about 40% of variations within proteomes can be explained by altered transcript levels [100]. This clearly demonstrates that transcriptome data are not sufficient to predict protein levels [101]. The need to overcome this limitation led to the rapid development of sophisticated proteomics techniques, of which mass spectrometry has emerged as the most effective and sensitive technology to quantify proteins in complex biological mixtures. Discovery proteomics (also known as shotgun proteomics) is routinely used to effectively characterize the proteome of interest, whereas targeted proteomics focuses on a predefined set of proteins, allowing a more accurate quantification with a high dynamic range.

Although data at the proteome level are essential to understanding disease-related biochemical networks, so far, mainly four high-throughput studies have investigated the impact of maternal diabetes on offspring proteomes (Table 4). Kopylov et al. compared cord blood samples from patients with different types of diabetes mellitus (GDM, type 1 diabetes, type 2 diabetes) who delivered either healthy newborns or newborns with

fetopathy complications. The most altered proteins in the cord blood across the groups were apolipoprotein M (APOM), ceruloplasmin (CP), plasminogen (PLG), angiotensinogen (AGT), kininogen-1 (KNG1), apolipoprotein A-I (APOA1), α -1-acid glycoprotein 2 (ORM2), serotransferrin (TF), histidine-rich glycoprotein (HRG), apolipoprotein D (APOD), and lumican (LUM). Bioinformatics analysis revealed processes such as inflammation, extracellular matrix remodeling, and lipid metabolism, etc., possibly altered due to maternal diabetes [102]. Altered lipid metabolism and possible relation to GDM-induced macrosomia was also shown in the study by Miao et al., who analyzed the cord blood of GDM patients whose offspring showed obesity at ages 6–7 years. In total, 318 proteins were identified by liquid chromatography with tandem mass spectrometry (LC-MS/MS), of which 36 were differentially abundant. The three randomly chosen proteins, rho guanine nucleotide exchange factor 11 (ARHGEF11), phospholipid transfer protein (PLTP), and lecithin-cholesterol acyltransferase (LCAT), were further validated by western blot (WB) and were consistent with LC-MS/MS results. The authors suggested a close relation of these proteins to abnormalities in glucose and lipid metabolism, while ARHGEF11 is known to influence embryo development. Furthermore, IPA revealed a connection of the differentially abundant proteins to adenocarcinoma. The authors concluded that GDM offspring might have an increased risk of adenocarcinoma, which has to be confirmed by follow-up studies [103]. Similar to PLTP and LCAT, another protein involved in lipoprotein metabolism, the cholesteryl ester transfer protein (CEPT), was found differentially abundant in a study by Liao et al. [104] comparing umbilical venous plasma samples from offspring of GDM patients and control subjects. Out of 780 identified proteins, 98 proteins were found to be differentially abundant in umbilical venous plasma of GDM patients compared to controls. Six of these proteins were also consistently regulated in maternal peripheral plasma samples, including CEPT and apolipoprotein M (APOM) that are known to be GDM-related. Notably, in line with the above-mentioned study by Kopylov et al. [102], APOM was one of the most elevated proteins in the cord blood as a response to maternal diabetes. Furthermore, CEPT concentration in umbilical venous plasma was found to be correlated with the low-density lipoprotein (LDL) levels. Alterations of CEPT abundance were confirmed using an enzyme-linked immunosorbent assay (ELISA) and remained significant after adjustment for age and neonatal gender. Additionally, bioinformatics-based IPA analysis predicted the follicle-stimulating hormone (FSH) as an upstream regulator of the detected differentially abundant proteins [104]. FSH is essential for normal ovarian follicular maturation [105]. In line with this, in the study by Clark et al., healthy follicles were decreased in ovaries from mice offspring after in utero GDM exposure and dietary stress during adulthood. In this study, aiming to investigate the role of GDM on the developmental origins of ovarian disorder, GDM was induced by feeding female mice with a high-fat, high-sucrose diet (HFHS) one week prior to mating and for the duration of gestation. Offspring of HFHS fed mice and control diet mice were further divided into two groups, with one given control and another group given an HFHS diet. Maternal GDM in the absence of dietary stress in offspring resulted in the alteration of 89 proteins in the offspring's ovaries. Canopy FGF signaling regulator 2 (CNPY2), deleted in azoospermia-associated protein 1 (DAZAP1), septin 7 (SEPT7), and serine/arginine-rich splicing factor 2 (SRSF2) were shown to be altered by GDM, adult dietary stress, or both. Overall, this study indicated the possible impact of GDM exposure in utero on the fertility and oocyte quality of offspring in later life.

Table 4. Summary of selected studies linking maternal diabetes with proteome profiles of offspring.

Species	Maternal Characteristics	Bio-Specimen	Major Findings in Offspring	Reference
Human	GDM, type 1 diabetes, type 2 diabetes	Cord blood	Altered abundance of APOM, CP, PLG, AGT, KNG1, APOA1, ORM2, TF, HRG, APOD, LUM; processes such as inflammation, extracellular matrix remodeling, lipid metabolism, etc. mainly affected	[102]
Human	GDM	Umbilical venous plasma	Altered abundance of CEPT and APOM; FSH as upstream regulator of the differentially abundant proteins	[104]
Human	GDM	Umbilical venous plasma	Altered abundance of PLTP and LCAT (related to abnormal glucose and lipid metabolism) and ARHGEF11 (known to influence embryo development)	[103]
Mouse	Diet-induced diabetes	Ovaries	Altered abundance of CNPY2, DAZAP1, SEPT7, and SRSF2; potential impact on fertility and oocyte quality of offspring in later life	[106]

7. Metabolomic Changes in Offspring after Exposure to Maternal Diabetes

Metabolomics addresses the quantitative profile of low-molecular-weight metabolites, such as amino acids, carbohydrates, lipids, or other compounds involved in a plethora of biological processes [50]. Since genetic and epigenetic regulation influences cellular homeostasis and leads to an altered metabolic output, the metabolome largely reflects environment–gene interactions and is a very sensitive measure of an organism’s physiological status [107]. To explore the metabolome, two distinct approaches are frequently utilized: the so-called untargeted approach, assessing the global profiles of all measurable analytes, and the targeted approach, focusing on a predefined set of compounds [108]. Even though the untargeted strategy offers an unbiased survey of molecules and can sometimes reveal novel, unexpected findings, many of the detected metabolites remain unannotated. However, a targeted approach, which is often used in hypothesis-driven studies and uses internal standards, allows accurate quantification of a variety of metabolites [109]. Mass spectrometry and nuclear magnetic resonance spectroscopy (NMR) are the two most commonly used analytical platforms in the field of metabolomics.

Given the constant transplacental supply of maternal metabolites towards the fetus and the fetuses’ own metabolism, metabolomics is a valuable tool to explore the effects of intrauterine exposure to elevated glucose at the molecular level. So far, GDM-related metabolomic studies are limited [110] and mainly refer to GDM-associated complications and their influence on the newborn cord blood metabolome (Table 5). Furthermore, it remains unclear if the metabolomic alterations observed in offspring born to diabetic women are due to an imbalanced maternal supply or alterations of the feto/placental metabolism or a combination of both.

To study the impact of GDM on cord plasma, Shokry et al. used LC-MS/MS to metabolically characterize samples from the PREOBE cohort [111]. Compared to non-GDM, elevated levels of the sum of hexoses were detected in both the maternal and cord blood, indicative of maternal hyperglycemia and increased glucose transport towards the fetus in GDM subjects. Importantly, uniquely in the cord blood but not in the maternal blood, free carnitine was significantly decreased. Furthermore, the same tendency was observed for acyl carnitines (AC), long-chain non-esterified fatty acids (NEFA), phospholipids (PL), specific Krebs cycle metabolites, and β -oxidation markers [112]. Moreover, also in the study by Dube et al., elevated cord blood glucose levels were found in newborns of GDM women, again reflecting the consequences of maternal hyperglycemia [113]. Interestingly,

using mass spectrometry-based untargeted metabolomics, alterations of phospholipid levels during childhood, associated with GDM and persisting during adolescence, were also found in the EPOCH cohort [81]. This study further confirmed an association of the phospholipid metabolic pattern with increased adiposity, impaired insulin sensitivity, and altered adipocytokines across the adolescent transition among girls exposed to in utero GDM [114]. Likewise, Ott et al. aimed to investigate whether women with GDM and their offspring show similar metabolomic patterns eight years after birth. Intergenerationally correlated metabolites included carnitine (C0), glycerophospholipid (PC ae C34:3), two biogenic amines (taurine, creatinine), an amino acid (proline), and sphingolipid (SM-(OH) C14:1). The authors suggested a possible long-term programming effect of maternal GDM on metabolic health in children [115]. Conversely, even though Shokry et al. also found altered metabolites in the cord blood, associated with anthropometric changes in newborn children of mothers with GDM and obesity, these alterations were not detected longitudinally. As a conclusion, the study postulated a lack of predictive power of the cord blood metabolome for the later development of the children [116]. Lu et al. compared cord blood samples of newborns from GDM and from non-GDM women, using flow injection analysis–electrospray ionization–tandem mass spectrometry (FIA-ESI-MS/MS). The authors demonstrated that phosphatidylcholine acyl-alkyl C 32:1 and proline were associated with maternal GDM. Further statistical analysis showed that this association was independent of known GDM risk factors. The authors hypothesized that such an independent association might support the idea that the fetal metabolome may contribute to the development of maternal GDM [117]. Interestingly, Cetin et al. demonstrated that although proline (Pro), methionine (Met), isoleucine (Ile), alanine (Ala), leucine (Leu), and phenylalanine (Phe) were elevated in the umbilical vein blood from offspring born to women with GDM, these amino acids were unchanged in the maternal circulation. Even though ornithine concentration was increased in both the maternal and umbilical vein blood in GDM pregnancies, the levels in the umbilical vein and maternal blood were not significantly correlated. Strikingly, elevated fetal glutamate (Glu) and decreased glutamine (Gln) were also observed while they were unchanged in the maternal circulation. In this context, an increased hepatic Gln-to-Glu conversion, as a consequence of endocrine changes in the fetus, was suggested [118]. Pitchika et al. used UHPLC-MS and non-targeted metabolomics to examine fasting serum samples from the TEENDIAB [119] and BABYDIAB/BABYDIET [120] cohorts. The study included fasting serum samples from offspring born to mothers with type 1 diabetes and a control group of newborns born to non-diabetic mothers but with fathers or siblings with type 1 diabetes. With this study design, the authors aimed to elucidate to what extent health complications in offspring are due to parental genetic transmission or due to intrauterine exposure to hyperglycemia. The authors found that offspring of mothers with type 1 diabetes are more prone to worsening of the metabolic profile than offspring of fathers with type 1 diabetes. This provides evidence that in utero exposure to hyperglycemia has more influence on offspring than parental genetic transmission. Furthermore, increased levels of fasting glucose, insulin, and C-peptide were found in offspring of mothers with type 1 diabetes, but no significant associations between maternal type 1 diabetes and metabolite concentrations in offspring were observed. Overall, the authors proposed that maternal type 1 diabetes is associated with the offspring's metabolic health, but this is unlikely to be caused by alterations in the offspring's metabolome [121]. Lowe et al. used LC-MS/MS-based targeted metabolomics to elucidate the effect of maternal hyperglycemia on newborn cord blood from the HAPO cohort. They found that the maternal response to a glucose load, as reflected by maternal 1h glucose levels, was correlated with concentrations of 3-hydroxybutyrate and its carnitine ester, glycerol, and medium-chain carnitine ester in the cord blood [122]. Walejko et al. used ¹H-NMR to study the effect of PGDM and GDM on serum metabolic changes in the cord blood at birth. The authors found that metabolites of the carbohydrate and choline metabolism were altered in the umbilical cord blood of newborns with both PGDM and GDM [123].

Peng et al. used liquid chromatography coupled to mass spectrometry to investigate the influences of GDM on the newborn meconium and urine metabolome. While in the urine, no significant differences between GDM and controls became apparent. Differences in the meconium metabolome pointed to significantly disrupted metabolic pathways, including lipid, amino acid, and purine metabolism. Moreover, the relationships between potential biomarkers and GDM risk were evaluated. Nine of them (argininosuccinic acid, methyladenosine, methylguanosine, aurodeoxycholic acid, glycocholic acid, hydroxyindoleacetyl glycine, oxotrihydroxyleukotriene B₄, tetrahydrodipicolinate, and DHAP (8:0)) showed the potential as markers for GDM-induced disorders [124]. In the study by Graca et al., using untargeted ultra-high-performance liquid chromatography-mass spectrometry (UPLC-MS)-based metabolomics, no significant alterations in the metabolome of amniotic fluid (AF) of GDM subjects, collected between gestational week 15 and 25, were detected [125]. It should be noted that AF from 10 weeks to 20 weeks is similar to fetal plasma, while the contribution of fetal urine is significant during the second half of the pregnancy [126].

Zhao et al. used ¹H-NMR-based untargeted metabolomics to investigate the crosstalk between maternal gut microbiota and neonatal blood metabolome from pregnancies with GDM. The study showed that the maternal fecal metabolome and the matched neonatal blood metabolome could be separated along the vector of maternal hyperglycemia. A multi-Omics associated approach detected eight metabolites contributing to the close connection between the maternal fecal and the neonatal blood metabolome. Notably, in the feces, metabolites involved in biotin metabolism (lysine, putrescine, guanidinoacetate, and hexadecanedioate) were negatively correlated with maternal hyperglycemia [127].

Only a limited number of studies used animal models to investigate samples not accessible in a non-invasive way. Isganaitis et al. developed the “haploinsufficient for insulin receptor substrate-1 (IRS1-het)” mouse model. During pregnancy, despite normal body weights and plasma glucose levels, the mice are insulin-resistant and hyperinsulinemic, reflecting isolated maternal IR. Using this model, gas chromatography coupled to mass spectrometry was used to measure the liver lipids levels. The results revealed alterations of several lipid classes, notably in the fraction of the 16:1n7 family. However, at six months of age, the mice showed only a trend towards increased triglyceride species, while phospholipids were significantly reduced. The authors concluded that maternal IR could, even in the absence of hyperglycemia or obesity, promote metabolic perturbation in male offspring [128]. The liver metabolome was also targeted in a study by Pereira et al., where the offspring from rats with maternal obesity and GDM was compared to the offspring of lean dams. The offspring were further divided into two groups, with one given a high-fat and -sucrose diet (HFS) and the other a low-fat diet (LF). The analysis of the hepatic metabolome revealed increased diacylglycerol and reduced phosphatidylethanolamine levels in the offspring of GDM dams compared to offspring of lean dams. The authors concluded that GDM might be a driver of hepatic steatosis and insulin resistance in offspring [129]. Renner et al. developed a transgenic pig model expressing mutant insulin C93S in pancreatic β cells. The model mimics isolated maternal hyperglycemia without confounding obesity during pregnancy. Using LC/MS-based targeted metabolomics to analyze the offspring's plasma metabolome, increased concentrations of lysine and α-amino adipic acid, as well as phospholipids, were revealed. Moreover, the ratio of total and short-chain acylcarnitines to carnitine was elevated, indicating an increased import of fatty acids into mitochondria and an increased β-oxidation rate. Overall, it was shown that in this large animal model, even mild maternal hyperglycemia is associated with alterations in the plasma metabolome of the neonatal offspring [130].

Table 5. Summary of selected studies linking maternal diabetes with metabolome profiles of offspring.

Species	Maternal Characteristics	Bio-Specimen	Major Findings in Offspring	Reference
Human	GDM	Blood	Concentrations of lysine, putrescine, guanidinoacetate, and hexadecanedioate were negatively correlated with maternal hyperglycemia	[127]
Human	GDM	Cord Blood	Phosphatidylcholine acyl-alkyl C 32:1 and proline levels were associated with maternal GDM	[117]
Human	GDM	Blood	Association of the phospholipid metabolic pattern with higher adiposity, impaired insulin sensitivity and altered adipocytokines across the adolescent transition, among girls exposed to in utero GDM	[114]
Human	GDM	Blood	Intergenerational correlation of metabolites (carnitine, PC ac C34:3, taurine, creatinine, proline, SM-(OH) C14:1) between women with GDM and offspring 8 years after birth	[115]
Human	GDM	Cord blood	Elevated concentrations of Pro, Met, Ile, Leu, Ala and Phe; potentially, increased Gln-to-Glu conversion	[118]
Human	GDM and PGDM	Cord blood	Altered concentrations of metabolites of carbohydrate and choline metabolism	[123]
Human	GDM and overweight/obesity	Cord blood	Alteration of metabolites associated with anthropometric changes in newborn children, which were not detected longitudinally	[116]
Human	GDM and overweight/obesity	Cord blood	Elevated total hexoses; decreased levels of free carnitine, acyl carnitines, long-chain non-esterified fatty acids, phospholipids, specific Krebs cycle metabolites, and β -oxidation markers in cord blood but not in maternal blood	[112]
Human	Hyperglycemia	Cord blood	Concentrations of 3-hydroxybutyrate and its carnitine ester, glycerol and medium chain carnitine esters correlated with maternal 1h glucose levels	[122]
Human	GDM	Urine and meconium	No difference in urine; evidence for disrupted metabolic pathways, including lipid, amino acid, and purine metabolism from meconium analysis; argininosuccinic acid, methyladenosine, methylguanosine, aurodeoxycholic acid, glycocholic acid, hydroxyindoleacetyl glycine, oxotrihydroxyleukotriene B ₄ , tetrahydrodipicolinate, and DHAP (8:0) suggested as markers for GDM-induced disorders	[124]
Human	Type 1 diabetes	Serum	No significant associations between maternal type 1 diabetes and metabolite concentrations in offspring	[121]

Table 5. Cont.

Species	Maternal Characteristics	Bio-Specimen	Major Findings in Offspring	Reference
Pig	Mutant insulin C93S causing hyperglycemia	Plasma	Increased concentrations of lysine, α -amino adipic acid and phospholipids; biochemical evidence for an increased mitochondrial import of fatty acids for β -oxidation	[130]
Rat	GDM	Liver	Increased levels of diacylglycerol and reduced levels of phosphatidylethanolamine	[129]
Mouse	IR	Liver	Altered concentrations of the 16:1n7 lipid family; at 6 months of age a trend towards increased triglyceride species, while phospholipids were significantly reduced	[128]

8. Microbiomics and Nutriomics Studies Addressing GDM Effects on Offspring

Microbiomics is a fast-growing field, characterizing and quantifying the community of microorganisms found in a certain habitat [131]. The microbial community, also known as microbiota, consists of various microorganisms, such as bacteria, fungi, etc. The rapid development of high-throughput analytical technologies facilitated a detailed investigation of the microbiota with regards to their genetic and functional divergence and caused paradigm shifts in our understanding of their roles in health and disease [132]. Especially the sequence analysis of small subunit ribosomal RNA (16S rRNA) genes as well as shotgun metagenomics sequencing, in which total DNA is sequenced, are the leading methods utilized for microbiome profiling. Both approaches allow an accurate quantitative determination of microorganisms and their taxa, which can be correlated with disease or other phenotypes of interest [50].

At first, the fetal gut was thought to be sterile at birth. However, recent studies indicate that colonization of the gastrointestinal tract may already occur during fetal development and could also be influenced by maternal environmental exposures and by the mode of birth (caesarean section or vaginal) [133]. So far, there are only a few studies investigating the influence of maternal diabetes on offspring microbiota. Furthermore, studies are often confounded by varying perinatal conditions known to affect the microbiota colonization of offspring. This prevents a clear distinction of the maternal diabetes effects from those of concomitant diseases. Despite this, it seems that specific taxa associated with maternal diabetes can be transmitted to the offspring, which differentiates their microbiota from the offspring of non-diabetic mothers. A comprehensive review of studies investigating the influence of maternal GDM on the neonatal microbiome was recently published [134]. Therefore, here we summarize only some major findings from the studies shown in Table 6. For instance, Ponzo et al. compared the microbiota of offspring born to GDM mothers versus normoglycemic mothers by 16S amplicon-based sequencing of fecal samples collected during the first week of life. The microbiota of infants from GDM women showed a lower complexity and higher inter-individual variability. Furthermore, the relative abundance of pro-inflammatory taxa, in particular *Escherichia* and *Parabacteroides*, was increased [135]. Similarly, Soderborg et al. investigated the gut microbiota from 2-week old neonates born to normal-weight or overweight/obese mothers with or without GDM and found evidence that GDM alone or together with maternal overweight/obesity influences the infant microbiota in a way that sets the stage for the future risk of inflammatory and metabolic diseases [136]. Furthermore, Hu et al. explored the diversity of the meconium microbiome to determine if it is affected by maternal diabetes (pre-pregnancy type 2 diabetes and GDM). The authors concluded that the meconium microbiome of infants born to mothers with diabetes is enriched with similar bacterial taxa as those reported in the fecal microbiome

of adult diabetic patients [137]. This finding might indicate a non-genetic risk of transmission of diabetes (i.e., through the microbiome). Therefore, it is interesting if similar findings are observed in longitudinal studies exploring the effect of maternal diabetes on the offspring microbiome postpartum. Using 16S rRNA gene amplicon sequencing, Crusell et al. compared feces from children of mothers with and without GDM. The samples were collected during the first week of life and later at an average age of 9 months. The results indicate that differences in glycemic control during late pregnancy are linked to relatively modest variations in the gut microbiota composition of offspring during the first week of life and nine months after birth. In addition, similar to the above-mentioned study by Ponzo et al. and the study by Su et al. [138], Crusell et al. found a lower richness of the gut microbiota in GDM neonates compared with neonates born to mothers without GDM. The authors also referred to the previous reports [139], where high-microbial richness was associated with metabolically more advantageous phenotypes (i.e., lower BMI, and higher insulin sensitivity, etc.). Furthermore, the authors found species in the gut microbiota that was similar to the microbiota observed in childhood obesity and in adults with type 2 diabetes [140]. In a longitudinal study by Hasan et al., stool samples from offspring of GDM and non-GDM mothers collected five years postpartum were analyzed for microbiome profiling. Interestingly, the *Anaerotruncus* genus was more abundant in the offspring of GDM mothers [141]. Of note, *Anaerotruncus* was also found to be enriched in the gut microbiota of GDM women even after the adjustment for pre-pregnancy BMI [142]. This may be one of the examples of an intergenerational concordance of microbial variation in mother–offspring pairs. Nevertheless, whether an increase in *Anaerotruncus* in the offspring microbiome is a risk factor for future metabolic disorders has to be elucidated in further studies.

Table 6. Summary of selected human studies linking maternal diabetes with microbiome profiles of offspring.

Maternal Characteristics	Bio-Specimen	Major Findings in Offspring	Reference
GDM	Feces	GDM alone or together with maternal overweight/obesity influences infant microbiota in a way that set the stage for future risks of inflammatory and metabolic disease	[136]
GDM	Feces	Glycemic regulation in late pregnancy is linked with relatively modest variation in the gut microbiota composition of the offspring at age 1 week and 9 months; lower richness of the gut microbiota in GDM neonates compared with neonates born to mothers without GDM	[140]
GDM	Feces	Increased relative abundance of pro-inflammatory taxa, in particular <i>Escherichia</i> and <i>Parabacteroides</i>	[135]
GDM	Feces	Increased abundance of <i>Anaerotruncus</i> genus	[141]
Type 2 PGDM GDM	Meconium	Enrichment of the meconium microbiome for the same bacterial taxa as reported in the fecal microbiome of adult diabetic patients	[137]

Nutriomics is formed by the combination of nutritional science and different Omics techniques, resulting in disciplines such as nutrigenomics, and nutriproteomics, etc. Taking into account the complexity of the human body and its interplay with food, it is conceivable that holistic molecular analyses of food–body interactions (i.e., nutri-omics) are essential to understanding the effects of nutrients [143]. Several studies have pointed to diet–gene interactions affecting glucose metabolism and being linked to diabetes (reviewed in [144]). Studying dietary interventions and personalized nutrition could reveal certain diet types, which could help prevent adverse fetal outcomes caused by maternal diabetes.

Studies investigating combinatorial effects of maternal diabetes, the type of offspring diet, and the influence of both on offspring health are limited (Table 7). Results from the longitudinal, large-scale cohort study by Chu Tint et al. suggested that a high placental inositol content may reduce the pro-adipogenic effects of maternal glycemia, resulting in lower birth weight and reduced adiposity of offspring. The authors used the longitudinal data from the Growing Up in Singapore Towards healthy Outcomes (GUSTO) cohort [145]. Maternal FPG and 2h plasma glucose (2 hPG) were obtained in pregnant women by a 75 g oral glucose tolerance test at around 26 weeks of gestation. Placental inositol was quantified by liquid chromatography-mass spectrometry. Interestingly, maternal glycemia and fetal birth weight (or abdominal adiposity) correlated positively only in the case of low, but not high, placental inositol content. The authors emphasized the anti-adipogenic effect of inositol during maternal hyperglycemia and pointed to the potential benefits of prenatal inositol supplementation [39]. Interestingly, a study by Pereira et al. found that metabolic disturbances observed in the liver from offspring of gestational diabetic dams were even worsened after the challenges of a high-fat diet. A low-fat diet did not show protective effects against these metabolic phenotypes (obesity, hepatic steatosis, and insulin resistance) [129] (see the chapter: Fetal metabolomic changes after exposure to maternal diabetes).

Table 7. Summary of selected studies investigating combinatorial effect of maternal diabetes and offspring nutrition on offspring health.

Species	Maternal Characteristics	Major Findings in Offspring	Reference
Human	Hyperglycemia	Positive correlation of maternal glycemia and fetal birth weight/abdominal adiposity in the case of low, but not high, placental inositol content	[39]
Rat	GDM	Metabolic disturbances in liver of offspring from gestational diabetic dams worsened upon a high-fat diet; no protective effect of a low-fat diet against metabolic changes (obesity, hepatic steatosis, insulin resistance)	[129]

9. Conclusions

Diabetes is a serious health concern for pregnant women and their offspring. In this article, we have reviewed the contributions of Omics technologies in studying the effects of maternal diabetes on offspring health. The transformation of complex and heterogeneous Omics data into biological meaning is a daunting task. In this regard, careful interpretation of results, especially from studies with limited numbers of samples, is necessary. Overall, there is increasing evidence pointing to molecular disturbances in offspring exposed in utero to maternal diabetes. Apparently, many characteristics that are based on observational cohort studies are reflected on molecular levels in Omics studies, demonstrating that maternal diabetes influences the cellular and organ systems of the offspring. This includes the predisposition of offspring to future obesity triggered by elevated maternal glucose levels. Other long-term offspring health complications include cardiovascular and neurodevelopmental disorders, as supported by Omics studies. It should be noted that the majority of the Omics studies reviewed here were performed at birth, and the knowledge about molecular derangements during earlier stages of embryo development is lacking. More Omics experiments using animal models would be valuable to close this knowledge gap and to reveal the most susceptible windows during development when alterations due to maternal diabetes manifest. Additional research is also warranted to determine if Omics data will result in new biomarkers for the diagnosis, treatment, and prevention of offspring health problems related to maternal diabetes.

Author Contributions: Conceptualization, B.S.; writing—original draft preparation, B.S.; Review and editing, J.B.S., L.V., F.F., E.K., S.R., T.F. and E.W.; Supervision T.F. and E.W. All authors have read and agreed to the published version of the manuscript.

Funding: This project has received funding from the European Union’s Horizon 2020 research and innovation program under the Marie Skłodowska-Curie grant agreement No. 812660 (DohART-NET).

Institutional Review Board Statement: Not applicable.

Informed Consent Statement: Not applicable.

Data Availability Statement: Not applicable.

Acknowledgments: All figures were adapted from the Servier Medical Art (<https://smart.servier.com/>, accessed on 28 October 2021) templates, licensed under a Creative Commons License attribution 3.0 Unported License.

Conflicts of Interest: The authors declare no conflict of interest.

Abbreviations

16S rRNA	16S ribosomal RNA
2 hPG	2-h plasma glucose
Ala	Alanine
ABCA1	ATP-binding cassette transporter A1
AC	Acyl-carnitine
ADIPOQ	Adiponectin
AF	Amniotic fluid
AGT	Angiotensinogen
Ahsp	α haemoglobin stabilizing protein
AMPK	AMP-activated protein kinase
APOA1	Apolipoprotein A-I
APOD	Apolipoprotein D
APOM	Apolipoprotein M
ARHGEF11	Rho guanine nucleotide exchange factor 11
BMI	Body mass index
CEPT	Cholesteryl ester transfer protein
ChiP	Chromatin immunoprecipitation assay
CNYP2	Canopy FGF signaling regulator 2
CP	Ceruloplasmin
CpG	Cytosine-guanine dinucleotide
CVD	Cardiovascular disorder
CYP2E1	Cytochrome P450 Family 2 Subfamily E Member 1
DAZAP1	Azoospermia Associated Protein 1
DEG	Differentially expressed genes
DNA	Deoxyribonucleic acid
EFSOCH	The Exeter Family Study of Childhood Health
EGR1	Early growth response 1
ELISA	Enzyme-linked immunosorbent assay
EPOCH	Exploring Perinatal Outcomes among Children
FIA-ESI-MS/MS	Flow injection analysis-electrospray ionization-tandem mass spectrometry
FOXO1	Forkhead box protein O1
FPG	Fasting plasma glucose
FSH	Follicle-stimulating hormone
GDM	Gestational diabetes mellitus
Gln	Glutamine
Glu	Glutamate
GWAS	Genome-wide association study
HAPO	The Hyperglycemia and Adverse Pregnancy Outcome
HFHS	High fat, high sucrose diet

HFS	High fat diet and sucrose diet
HIF1	Hypoxia-inducible factor 1
HRG	Histidine-rich glycoprotein
HUVEC	Human umbilical vein endothelial cells
Ile	Isoleucine
IPA	Ingenuity Pathway Analysis
IR	Insulin resistance
IRS1-het	Haploinsufficient for insulin receptor substrate-1
Kel	Kel metallo-endopeptidase
KNG1	Kinogen-1
LCAT	Lecithin-cholesterol acyltransferase
LC-MS/MS	Liquid Chromatography with tandem Mass Spectrometry
LDL	Low-density lipoprotein
Leu	Leucine
LF	Low fat diet
LGA	Large for gestational age
LPL	Lipoprotein lipase
LUM	Lumican
LV	Left ventricle
MEST	Mesoderm Specific Transcript
Met	Methionine
MHC	Major Histocompatibility Complex
MIA	Maternal immune activation
mRNA	Messenger RNA
NEFA	Non-esterified fatty acid
NGS	Next generation sequencing
NMR	Nuclear magnetic resonance
OGTT	Oral glucose tolerance test
OR2L13	Olfactory Receptor Family 2 Subfamily L Member 13
ORM2	α -1-acid glycoprotein 2
PACE	Pregnancy and Childhood epigenetics consortium
PCK1	Phosphoenolpyruvate Carboxykinase 1
PGDM	Pregestational diabetes mellitus
Phe	Phenylalanine
PL	Phospholipid
PLG	Plasminogen
PLTP	Phospholipid transfer protein
PPAR	Peroxisome proliferator-activated receptor
PPARGC1 α	Peroxisome proliferator-activated receptor- γ , co-activator 1, α
Pro	Proline
RDH16	Retinol Dehydrogenase 16
RNA	Ribonucleic acid
SETP7	Septin 7
SH3PXD2A	SH3 And PX Domains 2A
SLC6A4	Serotonin transporter gene
SNP	Single nucleotide polymorphism
SOD2	Superoxide dismutase 2
SRSF2	Serine and Arginine Rich Splicing Factor 2
STZ	Streptozotocin
TF	Serotransferrin
UHPLC-MS	Ultra-high-performance liquid chromatography Mass spectrometry
Vegfa	Vascular endothelial growth factor A
WB	Western blot
WGCNA	Weighted Correlation Network Analysis

References

1. Hadden, D.R.; McLaughlin, C. Normal and abnormal maternal metabolism during pregnancy. *Semin. Fetal Neonatal Med.* **2009**, *14*, 66–71. [[CrossRef](#)]
2. Herrera, E. Metabolic adaptations in pregnancy and their implications for the availability of substrates to the fetus. *Eur. J. Clin. Nutr.* **2000**, *54*, S47–S51. [[CrossRef](#)] [[PubMed](#)]
3. Zeng, Z.; Liu, F.; Li, S. Metabolic Adaptations in Pregnancy: A Review. *Ann. Nutr. Metab.* **2017**, *70*, 59–65. [[CrossRef](#)] [[PubMed](#)]
4. Parrettini, S.; Caroli, A.; Torlone, E. Nutrition and Metabolic Adaptations in Physiological and Complicated Pregnancy: Focus on Obesity and Gestational Diabetes. *Front. Endocrinol.* **2020**, *11*, 611929. [[CrossRef](#)] [[PubMed](#)]
5. Holme, A.M.; Roland, M.C.; Lorentzen, B.; Michelsen, T.M.; Henriksen, T. Placental glucose transfer: A human in vivo study. *PLoS ONE* **2015**, *10*, e0117084. [[CrossRef](#)] [[PubMed](#)]
6. Butte, N.F. Carbohydrate and lipid metabolism in pregnancy: Normal compared with gestational diabetes mellitus. *Am. J. Clin. Nutr.* **2000**, *71*, S1256–S1261. [[CrossRef](#)]
7. Di Cianni, G.; Miccoli, R.; Volpe, L.; Lencioni, C.; Del Prato, S. Intermediate metabolism in normal pregnancy and in gestational diabetes. *Diabetes Metab. Res. Rev.* **2003**, *19*, 259–270. [[CrossRef](#)]
8. Kampmann, U.; Knorr, S.; Fuglsang, J.; Ovesen, P. Determinants of Maternal Insulin Resistance during Pregnancy: An Updated Overview. *J. Diabetes Res.* **2019**, *2019*, 5320156. [[CrossRef](#)]
9. Ernst, S.; Demirci, C.; Valle, S.; Velazquez-Garcia, S.; Garcia-Ocana, A. Mechanisms in the adaptation of maternal beta-cells during pregnancy. *Diabetes Manag.* **2011**, *1*, 239–248. [[CrossRef](#)]
10. Napso, T.; Yong, H.E.J.; Lopez-Tello, J.; Sferruzzi-Perri, A.N. The Role of Placental Hormones in Mediating Maternal Adaptations to Support Pregnancy and Lactation. *Front. Physiol.* **2018**, *9*, 1091. [[CrossRef](#)]
11. Herrera, E.; Desoye, G. Maternal and fetal lipid metabolism under normal and gestational diabetic conditions. *Horm. Mol. Biol. Clin. Investig.* **2016**, *26*, 109–127. [[CrossRef](#)]
12. Buchanan, T.A.; Xiang, A.; Kjos, S.L.; Watanabe, R. What is gestational diabetes? *Diabetes Care* **2007**, *30* (Suppl. 2), S105–S111. [[CrossRef](#)]
13. Howe, C.G.; Cox, B.; Fore, R.; Jungius, J.; Kvist, T.; Lent, S.; Miles, H.E.; Salas, L.A.; Rifas-Shiman, S.; Starling, A.P.; et al. Maternal Gestational Diabetes Mellitus and Newborn DNA Methylation: Findings From the Pregnancy and Childhood Epigenetics Consortium. *Diabetes Care* **2020**, *43*, 98–105. [[CrossRef](#)] [[PubMed](#)]
14. Chen, L.; Mayo, R.M.; Chatry, A.; Hu, G. Gestational Diabetes Mellitus: Its Epidemiology and Implication beyond Pregnancy. *Curr. Epidemiol. Rep.* **2016**, *3*, 1–11. [[CrossRef](#)]
15. DeSisto, C.L.; Kim, S.Y.; Sharma, A.J. Prevalence estimates of gestational diabetes mellitus in the United States, Pregnancy Risk Assessment Monitoring System (PRAMS), 2007–2010. *Prev. Chronic Dis.* **2014**, *11*, E104. [[CrossRef](#)] [[PubMed](#)]
16. Sacks, D.A.; Hadden, D.R.; Maresh, M.; Deerochanawong, C.; Dyer, A.R.; Metzger, B.E.; Lowe, L.P.; Coustan, D.R.; Hod, M.; Oats, J.J.; et al. Frequency of gestational diabetes mellitus at collaborating centers based on IADPSG consensus panel-recommended criteria: The Hyperglycemia and Adverse Pregnancy Outcome (HAPO) Study. *Diabetes Care* **2012**, *35*, 526–528. [[CrossRef](#)]
17. American Diabetes Association. Diagnosis and Classification of Diabetes Mellitus. *Diabetes Care* **2014**, *37*, S81–S90. [[CrossRef](#)] [[PubMed](#)]
18. Ravnsborg, T.; Svaneklink, S.; Andersen, L.L.T.; Larsen, M.R.; Jensen, D.M.; Overgaard, M. First-trimester proteomic profiling identifies novel predictors of gestational diabetes mellitus. *PLoS ONE* **2019**, *14*, e0214457. [[CrossRef](#)]
19. Damm, P.; Houshmand-Oregaard, A.; Kelstrup, L.; Lauenborg, J.; Mathiesen, E.R.; Clausen, T.D. Gestational diabetes mellitus and long-term consequences for mother and offspring: A view from Denmark. *Diabetologia* **2016**, *59*, 1396–1399. [[CrossRef](#)]
20. Ruiz-Palacios, M.; Ruiz-Alcaraz, A.J.; Sanchez-Campillo, M.; Larque, E. Role of Insulin in Placental Transport of Nutrients in Gestational Diabetes Mellitus. *Ann. Nutr. Metab.* **2017**, *70*, 16–25. [[CrossRef](#)] [[PubMed](#)]
21. Pedersen, J. Diabetes and pregnancy; blood sugar of newborn infants during fasting and glucose administration. *Ugeskr Laeger* **1952**, *114*, 685.
22. Ornoy, A.; Reece, E.A.; Pavlinkova, G.; Kappen, C.; Miller, R.K. Effect of maternal diabetes on the embryo, fetus, and children: Congenital anomalies, genetic and epigenetic changes and developmental outcomes. *Birth Defects Res. C Embryo Today* **2015**, *105*, 53–72. [[CrossRef](#)] [[PubMed](#)]
23. Lin, S.F.; Kuo, C.F.; Chiou, M.J.; Chang, S.H. Maternal and fetal outcomes of pregnant women with type 1 diabetes, a national population study. *Oncotarget* **2017**, *8*, 80679–80687. [[CrossRef](#)]
24. Broughton, C.; Douek, I. An overview of the management of diabetes from pre-conception, during pregnancy and in the postnatal period. *Clin. Med.* **2019**, *19*, 399–402. [[CrossRef](#)] [[PubMed](#)]
25. Mitanchez, D.; Yzydorczyk, C.; Simeoni, U. What neonatal complications should the pediatrician be aware of in case of maternal gestational diabetes? *World J. Diabetes* **2015**, *6*, 734–743. [[CrossRef](#)]
26. Kawakita, T.; Bowers, K.; Hazrati, S.; Zhang, C.; Grewal, J.; Chen, Z.; Sun, L.; Grantz, K.L. Increased Neonatal Respiratory Morbidity Associated with Gestational and Pregestational Diabetes: A Retrospective Study. *Am. J. Perinatol.* **2017**, *34*, 1160–1168. [[CrossRef](#)]
27. Boghossian, N.S.; Yeung, E.; Albert, P.S.; Mendola, P.; Laughon, S.K.; Hinkle, S.N.; Zhang, C. Changes in diabetes status between pregnancies and impact on subsequent newborn outcomes. *Am. J. Obstet. Gynecol.* **2014**, *210*, 431.e1–14. [[CrossRef](#)] [[PubMed](#)]

28. Forsbach-Sanchez, G.; Vasquez-Lara, J.; Hernandez-Herrera, R.; Tamez-Perez, H.E. Neonatal morbidity associated to gestational diabetes. A descriptive study on 74 patients. *Rev. Med. Inst. Mex. Seguro Soc.* **2008**, *46*, 141–144.
29. Karczewski, K.J.; Snyder, M.P. Integrative omics for health and disease. *Nat. Rev. Genet.* **2018**, *19*, 299–310. [[CrossRef](#)] [[PubMed](#)]
30. Huhn, E.A.; Rossi, S.W.; Hoesli, I.; Gobl, C.S. Controversies in Screening and Diagnostic Criteria for Gestational Diabetes in Early and Late Pregnancy. *Front. Endocrinol.* **2018**, *9*, 696. [[CrossRef](#)]
31. Albl, B.; Haesner, S.; Braun-Reichhart, C.; Streckel, E.; Renner, S.; Seeliger, F.; Wolf, E.; Wanke, R.; Blutke, A. Tissue Sampling Guides for Porcine Biomedical Models. *Toxicol. Pathol.* **2016**, *44*, 414–420. [[CrossRef](#)]
32. Pasek, R.C.; Gannon, M. Advancements and challenges in generating accurate animal models of gestational diabetes mellitus. *Am. J. Physiol. Endocrinol. Metab.* **2013**, *305*, E1327–E1338. [[CrossRef](#)]
33. Friedman, J.E. Developmental Programming of Obesity and Diabetes in Mouse, Monkey, and Man in 2018: Where are We Headed? *Diabetes* **2018**, *67*, 2137–2151. [[CrossRef](#)]
34. Zettler, S.; Renner, S.; Kemter, E.; Hinrichs, A.; Klymiuk, N.; Backman, M.; Riedel, E.O.; Mueller, C.; Streckel, E.; Braun-Reichhart, C.; et al. A decade of experience with genetically tailored pig models for diabetes and metabolic research. *Anim. Reprod.* **2020**, *17*, e20200064. [[CrossRef](#)]
35. Renner, S.; Blutke, A.; Clauss, S.; Deeg, C.A.; Kemter, E.; Merkus, D.; Wanke, R.; Wolf, E. Porcine models for studying complications and organ crosstalk in diabetes mellitus. *Cell Tissue Res.* **2020**, *380*, 341–378. [[CrossRef](#)] [[PubMed](#)]
36. Renner, S.; Dobenecker, B.; Blutke, A.; Zöls, S.; Wanke, R.; Ritzmann, M.; Wolf, E. Comparative aspects of rodent and nonrodent animal models for mechanistic and translational diabetes research. *Theriogenology* **2016**, *86*, 406–421. [[CrossRef](#)]
37. Litten-Brown, J.C.; Corson, A.M.; Clarke, L. Porcine models for the metabolic syndrome, digestive and bone disorders: A general overview. *Animal* **2010**, *4*, 899–920. [[CrossRef](#)]
38. Souza, R.T.; Mayrink, J.; Leite, D.F.; Costa, M.L.; Calderon, I.M.; Rocha Filho, E.A.; Vettorazzi, J.; Feitosa, F.E.; Cecatti, J.G.; Preterm, S.S.G. Metabolomics applied to maternal and perinatal health: A review of new frontiers with a translation potential. *Clinics* **2019**, *74*, e894. [[CrossRef](#)]
39. Chu, A.H.Y.; Tint, M.T.; Chang, H.F.; Wong, G.; Yuan, W.L.; Tull, D.; Nijagal, B.; Narayana, V.K.; Meikle, P.J.; Chang, K.T.E.; et al. High placental inositol content associated with suppressed pro-adipogenic effects of maternal glycaemia in offspring: The GUSTO cohort. *Int. J. Obes.* **2021**, *45*, 247–257. [[CrossRef](#)] [[PubMed](#)]
40. Lizárraga, D.; García-Gasca, A. The Placenta as a Target of Epigenetic Alterations in Women with Gestational Diabetes Mellitus and Potential Implications for the Offspring. *Epigenomes* **2021**, *5*, 13. [[CrossRef](#)]
41. Valencia-Ortega, J.; Saucedo, R.; Sánchez-Rodríguez, M.A.; Cruz-Durán, J.G.; Martínez, E.G.R. Epigenetic Alterations Related to Gestational Diabetes Mellitus. *Int. J. Mol. Sci.* **2021**, *22*, 9462. [[CrossRef](#)]
42. Collins, F.S.; Green, E.D.; Guttmacher, A.E.; Guyer, M.S. A vision for the future of genomics research. *Nature* **2003**, *422*, 835–847. [[CrossRef](#)]
43. Tam, V.; Patel, N.; Turcotte, M.; Bossé, Y.; Paré, G.; Meyre, D. Benefits and limitations of genome-wide association studies. *Nat. Rev. Genet.* **2019**, *20*, 467–484. [[CrossRef](#)] [[PubMed](#)]
44. Derrai, J.G.B.; Maessen, S.E.; Gibbins, J.D.; Cutfield, W.S.; Lundgren, M.; Ahlsson, F. Large-for-gestational-age phenotypes and obesity risk in adulthood: A study of 195,936 women. *Sci. Rep.* **2020**, *10*, 2157. [[CrossRef](#)]
45. Boney, C.M.; Verma, A.; Tucker, R.; Vohr, B.R. Metabolic syndrome in childhood: Association with birth weight, maternal obesity, and gestational diabetes mellitus. *Pediatrics* **2005**, *115*, e290–e296. [[CrossRef](#)] [[PubMed](#)]
46. Kong, L.; Nilsson, I.A.K.; Gissler, M.; Lavebratt, C. Associations of Maternal Diabetes and Body Mass Index With Offspring Birth Weight and Prematurity. *JAMA Pediatr.* **2019**, *173*, 371–378. [[CrossRef](#)] [[PubMed](#)]
47. Knight, B.; Shields, B.M.; Hattersley, A.T. The Exeter Family Study of Childhood Health (EFSOCH): Study protocol and methodology. *Paediatr. Perinat. Epidemiol.* **2006**, *20*, 172–179. [[CrossRef](#)]
48. Coustan, D.R.; Lowe, L.P.; Metzger, B.E. The hyperglycemia and adverse pregnancy outcome (HAPO) study: Can we use the results as a basis for change? *J. Matern. Fetal Neonatal Med.* **2010**, *23*, 204–209. [[CrossRef](#)]
49. Hughes, A.E.; Nodzinski, M.; Beaumont, R.N.; Talbot, O.; Shields, B.M.; Scholtens, D.M.; Knight, B.A.; Lowe, W.L., Jr.; Hattersley, A.T.; Freathy, R.M. Fetal Genotype and Maternal Glucose Have Independent and Additive Effects on Birth Weight. *Diabetes* **2018**, *67*, 1024–1029. [[CrossRef](#)]
50. Hasin, Y.; Seldin, M.; Lusis, A. Multi-omics approaches to disease. *Genome Biol.* **2017**, *18*, 83. [[CrossRef](#)]
51. Feil, R.; Fraga, M.F. Epigenetics and the environment: Emerging patterns and implications. *Nat. Rev. Genet.* **2012**, *13*, 97–109. [[CrossRef](#)]
52. Bird, A. DNA methylation patterns and epigenetic memory. *Genes Dev.* **2002**, *16*, 6–21. [[CrossRef](#)]
53. Tirado-Magallanes, R.; Rebbani, K.; Lim, R.; Pradhan, S.; Benoukraf, T. Whole genome DNA methylation: Beyond genes silencing. *Oncotarget* **2017**, *8*, 5629–5637. [[CrossRef](#)]
54. Finer, S.; Mathews, C.; Lowe, R.; Smart, M.; Hillman, S.; Foo, L.; Sinha, A.; Williams, D.; Rakyan, V.K.; Hitman, G.A. Maternal gestational diabetes is associated with genome-wide DNA methylation variation in placenta and cord blood of exposed offspring. *Hum. Mol. Genet.* **2015**, *24*, 3021–3029. [[CrossRef](#)] [[PubMed](#)]
55. Moen, G.H.; Sommer, C.; Prasad, R.B.; Sletner, L.; Qvigstad, E.; Birkeland, K.I. MECHANISMS IN ENDOCRINOLOGY: Epigenetic modifications and gestational diabetes: A systematic review of published literature. *Eur. J. Endocrinol.* **2017**, *176*, R247–R267. [[CrossRef](#)] [[PubMed](#)]

56. Franzago, M.; Fraticelli, F.; Stuppia, L.; Vitacolonna, E. Nutrigenetics, epigenetics and gestational diabetes: Consequences in mother and child. *Epigenetics* **2019**, *14*, 215–235. [[CrossRef](#)]
57. Stupecka-Ziemilska, M.; Wychowański, P.; Puzianowska-Kuznicka, M. Gestational Diabetes Mellitus Affects Offspring's Epigenome. Is There a Way to Reduce the Negative Consequences? *Nutrients* **2020**, *12*, 2792. [[CrossRef](#)] [[PubMed](#)]
58. Chu, A.H.Y.; Godfrey, K.M. Gestational Diabetes Mellitus and Developmental Programming. *Ann. Nutr. Metab.* **2020**, *76* (Suppl. 3), 4–15. [[CrossRef](#)]
59. Dluski, D.F.; Wolinska, E.; Skrzypczak, M. Epigenetic Changes in Gestational Diabetes Mellitus. *Int. J. Mol. Sci.* **2021**, *22*, 7649. [[CrossRef](#)] [[PubMed](#)]
60. Lesseur, C.; Armstrong, D.A.; Paquette, A.G.; Li, Z.; Padbury, J.F.; Marsit, C.J. Maternal obesity and gestational diabetes are associated with placental leptin DNA methylation. *Am. J. Obstet. Gynecol.* **2014**, *211*, 654.e1–654.e9. [[CrossRef](#)]
61. Gagné-Ouellet, V.; Breton, E.; Thibeault, K.; Fortin, C.-A.; Cardenas, A.; Guérin, R.; Perron, P.; Hivert, M.-F.; Bouchard, L. Mediation Analysis Supports a Causal Relationship between Maternal Hyperglycemia and Placental DNA Methylation Variations at the Leptin Gene Locus and Cord Blood Leptin Levels. *Int. J. Mol. Sci.* **2020**, *21*, 329. [[CrossRef](#)]
62. Allard, C.; Desgagné, V.; Patenaude, J.; Lacroix, M.; Guillemette, L.; Battista, M.C.; Doyon, M.; Ménard, J.; Ardilouze, J.L.; Perron, P.; et al. Mendelian randomization supports causality between maternal hyperglycemia and epigenetic regulation of leptin gene in newborns. *Epigenetics* **2015**, *10*, 342–351. [[CrossRef](#)] [[PubMed](#)]
63. Côté, S.; Gagné-Ouellet, V.; Guay, S.-P.; Allard, C.; Houde, A.-A.; Perron, P.; Baillargeon, J.-P.; Gaudet, D.; Guérin, R.; Brisson, D.; et al. PPARGC1 α gene DNA methylation variations in human placenta mediate the link between maternal hyperglycemia and leptin levels in newborns. *Clin. Epigenetics* **2016**, *8*, 72. [[CrossRef](#)]
64. Friedman, J. Leptin at 20: An overview. *J. Endocrinol.* **2014**, *223*. [[CrossRef](#)]
65. Flenkenthaler, F.; Ländström, E.; Shashikadze, B.; Backman, M.; Blutke, A.; Philippou-Massier, J.; Renner, S.; Hrabe de Angelis, M.; Wanke, R.; Blum, H.; et al. Differential Effects of Insulin-Deficient Diabetes Mellitus on Visceral vs. Subcutaneous Adipose Tissue—Multi-omics Insights From the Munich MIDY Pig Model. *Front. Med.* **2021**, *8*. [[CrossRef](#)]
66. Mantzoros, C.S.; Rifas-Shiman, S.L.; Williams, C.J.; Fargnoli, J.L.; Kelesidis, T.; Gillman, M.W. Cord blood leptin and adiponectin as predictors of adiposity in children at 3 years of age: A prospective cohort study. *Pediatrics* **2009**, *123*, 682–689. [[CrossRef](#)]
67. Bouchard, L.; Hivert, M.-F.; Guay, S.-P.; St-Pierre, J.; Perron, P.; Brisson, D. Placental adiponectin gene DNA methylation levels are associated with mothers' blood glucose concentration. *Diabetes* **2012**, *61*, 1272–1280. [[CrossRef](#)]
68. Houde, A.-A.; Hivert, M.-F.; Bouchard, L. Fetal epigenetic programming of adipokines. *Adipocyte* **2013**, *2*, 41–46. [[CrossRef](#)]
69. Houde, A.A.; St-Pierre, J.; Hivert, M.F.; Baillargeon, J.P.; Perron, P.; Gaudet, D.; Brisson, D.; Bouchard, L. Placental lipoprotein lipase DNA methylation levels are associated with gestational diabetes mellitus and maternal and cord blood lipid profiles. *J. Dev. Orig. Health Dis.* **2014**, *5*, 132–141. [[CrossRef](#)] [[PubMed](#)]
70. Gagné-Ouellet, V.; Houde, A.-A.; Guay, S.-P.; Perron, P.; Gaudet, D.; Guérin, R.; Jean-Patrice, B.; Hivert, M.-F.; Brisson, D.; Bouchard, L. Placental lipoprotein lipase DNA methylation alterations are associated with gestational diabetes and body composition at 5 years of age. *Epigenetics* **2017**, *12*, 616–625. [[CrossRef](#)] [[PubMed](#)]
71. Blazevic, S.; Horvaticek, M.; Kesic, M.; Zill, P.; Hranilovic, D.; Ivanisevic, M.; Desoye, G.; Stefulj, J. Epigenetic adaptation of the placental serotonin transporter gene (SLC6A4) to gestational diabetes mellitus. *PLoS ONE* **2017**, *12*, e0179934. [[CrossRef](#)]
72. Muller, C.L.; Anacker, A.M.J.; Veenstra-VanderWeele, J. The serotonin system in autism spectrum disorder: From biomarker to animal models. *Neuroscience* **2016**, *321*, 24–41. [[CrossRef](#)]
73. Rowland, J.; Wilson, C.A. The association between gestational diabetes and ASD and ADHD: A systematic review and meta-analysis. *Sci. Rep.* **2021**, *11*, 5136. [[CrossRef](#)]
74. Felix, J.F.; Joubert, B.R.; Baccarelli, A.A.; Sharp, G.C.; Almqvist, C.; Annesi-Maesano, I.; Arshad, H.; Baiz, N.; Bakermans-Kranenburg, M.J.; Bakulski, K.M.; et al. Cohort Profile: Pregnancy And Childhood Epigenetics (PACE) Consortium. *Int. J. Epidemiol.* **2018**, *47*, 22–23. [[CrossRef](#)]
75. Wang, X.; Lu, J.; Xie, W.; Lu, X.; Liang, Y.; Li, M.; Wang, Z.; Huang, X.; Tang, M.; Pfaff, D.W.; et al. Maternal diabetes induces autism-like behavior by hyperglycemia-mediated persistent oxidative stress and suppression of superoxide dismutase 2. *Proc. Natl. Acad. Sci. USA* **2019**, *116*, 23743–23752. [[CrossRef](#)] [[PubMed](#)]
76. Weng, X.; Liu, F.; Zhang, H.; Kan, M.; Wang, T.; Dong, M.; Liu, Y. Genome-wide DNA methylation profiling in infants born to gestational diabetes mellitus. *Diabetes Res. Clin. Pract.* **2018**, *142*, 10–18. [[CrossRef](#)] [[PubMed](#)]
77. El Hajj, N.; Plushch, G.; Schneider, E.; Dittrich, M.; Muller, T.; Korenkov, M.; Aretz, M.; Zechner, U.; Lehnen, H.; Haaf, T. Metabolic programming of MEST DNA methylation by intrauterine exposure to gestational diabetes mellitus. *Diabetes* **2013**, *62*, 1320–1328. [[CrossRef](#)]
78. Shiau, S.; Wang, L.; Liu, H.; Zheng, Y.; Drong, A.; Joyce, B.T.; Wang, J.; Li, W.; Leng, J.; Shen, Y.; et al. Prenatal gestational diabetes mellitus exposure and accelerated offspring DNA methylation age in early childhood. *Epigenetics* **2021**, *16*, 186–195. [[CrossRef](#)] [[PubMed](#)]
79. West, N.A.; Kechris, K.; Dabelea, D. Exposure to Maternal Diabetes in Utero and DNA Methylation Patterns in the Offspring. *Immunometabolism* **2013**, *1*, 1–9. [[CrossRef](#)]
80. Yang, I.V.; Zhang, W.; Davidson, E.J.; Fingerlin, T.E.; Kechris, K.; Dabelea, D. Epigenetic marks of in utero exposure to gestational diabetes and childhood adiposity outcomes: The EPOCH study. *Diabet. Med.* **2018**, *35*, 612–620. [[CrossRef](#)]

81. Crume, T.L.; Ogden, L.; West, N.A.; Vehik, K.S.; Scherzinger, A.; Daniels, S.; McDuffie, R.; Bischoff, K.; Hamman, R.F.; Norris, J.M.; et al. Association of exposure to diabetes in utero with adiposity and fat distribution in a multiethnic population of youth: The Exploring Perinatal Outcomes among Children (EPOCH) Study. *Diabetologia* **2011**, *54*, 87–92. [[CrossRef](#)]
82. Hjort, L.; Martino, D.; Grunnet, L.G.; Naeem, H.; Maksimovic, J.; Olsson, A.H.; Zhang, C.; Ling, C.; Olsen, S.F.; Saffery, R.; et al. Gestational diabetes and maternal obesity are associated with epigenome-wide methylation changes in children. *JCI Insight* **2018**, *3*. [[CrossRef](#)] [[PubMed](#)]
83. Jung, Y.; Goldman, D. Role of RNA modifications in brain and behavior. *Genes Brain Behav.* **2018**, *17*, e12444. [[CrossRef](#)]
84. Lowe, R.; Shirley, N.; Bleackley, M.; Dolan, S.; Shafee, T. Transcriptomics technologies. *PLoS Comput. Biol.* **2017**, *13*, e1005457. [[CrossRef](#)] [[PubMed](#)]
85. Marguerat, S.; Bahler, J. RNA-seq: From technology to biology. *Cell Mol. Life Sci.* **2010**, *67*, 569–579. [[CrossRef](#)]
86. Sozoniuk, M.; Chrobak, L.; Kowalczyk, K.; Kankofer, M. Is it useful to use several “omics” for obtaining valuable results? *Mol. Biol. Rep.* **2019**, *46*. [[CrossRef](#)]
87. Ambra, R.; Manca, S.; Palumbo, M.C.; Leoni, G.; Natarelli, L.; De Marco, A.; Consoli, A.; Pandolfi, A.; Virgili, F. Transcriptome analysis of human primary endothelial cells (HUVEC) from umbilical cords of gestational diabetic mothers reveals candidate sites for an epigenetic modulation of specific gene expression. *Genomics* **2014**, *103*, 337–348. [[CrossRef](#)]
88. Koskinen, A.; Lehtoranta, L.; Laiho, A.; Laine, J.; Kaapa, P.; Soukka, H. Maternal diabetes induces changes in the umbilical cord gene expression. *Placenta* **2015**, *36*, 767–774. [[CrossRef](#)]
89. Casanovas, J.; Jo, Y.; Rao, X.; Xuei, X.; Brown, M.E.; Kua, K.L. High glucose alters fetal rat islet transcriptome and induces progeny islet dysfunction. *J. Endocrinol.* **2019**, *240*, 309–323. [[CrossRef](#)]
90. Inoguchi, Y.; Ichiyonagi, K.; Ohishi, H.; Maeda, Y.; Sonoda, N.; Ogawa, Y.; Inoguchi, T.; Sasaki, H. Poorly controlled diabetes during pregnancy and lactation activates the Foxo1 pathway and causes glucose intolerance in adult offspring. *Sci. Rep.* **2019**, *9*, 10181. [[CrossRef](#)]
91. Backman, M.; Flenkenthaler, F.; Blutke, A.; Dahlhoff, M.; Landstrom, E.; Renner, S.; Philippou-Massier, J.; Krebs, S.; Rathkolb, B.; Prehn, C.; et al. Multi-omics insights into functional alterations of the liver in insulin-deficient diabetes mellitus. *Mol. Metab.* **2019**, *26*, 30–44. [[CrossRef](#)] [[PubMed](#)]
92. Page, K.A.; Luo, S.; Wang, X.; Chow, T.; Alves, J.; Buchanan, T.A.; Xiang, A.H. Children Exposed to Maternal Obesity or Gestational Diabetes Mellitus During Early Fetal Development Have Hypothalamic Alterations that Predict Future Weight Gain. *Diabetes Care* **2019**, *42*, 1473–1480. [[CrossRef](#)] [[PubMed](#)]
93. Camprubi Robles, M.; Campoy, C.; Garcia Fernandez, L.; Lopez-Pedrosa, J.M.; Rueda, R.; Martin, M.J. Maternal Diabetes and Cognitive Performance in the Offspring: A Systematic Review and Meta-Analysis. *PLoS ONE* **2015**, *10*, e0142583. [[CrossRef](#)]
94. Aviel-Shekler, K.; Hamshawi, Y.; Sirhan, W.; Getselter, D.; Srikanth, K.D.; Malka, A.; Piran, R.; Elliott, E. Gestational diabetes induces behavioral and brain gene transcription dysregulation in adult offspring. *Transl. Psychiatry* **2020**, *10*, 412. [[CrossRef](#)] [[PubMed](#)]
95. Money, K.M.; Barke, T.L.; Serezani, A.; Gannon, M.; Garbett, K.A.; Aronoff, D.M.; Mirmics, K. Gestational diabetes exacerbates maternal immune activation effects in the developing brain. *Mol. Psychiatry* **2018**, *23*, 1920–1928. [[CrossRef](#)]
96. Ke, Q.; Costa, M. Hypoxia-inducible factor-1 (HIF-1). *Mol. Pharmacol.* **2006**, *70*, 1469–1480. [[CrossRef](#)] [[PubMed](#)]
97. Cerychova, R.; Bohuslavova, R.; Papousek, F.; Sedmera, D.; Abaffy, P.; Benes, V.; Kolar, F.; Pavlinkova, G. Adverse effects of Hif1a mutation and maternal diabetes on the offspring heart. *Cardiovasc. Diabetol.* **2018**, *17*, 68. [[CrossRef](#)] [[PubMed](#)]
98. Yu, Y.; Arah, O.A.; Liew, Z.; Cnattingius, S.; Olsen, J.; Sorensen, H.T.; Qin, G.; Li, J. Maternal diabetes during pregnancy and early onset of cardiovascular disease in offspring: Population based cohort study with 40 years of follow-up. *BMJ* **2019**, *367*, l6398. [[CrossRef](#)]
99. Preston, C.C.; Larsen, T.D.; Eclow, J.A.; Louwagie, E.J.; Gandy, T.C.T.; Faustino, R.S.; Baack, M.L. Maternal High Fat Diet and Diabetes Disrupts Transcriptomic Pathways That Regulate Cardiac Metabolism and Cell Fate in Newborn Rat Hearts. *Front. Endocrinol.* **2020**, *11*, 570846. [[CrossRef](#)] [[PubMed](#)]
100. Vogel, C.; Marcotte, E.M. Insights into the regulation of protein abundance from proteomic and transcriptomic analyses. *Nat. Rev. Genet.* **2012**, *13*, 227–232. [[CrossRef](#)]
101. Liu, Y.; Beyer, A.; Aebersold, R. On the Dependency of Cellular Protein Levels on mRNA Abundance. *Cell* **2016**, *165*, 535–550. [[CrossRef](#)] [[PubMed](#)]
102. Kopylov, A.; Papysheva, O.; Gribova, I.; Kotaysch, G.; Kharitonova, L.; Mayatskaya, T.; Sokerina, E.; Kaysheva, A.; Morozov, S. Molecular pathophysiology of diabetes mellitus during pregnancy with antenatal complications. *Sci. Rep.* **2020**, *10*, 19641. [[CrossRef](#)] [[PubMed](#)]
103. Miao, Z.; Wang, J.; Wang, F.; Liu, L.; Ding, H.; Shi, Z. Comparative proteomics of umbilical vein blood plasma from normal and gestational diabetes mellitus patients reveals differentially expressed proteins associated with childhood obesity. *Proteom. Clin. Appl.* **2016**, *10*, 1122–1131. [[CrossRef](#)] [[PubMed](#)]
104. Liao, Y.; Xu, G.F.; Jiang, Y.; Zhu, H.; Sun, L.J.; Peng, R.; Luo, Q. Comparative proteomic analysis of maternal peripheral plasma and umbilical venous plasma from normal and gestational diabetes mellitus pregnancies. *Medicine* **2018**, *97*, e12232. [[CrossRef](#)]
105. Kumar, T.R.; Wang, Y.; Lu, N.; Matzuk, M.M. Follicle stimulating hormone is required for ovarian follicle maturation but not male fertility. *Nat. Genet.* **1997**, *15*, 201–204. [[CrossRef](#)] [[PubMed](#)]

106. Clark, K.L.; Talton, O.O.; Ganesan, S.; Schulz, L.C.; Keating, A.F. Developmental origins of ovarian disorder: Impact of maternal lean gestational diabetes on the offspring ovarian proteome in micedagger. *Biol. Reprod.* **2019**, *101*, 771–781. [[CrossRef](#)] [[PubMed](#)]
107. Bouatra, S.; Aziat, F.; Mandal, R.; Guo, A.C.; Wilson, M.R.; Knox, C.; Bjorndahl, T.C.; Krishnamurthy, R.; Saleem, F.; Liu, P.; et al. The human urine metabolome. *PLoS ONE* **2013**, *8*, e73076. [[CrossRef](#)]
108. Roberts, L.D.; Souza, A.L.; Gerszten, R.E.; Clish, C.B. Targeted metabolomics. *Curr. Protoc. Mol. Biol.* **2012**, *98*, 30–32. [[CrossRef](#)]
109. Johnson, C.H.; Ivanisevic, J.; Siuzdak, G. Metabolomics: Beyond biomarkers and towards mechanisms. *Nat. Rev. Mol. Cell Biol.* **2016**, *17*, 451–459. [[CrossRef](#)]
110. Chen, Q.; Francis, E.; Hu, G.; Chen, L. Metabolomic profiling of women with gestational diabetes mellitus and their offspring: Review of metabolomics studies. *J. Diabetes Complicat.* **2018**, *32*, 512–523. [[CrossRef](#)]
111. Berglund, S.K.; Garcia-Valdes, L.; Torres-Espinola, F.J.; Segura, M.T.; Martinez-Zaldivar, C.; Aguilar, M.J.; Agil, A.; Lorente, J.A.; Florido, J.; Padilla, C.; et al. Maternal, fetal and perinatal alterations associated with obesity, overweight and gestational diabetes: An observational cohort study (PREOBE). *BMC Public Health* **2016**, *16*, 207. [[CrossRef](#)]
112. Shokry, E.; Marchioro, L.; Uhl, O.; Bermudez, M.G.; Garcia-Santos, J.A.; Segura, M.T.; Campoy, C.; Koletzko, B. Impact of maternal BMI and gestational diabetes mellitus on maternal and cord blood metabolome: Results from the PREOBE cohort study. *Acta Diabetol.* **2019**, *56*, 421–430. [[CrossRef](#)]
113. Dube, M.C.; Morisset, A.S.; Tchernof, A.; Weisnagel, S.J. Cord blood C-peptide levels relate to the metabolic profile of women with and without gestational diabetes. *Acta Obstet. Gynecol. Scand.* **2012**, *91*, 1469–1473. [[CrossRef](#)]
114. Perng, W.; Ringham, B.M.; Smith, H.A.; Michelotti, G.; Kechris, K.M.; Dabelea, D. A prospective study of associations between in utero exposure to gestational diabetes mellitus and metabolomic profiles during late childhood and adolescence. *Diabetologia* **2020**, *63*, 296–312. [[CrossRef](#)]
115. Ott, R.; Pawlow, X.; Weiss, A.; Hofelich, A.; Herbst, M.; Hummel, N.; Prehn, C.; Adamski, J.; Romisch-Margl, W.; Kastenmuller, G.; et al. Intergenerational Metabolomic Analysis of Mothers with a History of Gestational Diabetes Mellitus and Their Offspring. *Int. J. Mol. Sci.* **2020**, *21*, 9647. [[CrossRef](#)]
116. Shokry, E.; Marchioro, L.; Uhl, O.; Bermudez, M.G.; Garcia-Santos, J.A.; Segura, M.T.; Campoy, C.; Koletzko, B. Transgenerational cycle of obesity and diabetes: Investigating possible metabolic precursors in cord blood from the PREOBE study. *Acta Diabetol.* **2019**, *56*, 1073–1082. [[CrossRef](#)] [[PubMed](#)]
117. Lu, Y.P.; Reichetzer, C.; Prehn, C.; von Websky, K.; Slowinski, T.; Chen, Y.P.; Yin, L.H.; Kleuser, B.; Yang, X.S.; Adamski, J.; et al. Fetal Serum Metabolites Are Independently Associated with Gestational Diabetes Mellitus. *Cell Physiol. Biochem.* **2018**, *45*, 625–638. [[CrossRef](#)] [[PubMed](#)]
118. Cetin, I.; de Santis, M.S.N.; Taricco, E.; Radaelli, T.; Teng, C.; Ronzoni, S.; Spada, E.; Milani, S.; Pardi, G. Maternal and fetal amino acid concentrations in normal pregnancies and in pregnancies with gestational diabetes mellitus. *Am. J. Obstet. Gynecol.* **2005**, *192*, 610–617. [[CrossRef](#)]
119. Ziegler, A.G.; Meier-Stiegen, F.; Winkler, C.; Bonifacio, E. Prospective evaluation of risk factors for the development of islet autoimmunity and type 1 diabetes during puberty—TEENDIAB: Study design. *Pediatr. Diabetes* **2012**, *13*, 419–424. [[CrossRef](#)]
120. Ziegler, A.G.; Hummel, M.; Schenker, M.; Bonifacio, E. Autoantibody appearance and risk for development of childhood diabetes in offspring of parents with type 1 diabetes: The 2-year analysis of the German BABYDIAB Study. *Diabetes* **1999**, *48*, 460–468. [[CrossRef](#)] [[PubMed](#)]
121. Pitchika, A.; Jolink, M.; Winkler, C.; Hummel, S.; Hummel, N.; Krumsiek, J.; Kastenmuller, G.; Raab, J.; Kordonouri, O.; Ziegler, A.G.; et al. Associations of maternal type 1 diabetes with childhood adiposity and metabolic health in the offspring: A prospective cohort study. *Diabetologia* **2018**, *61*, 2319–2332. [[CrossRef](#)]
122. Lowe, W.L., Jr.; Bain, J.R.; Nodzinski, M.; Reisetter, A.C.; Muehlbauer, M.J.; Stevens, R.D.; Ilkayeva, O.R.; Lowe, L.P.; Metzger, B.E.; Newgard, C.B.; et al. Maternal BMI and Glycemia Impact the Fetal Metabolome. *Diabetes Care* **2017**, *40*, 902–910. [[CrossRef](#)]
123. Walejko, J.M.; Chelliah, A.; Keller-Wood, M.; Wasserfall, C.; Atkinson, M.; Gregg, A.; Edison, A.S. Diabetes Leads to Alterations in Normal Metabolic Transitions of Pregnancy as Revealed by Time-Course Metabolomics. *Metabolites* **2020**, *10*, 350. [[CrossRef](#)]
124. Peng, S.; Zhang, J.; Liu, L.; Zhang, X.; Huang, Q.; Alamdar, A.; Tian, M.; Shen, H. Newborn meconium and urinary metabolome response to maternal gestational diabetes mellitus: A preliminary case-control study. *J. Proteome Res.* **2015**, *14*, 1799–1809. [[CrossRef](#)]
125. Graca, G.; Goodfellow, B.J.; Barros, A.S.; Diaz, S.; Duarte, I.F.; Spagou, K.; Veselkov, K.; Want, E.J.; Lindon, J.C.; Carreira, I.M.; et al. UPLC-MS metabolic profiling of second trimester amniotic fluid and maternal urine and comparison with NMR spectral profiling for the identification of pregnancy disorder biomarkers. *Mol. Biosyst.* **2012**, *8*, 1243–1254. [[CrossRef](#)]
126. Underwood, M.A.; Gilbert, W.M.; Sherman, M.P. Amniotic Fluid: Not Just Fetal Urine Anymore. *J. Perinatol.* **2005**, *25*, 341–348. [[CrossRef](#)]
127. Zhao, C.; Ge, J.; Li, X.; Jiao, R.; Li, Y.; Quan, H.; Li, J.; Guo, Q.; Wang, W. Integrated metabolome analysis reveals novel connections between maternal fecal metabolome and the neonatal blood metabolome in women with gestational diabetes mellitus. *Sci. Rep.* **2020**, *10*, 3660. [[CrossRef](#)] [[PubMed](#)]
128. Isganaitis, E.; Woo, M.; Ma, H.; Chen, M.; Kong, W.; Lytras, A.; Sales, V.; Decoste-Lopez, J.; Lee, K.J.; Leatherwood, C.; et al. Developmental programming by maternal insulin resistance: Hyperinsulinemia, glucose intolerance, and dysregulated lipid metabolism in male offspring of insulin-resistant mice. *Diabetes* **2014**, *63*, 688–700. [[CrossRef](#)] [[PubMed](#)]

129. Pereira, T.J.; Fonseca, M.A.; Campbell, K.E.; Moyce, B.L.; Cole, L.K.; Hatch, G.M.; Doucette, C.A.; Klein, J.; Aliani, M.; Dolinsky, V.W. Maternal obesity characterized by gestational diabetes increases the susceptibility of rat offspring to hepatic steatosis via a disrupted liver metabolome. *J. Physiol.* **2015**, *593*, 3181–3197. [[CrossRef](#)]
130. Renner, S.; Martins, A.S.; Streckel, E.; Braun-Reichhart, C.; Backman, M.; Prehn, C.; Klymiuk, N.; Bahr, A.; Blutke, A.; Landbrecht-Schessl, C.; et al. Mild maternal hyperglycemia in INS (C93S) transgenic pigs causes impaired glucose tolerance and metabolic alterations in neonatal offspring. *Dis. Model. Mech.* **2019**, *12*. [[CrossRef](#)]
131. Kumar, P.S. Microbiomics: Were we all wrong before? *Periodontology 2000* **2021**, *85*, 8–11. [[CrossRef](#)] [[PubMed](#)]
132. Berg, G.; Rybakova, D.; Fischer, D.; Cernava, T.; Vergès, M.-C.C.; Charles, T.; Chen, X.; Cocolin, L.; Eversole, K.; Corral, G.H.; et al. Microbiome definition re-visited: Old concepts and new challenges. *Microbiome* **2020**, *8*, 103. [[CrossRef](#)]
133. Walker, R.W.; Clemente, J.C.; Peter, I.; Loos, R.J.F. The prenatal gut microbiome: Are we colonized with bacteria in utero? *Pediatr. Obes.* **2017**, *12* (Suppl. 1), 3–17. [[CrossRef](#)]
134. Han, S.; Ellberg, C.C.; Olomu, I.N.; Vyas, A.K. Gestational microbiome: Metabolic perturbations and developmental programming. *Reproduction* **2021**, *162*, R85–R98. [[CrossRef](#)]
135. Ponzo, V.; Ferrocino, I.; Zarovska, A.; Amenta, M.B.; Leone, F.; Monzeglio, C.; Rosato, R.; Pellegrini, M.; Gambino, R.; Cassader, M.; et al. The microbiota composition of the offspring of patients with gestational diabetes mellitus (GDM). *PLoS ONE* **2019**, *14*, e0226545. [[CrossRef](#)] [[PubMed](#)]
136. Soderborg, T.K.; Carpenter, C.M.; Janssen, R.C.; Weir, T.L.; Robertson, C.E.; Ir, D.; Young, B.E.; Krebs, N.F.; Hernandez, T.L.; Barbour, L.A.; et al. Gestational Diabetes Is Uniquely Associated With Altered Early Seeding of the Infant Gut Microbiota. *Front. Endocrinol.* **2020**, *11*. [[CrossRef](#)]
137. Hu, J.; Nomura, Y.; Bashir, A.; Fernandez-Hernandez, H.; Itzkowitz, S.; Pei, Z.; Stone, J.; Loudon, H.; Peter, I. Diversified microbiota of meconium is affected by maternal diabetes status. *PLoS ONE* **2013**, *8*, e78257. [[CrossRef](#)]
138. Su, M.; Nie, Y.; Shao, R.; Duan, S.; Jiang, Y.; Wang, M.; Xing, Z.; Sun, Q.; Liu, X.; Xu, W. Diversified gut microbiota in newborns of mothers with gestational diabetes mellitus. *PLoS ONE* **2018**, *13*, e0205695. [[CrossRef](#)]
139. Le Chatelier, E.; Nielsen, T.; Qin, J.; Pridfti, E.; Hildebrand, F.; Falony, G.; Almeida, M.; Arumugam, M.; Batto, J.-M.; Kennedy, S.; et al. Richness of human gut microbiome correlates with metabolic markers. *Nature* **2013**, *500*, 541–546. [[CrossRef](#)] [[PubMed](#)]
140. Crusell, M.K.W.; Hansen, T.H.; Nielsen, T.; Allin, K.H.; Rühlemann, M.C.; Damm, P.; Vestergaard, H.; Rørbye, C.; Jørgensen, N.R.; Christiansen, O.B.; et al. Comparative Studies of the Gut Microbiota in the Offspring of Mothers With and Without Gestational Diabetes. *Front. Cell. Infect. Microbiol.* **2020**, *10*. [[CrossRef](#)] [[PubMed](#)]
141. Hasan, S.; Aho, V.; Pereira, P.; Paulin, L.; Koivusalo, S.B.; Auvinen, P.; Eriksson, J.G. Gut microbiome in gestational diabetes: A cross-sectional study of mothers and offspring 5 years postpartum. *Acta Obstet. Gynecol. Scand.* **2018**, *97*, 38–46. [[CrossRef](#)] [[PubMed](#)]
142. Crusell, M.K.W.; Hansen, T.H.; Nielsen, T.; Allin, K.H.; Rühlemann, M.C.; Damm, P.; Vestergaard, H.; Rørbye, C.; Jørgensen, N.R.; Christiansen, O.B.; et al. Gestational diabetes is associated with change in the gut microbiota composition in third trimester of pregnancy and postpartum. *Microbiome* **2018**, *6*, 89. [[CrossRef](#)] [[PubMed](#)]
143. Kato, H.; Takahashi, S.; Saito, K. Omics and integrated omics for the promotion of food and nutrition science. *J. Tradit. Complement. Med.* **2011**, *1*, 25–30. [[CrossRef](#)]
144. Ren, X.; Li, X. Advances in Research on Diabetes by Human Nutriomics. *Int. J. Mol. Sci.* **2019**, *20*, 5375. [[CrossRef](#)]
145. Soh, S.E.; Tint, M.T.; Gluckman, P.D.; Godfrey, K.M.; Rifkin-Graboi, A.; Chan, Y.H.; Stünkel, W.; Holbrook, J.D.; Kwek, K.; Chong, Y.S.; et al. Cohort profile: Growing Up in Singapore Towards healthy Outcomes (GUSTO) birth cohort study. *Int. J. Epidemiol.* **2014**, *43*, 1401–1409. [[CrossRef](#)]

2.1.2. Previous studies on effects of maternal hyperglycemia on offspring using transgenic animal models

Animal models expressing mutant insulin allow the modelling of effects of isolated maternal hyperglycemia without confounding obesity on offspring and provide insights into pre-conceptual diabetes mellitus (PCDM) [47]. Several studies used offspring born to the Akita mice model, which bears an autosomal dominant mutation causing chronic hypoinsulinemia and hyperglycemia. Chang et al. showed marked size reduction and delayed maturation of preovulatory oocytes in Akita mice when compared with control animals. Furthermore, histological evaluation revealed smaller and less developed ovarian follicles and an increased number of apoptotic foci. The authors proposed that smaller follicle and oocyte sizes may reflect abnormal cell growth and survival [48]. At postnatal day 2 wild-type offspring born to Akita mice had higher transcript levels of several nephron progenitor markers. At postnatal day 34 the total nephron numbers were decreased by around 20% (compared to controls). Additionally, the number of early-developing nephrons was reduced, together with decreased expression of the intracellular domain of Notch1 and the canonical Wnt target lymphoid enhancer binding factor 1. The authors concluded that *in utero* exposure to maternal diabetes impairs the differentiation of nephron progenitors into nephrons, potentially by repression of the Notch and Wnt/ β -catenin signalling pathways [49]. Grasmann et al. investigated the effect of parental diabetes in offspring born to Akita mice. Offspring of parental diabetes had impaired glucose tolerance. Furthermore, lower body weight alongside lower whole-body bone mineral density and trabecular bone mass was observed. Interestingly, the magnitude of phenotypic changes in offspring caused by maternal and paternal diabetes differed. Furthermore, metabolic alterations were in general more severe in male offspring of maternal diabetes. Female wildtype offspring of diabetic fathers were the least affected [50]. Metabolic alterations, specifically changes in myocardial triglyceride homeostasis, were observed in wild-type offspring of Akita mice. The transcript levels of genes involved in lipid metabolism genes (peroxisomal proliferator-activated receptor α , lipoprotein lipase, fatty acid translocase, and fatty acid transport protein 1) were reduced. Furthermore, their expression levels were highly correlated, suggestive of orchestrated down-regulation. The authors showed that maternal diabetes in

Ins2^{Akita} mice offspring does not cause cardiac hypertrophy or triglycerides accumulation in the fetal heart, possibly because of a coordinated down-regulation of genes to protect against increased myocardial fatty acid uptake [51].

Although studies from mice pups provide valuable insights into maternally induced alterations, mice offspring are born at a less mature stage than human offspring. Therefore, the influence of maternal diabetes in the second half of pregnancy is difficult to model in rodents. Conversely, similar to human babies, piglets are born in a more mature state compared to rodent pups and are therefore also exposed to maternal glycemia in a later developmental phase [52]. Additionally, pig and human embryos share similarities in the timing of embryonic genome activation and in metabolic characteristics [47]. Furthermore, changes in energy metabolism during both normal and pathological birth occur similarly in pigs and humans (reviewed in [11]). Renner et al. developed a transgenic pig model expressing mutant insulin C93S in pancreatic β cells. This model allows to study an isolated maternal hyperglycemia without confounding obesity during pregnancy. The authors found increased concentrations of lysine and α -aminoadipic acid, as well as phospholipids, in piglets born to diabetic mothers. Furthermore, the ratio of total and short-chain acylcarnitines to carnitine was elevated, indicating an increased import of fatty acids into mitochondria and an increased β -oxidation. Overall, it was shown that maternal hyperglycemia, even in the absence of maternal and neonatal obesity was associated with alterations in the neonatal offspring's plasma metabolome [41]. Molecular profiling of plasma provides a global picture of whole-body metabolism. However, the investigation of different organs is crucial to reveal the tissue-specific manifestations of developmental programming of maternal diabetes. In the context of metabolic alterations, the liver is highly relevant as it is a key metabolic hub of the organism. Comparative studies revealed high anatomic and functional similarities between pig and human liver [53, 54], making the pig a suitable model to recapitulate various human liver conditions.

2.2. Article 2

This chapter contains research article published in *Molecular Metabolism* (2023) with the title:

Maternal hyperglycemia induces alterations in hepatic amino acid, glucose and lipid metabolism of neonatal offspring: Multi-omics insights from a diabetic pig model

Bachuki Shashikadze, Libera Valla, Salvo Danilo Lombardo, Cornelia Prehn, Mark Haid, Fabien Riols, Jan Bernd Stöckl, Radwa Elkhateib, Simone Renner, Birgit Rathkolb, Jörg Menche, Martin Hrabě de Angelis, Eckhard Wolf, Elisabeth Kemter, Thomas Fröhlich

Author contributions:

B.S., L.V., E.W., E.K. and T.F.: Conceptualization; B.S.: Methodology, Software, Data curation and analysis, Writing- Original draft; B.S., L.V., S.D.L., R.E., B.R., J.M. and M.H.d.A.: Investigation; C.P., F.R., M.H.: Metabolomics measurements; L.V., S.D.L., J.B.S., S.R., E.W., E.K. and T.F.: Writing- Reviewing and Editing; E.W., E.K. and T.F.: Supervision, Resources, Funding acquisition

Maternal hyperglycemia induces alterations in hepatic amino acid, glucose and lipid metabolism of neonatal offspring: Multi-omics insights from a diabetic pig model



Bachuki Shashikadze¹, Libera Valla^{2,3}, Salvo Danilo Lombardo^{4,5,6}, Cornelia Prehn⁷, Mark Haid⁷, Fabien Riols⁷, Jan Bernd Stöckl¹, Radwa Elkhateib¹, Simone Renner^{2,8,9}, Birgit Rathkolb^{2,8,10}, Jörg Menche^{4,5,8,11}, Martin Hrabě de Angelis^{8,10,12}, Eckhard Wolf^{1,2,8,9}, Elisabeth Kemter^{2,8,9,13,**}, Thomas Fröhlich^{1,13,*}

ABSTRACT

Objective: To gain mechanistic insights into adverse effects of maternal hyperglycemia on the liver of neonates, we performed a multi-omics analysis of liver tissue from piglets developed in genetically diabetic (mutant *INS* gene induced diabetes of youth; MIDY) or wild-type (WT) pigs. **Methods:** Proteome, metabolome and lipidome profiles of liver and clinical parameters of serum samples from 3-day-old WT piglets (n = 9) born to MIDY mothers (PHG) were compared with those of WT piglets (n = 10) born to normoglycemic mothers (PNG). Furthermore, protein–protein interaction network analysis was used to reveal highly interacting proteins that participate in the same molecular mechanisms and to relate these mechanisms with human pathology.

Results: Hepatocytes of PHG displayed pronounced lipid droplet accumulation, although the abundances of central lipogenic enzymes such as fatty acid-synthase (FASN) were decreased. Additionally, circulating triglyceride (TG) levels were reduced as a trend. Serum levels of non-esterified free fatty acids (NEFA) were elevated in PHG, potentially stimulating hepatic gluconeogenesis. This is supported by elevated hepatic phosphoenolpyruvate carboxykinase (PCK1) and circulating alanine transaminase (ALT) levels. Even though targeted metabolomics showed strongly elevated phosphatidylcholine (PC) levels, the abundances of multiple key enzymes involved in major PC synthesis pathways — most prominently those from the Kennedy pathway — were paradoxically reduced in PHG liver. Conversely, enzymes involved in PC excretion and breakdown such as PC-specific translocase ATP-binding cassette 4 (ABCB4) and phospholipase A2 were increased in abundance.

Conclusions: Our study indicates that maternal hyperglycemia without confounding obesity induces profound molecular changes in the liver of neonatal offspring. In particular, we found evidence for stimulated gluconeogenesis and hepatic lipid accumulation independent of *de novo* lipogenesis. Reduced levels of PC biosynthesis enzymes and increased levels of proteins involved in PC translocation or breakdown may represent counter-regulatory mechanisms to maternally elevated PC levels. Our comprehensive multi-omics dataset provides a valuable resource for future meta-analysis studies focusing on liver metabolism in newborns from diabetic mothers.

© 2023 The Authors. Published by Elsevier GmbH. This is an open access article under the CC BY license (<http://creativecommons.org/licenses/by/4.0/>).

Keywords Maternal diabetes; Neonates; Liver; Pig model; Proteomics; Metabolomics; Protein–protein interaction; Clinical parameters

¹Laboratory for Functional Genome Analysis (LAFUGA), Gene Center, LMU Munich, 81377 Munich, Germany ²Molecular Animal Breeding and Biotechnology, Gene Center and Department of Veterinary Sciences, LMU Munich, 81377 Munich, Germany ³MWM Biomodels GmbH, 84184 Tiefenbach, Germany ⁴Max Perutz Labs, Vienna Biocenter Campus (VBC), 1030 Vienna, Austria ⁵University of Vienna, Center for Molecular Biology, Department of Structural and Computational Biology, 1030 Vienna, Austria ⁶CeMM Research Center for Molecular Medicine of the Austrian Academy of Sciences, 1090 Vienna, Austria ⁷Metabolomics and Proteomics Core (MPC), Helmholtz Zentrum München, 85764 Neuherberg, Germany ⁸German Center for Diabetes Research (DZD), 85764 Neuherberg, Germany ⁹Center for Innovative Medical Models (CIMM), LMU Munich, 85764 Oberschleißheim, Germany ¹⁰Institute of Experimental Genetics, German Mouse Clinic, Helmholtz Munich, 85764 Neuherberg, Germany ¹¹University of Vienna, Faculty of Mathematics, 1090 Vienna, Austria ¹²Experimental Genetics, School of Life Science Weihenstephan, Technische Universität München, 85354 Freising, Germany

¹³ Contributed equally.

*Corresponding author. Gene Center, LMU Munich, Feodor-Lynen-Str. 25, 81377 Munich, Germany. E-mail: fröhlich@genzentrum.lmu.de (T. Fröhlich).

**Corresponding author. Gene Center, LMU Munich, Feodor-Lynen-Str. 25, 81377 Munich, Germany. E-mail: kemter@genzentrum.lmu.de (E. Kemter).

Received March 2, 2023 • Revision received June 12, 2023 • Accepted June 29, 2023 • Available online 4 July 2023

<https://doi.org/10.1016/j.molmet.2023.101768>

Original Article

Abbreviations			
AGC	automatic gain control	MF	molecular function
BGC	blood glucose concentration	MIDY	mutant <i>INS</i> gene induced diabetes of youth
BP	biological process	NAFLD	non-alcoholic fatty liver disease
CC	cellular component	NCE	normalized collision energy
CIA	co-inertia analysis	NEFA	non-esterified free fatty acids
DIA	data independent acquisition	OPLS-DA	orthogonal projection to latent structures discriminant analysis
DNL	<i>de novo</i> lipogenesis	ORA	over-representation analysis
GDA	gene-disease association	PC	phosphatidylcholine
GDM	gestational diabetes mellitus	PCA	principal component analysis
GO	gene ontology	PE	phosphatidylethanolamine
GPF	gas phase fractionation	PHG	wild-type piglet born to transgenic hyperglycemic pig
GWAS	genome-wide association studies	PNG	wild-type piglet born to normoglycemic pig
HOMA-IR	homeostatic model assessment for insulin resistance	PPI	protein-protein interaction network
KEGG	Kyoto Encyclopedia of Genes and Genomes	QUICKI	quantitative insulin sensitivity check index
LC-MS/MS	nano-liquid chromatography–tandem mass spectrometry analysis	SIDD	severe insulin deficient diabetes
LOOCV	leave-one-out cross-validation	SM	sphingolipid
		TG	triglyceride
		VIP	variance importance in projection
		WT	wild-type

1. INTRODUCTION

A disturbed prenatal environment is considered a risk factor for health complications in offspring [1]. The environment of the developing fetus is influenced by an altered maternal nutritional and metabolic state [2,3]. For example, *in utero* exposure to elevated maternal glucose can trigger long-term consequences in the physiology and metabolism of the offspring [4]. Offspring of mothers with gestational diabetes mellitus (GDM) have a fourfold increased risk of developing a metabolic syndrome [5]. So far, hyperglycemia-related fetal programming has been mainly investigated by epidemiological studies and reports at the molecular level are scarce. Furthermore, human patient data have the drawback that confounding factors, such as the mother's lifestyle and medical history, are frequently not completely recorded. On the other hand, animal models living in controlled laboratory conditions with standardized tissue sampling [6] allow differentiating the sole consequences of maternal hyperglycemia from those of comorbidities. The pig is a promising large animal model to fill the gap between proof-of-concept studies and clinical trials [7–9]. In the context of diabetes and pregnancy, it is worth mentioning that pig offspring, similar to human babies, are born in a more mature state compared to rodent pups and are therefore also exposed to maternal glycemia in a later developmental phase [10]. Furthermore, piglets show similarities to human physiology in terms of changes in energy metabolism during both normal and pathological birth (reviewed in [11]). Since the liver is responsible for maintaining normal blood glucose levels alongside the homeostasis of other relevant metabolites such as lipids and amino acids [12], it is especially relevant for the consequences of maternal diabetes on offspring. Furthermore, as a major metabolic organ, the liver is highly relevant in the context of metabolic syndromes. Interestingly, previous studies of both human cohorts and rodent models suggest that maternal diabetes may be associated with offspring markers of liver pathology mainly related to an aberrant lipid metabolism [13–17]. The involvement of metabolic organs in neonatal complications is further suggested by the study of Renner et al. where it was found that maternal hyperglycemia, even in the absence of maternal and neonatal obesity, was associated with alterations in the neonatal offspring's plasma metabolome (such as amino acids and lipids) [18]. The detection of molecular changes induced by prenatal exposure to maternal hyperglycemia and underlying biological

pathways could provide the basis for novel intervention strategies which could have far-reaching implications for child health care. In this study, we address hepatic proteome and metabolome alterations alongside clinical-chemical changes and histomorphological findings in piglets developed in genetically hyperglycemic *INS*^{C94Y} transgenic pigs, a model for mutant *INS* gene induced diabetes of youth (MIDY) [19].

2. MATERIALS AND METHODS

2.1. Biological samples

In this study, the hepatic proteome, metabolome as well as clinical-chemical parameters in serum from 3-day-old wild-type (WT) piglets born to hyperglycemic mothers (PHG) expressing the mutant insulin C94Y [19] were compared to the profiles of WT piglets born to normoglycemic mothers (PNG). To further complement molecular findings histomorphological evaluation of the liver was performed. The hyperglycemic *INS*^{C94Y} transgenic pig model was obtained using the *INS*^{C94Y} expression vector, including the porcine *INS* gene with a point mutation introducing a Cys → Tyr exchange in position 94, which disrupts one of the two disulfide bonds between the A- and B-chain of the mature insulin molecule. This generates a misfolded insulin protein that induces endoplasmic reticulum stress in the β-cells, resulting in early-onset permanent insulin-deficient diabetes mellitus and β-cell loss [19]. The non-diabetic and diabetic sows used in this project were half-siblings produced by mating a diabetic boar with different WT sows. The piglets of the PHG and PNG groups were derived from mating of non-diabetic and diabetic sows with the same WT boar, reducing genetic variance. The diabetic sows were treated daily with a combination of long-acting and short-acting insulin, to ensure a blood glucose concentration (BGC) in a physiological range (around 150 mg/dL). This physiological range was maintained in the diabetic sows also during the mating and during the first 3 weeks of pregnancy to ensure the pregnancy state. After this period, the amount of insulin administered was reduced, to obtain a BGC of around 300 mg/dL, which corresponds to a pathological diabetic situation during pregnancy. 30 min after birth and before first milk intake, blood glucose of newborn piglets was measured by ear vein puncture using a glucometer (FreeStyle-Freedom Lite). In addition, venous EDTA plasma samples of offspring were collected, stored at –80 °C for determination of insulin

concentration. Sows were housed in groups under control conditions, with free access to water and fed with commercial food once per day. Shortly before giving birth, sows were separated into a separate pen in the farrowing unit. Newborn piglets were housed in the farrowing pen together with the mother, and a heated nest was offered to the piglets. At an age of 3 days, non-fasted piglets underwent necropsy. Tissues were collected by random systematic sampling [6], shock-frozen on dry ice and stored at -80°C until analysis. For omics analyses, all samples were processed in parallel to avoid possible bias related to different storage times. All experiments were performed according to the German Animal Welfare Act (Deutsches Tierschutzgesetz), following the ARRIVE guidelines and Directive 2010/63/EU.

2.2. Proteomics

2.2.1. Sample preparation

Frozen liver tissue samples were transferred into prechilled tubes and cryo-pulverized in a CPO2 Automated Dry Pulverizer (Covaris, Woburn, MA, USA) using an impact level of 3 according to the manufacturer's instructions. Powdered tissue was lysed in 8 M urea/0.5 M ammonium bicarbonate (Roche Diagnostics, Mannheim, Germany) by ultrasonication (18 cycles of 10 s) using a Sonopuls HD3200 (Bandelin, Berlin, Germany). Pierce 660 nm Protein Assay (Thermo Fisher Scientific, Rockford, IL, USA) was used for protein quantification. 20 μL of lysate containing 20 μg of protein were processed for digestion. Disulfide bonds were reduced with 45 mM dithiothreitol/20 mM tris(2-carboxyethyl) phosphine (30 min, 56°C). Reduced cysteine side chains were alkylated by adding 100 mM iodoacetamide (30 min, room temperature), followed by quenching the remaining iodoacetamide with dithiothreitol (90 mM, 15 min, room temperature). Sequential 2-step digestion was performed, firstly with Lys-C (FUJIFILM Wako Chemicals Europe GmbH, Neuss, Germany) for 4 h (1:50 enzyme to protein ratio) and subsequently with modified porcine trypsin (Promega, Madison, WI, USA) for 16 h at 37°C (1:50 enzyme to protein ratio). After digestion, samples were dried before analysis using a vacuum centrifuge.

2.2.2. Nano-liquid chromatography–tandem mass spectrometry analysis

Nano-liquid chromatography–tandem mass spectrometry (LC-MS/MS) analysis was performed on an UltiMate 3000 nano-LC system coupled to a Q Exactive HF-X Orbitrap mass spectrometer via a nano-electrospray ion source (all Thermo Fisher Scientific). 1 μg of peptides were transferred to a PepMap 100 C18 trap column (100 $\mu\text{m} \times 2\text{ cm}$, 5 μM particles, Thermo Fisher Scientific) and separated on an analytical column (PepMap RSLC C18, 75 $\mu\text{m} \times 50\text{ cm}$, 2 μm particles, Thermo Fisher Scientific) at 250 nL/min with an 80-min gradient of 5–20% of solvent B followed by a 9-min increase to 40%. After the gradient, the column was washed with 85% solvent B for 9 min, followed by 10-min re-equilibration with 3% solvent B. Mobile phases A and B were 99.9/0.1% water/formic acid (v/v) and 99.9/0.1% acetonitrile/formic acid (v/v), respectively. Gas phase fractionation (GPF)-based chromatogram libraries [20] were built using 6 injections of pooled samples with $25 \times 4\text{ m/z}$ -wide data-independent acquisition (DIA) (30,000 resolution, AGC target $1\text{e}6$ maximum inject time 55 ms, NCE 27, +3H assumed charge state) spectra using a staggered window pattern with window placements optimized by Skyline (v.22.2) (i.e. 400.43–502.48, 500.48–602.52, 600.52–702.57, 700.57–802.61, 800.61–902.66, 900.66–1002.70), yielding $300 \times 2\text{ m/z}$ -wide windows spanning from 400 to 1000 m/z after deconvolution. For DIA measurements, $50 \times 12\text{ m/z}$ -wide (in the range of 400–1000 m/z)

precursor isolation window DIA spectra (15,000 resolution, AGC target $1\text{e}6$, maximum inject time 20 ms, NCE 27) was acquired as described in [21] using a staggered window pattern [22]. Window placements were calculated by Skyline software [23]. Precursor spectra (in the range of 390–1010 m/z , 60,000 resolution, AGC target $1\text{e}6$, max IIT 60 ms, +3H assumed charge state) were interspersed every 50 MS/MS spectra.

2.2.3. Peptide and protein identification and quantification

Protein intensities were extracted from the DIA data using predicted spectral libraries generated by DIA-NN's (v1.8.1) built-in deep-learning-based spectra and retention time predictor which was further refined by the experimental data from project-specific GPF-based library (also generated by DIA-NN). For this, the *Sus scrofa* protein database (UniProt Reference Proteome – Taxonomy 9823 – Proteome ID UP000008227, 49,792 entries) alongside the MaxQuant contaminants fasta file [24] were used. Only tryptic peptides with a maximum of one missed cleavage and charge state of +2, +3 and +4 were considered. Cysteine carbamidomethylation was selected as a fixed modification and the quantification strategy was set to robust LC (high precision mode). Retention time correction was performed automatically by DIA-NN and quantification strategy was set to Robust LC (high accuracy mode). Similarly, mass tolerance was determined automatically by DIA-NN and was set to 9 ppm and 18 ppm for MS1 and MS2, respectively. The "Genes" column was used to count unique proteins. All other settings were left default. DIA-NN's main output containing precursor level data was used for the downstream analysis in R using custom scripts. Briefly, the output was filtered at 1% false-discovery rate, using both global and run-specific q-values for precursors and global q-values for protein groups. Peptides derived from potential contaminants, non-proteotypic peptides and peptides with a low signal quality were removed. Precursor intensities for different charge states were summed to derive peptide intensities. Normalization of raw intensities was performed using the MaxLFQ algorithm [25]. Proteins detected in at least 60% of all replicates were kept for quantitative analysis. To handle missing values, data imputation was performed using a random forest algorithm with the R package *MissForest* [26].

2.2.4. Western blot quantification

Powdered liver tissue was lysed in Laemmli extraction buffer supplemented with protease and phosphatase inhibitors (Complete®, Sigma-Aldrich) and protein concentration was determined by BCA assay. Equal amount of denatured tissue lysate per lane was separated on SDS-polyacrylamide minigels and blotted on PVDF membranes. Equal loading was controlled by Ponceau staining. The following primary antibodies were used: rabbit polyclonal antibody against ALDH1L2 (no. 21391-1-AP, dilution 1:4000, proteintech), rabbit polyclonal antibody against claudin 15 (no. 38-9200, dilution 1:1000, Thermo Scientific), rabbit polyclonal antibody against RAB3D (no. 12320-1-AP, dilution 1:1500, proteintech), and mouse monoclonal antibody against pan-actin (no. MAB1501, dilution 1:40,000; Sigma Aldrich). As secondary antibodies, HRP-labeled goat polyclonal antibody against rabbit IgG (no. 7074, dilution 1:2,000, Cell Signaling) and HRP-labeled goat polyclonal antibody against mouse IgG (no. 115-035-146, dilution 1:10,000, Jackson ImmunoResearch), respectively, were used. Bound antibodies were visualized using SuperSignal™ ECL reagents (Thermo Fisher Scientific) and ECL ChemoStar Imager (INTAS). Stripping was done to analyze ratio of various protein abundances and the reference protein. Therefore, membranes were incubated with the stripping buffer (2% SDS, 62.5 mM Tris/HCl, pH 6.7, and 100 mM

Original Article

beta-mercaptoethanol) for 60 min at 70 °C. Afterward, membranes were washed, blocked, and incubated with the next primary antibody. Signal intensities were quantified using ImageQuant (GE Healthcare). Standardization of equal loading was referred to the signal intensities of pan-actin of the corresponding PVDF membrane. Data are shown as mean \pm SD.

2.2.5. STRING network construction and characteristics

The pig-specific and human-specific networks were downloaded from STRING database v11.5 (<https://string-db.org/>) [27]. This large database includes several sources of information grouped in 7 evidence channels: neighborhood, fusion, co-occurrence, co-expression, experiments, knowledge, and text-mining. Each of these sources reflects different information (i.e. computational prediction of protein proximity, protein expression, literature knowledge) and contributes to obtaining a combined score. This is a metric that considers the probability of different evidence channels and corrects for the probability of randomly observing an interaction between two proteins. In both pig and human, we took into consideration 4 possible networks: full, full with high confidence interactions (combined score >0.7), physical (direct interactions only), and physical with high confidence (direct interactions and combined score >0.7). Based on the network connectivity of the differentially abundant proteins, we decided to proceed with our analyses with the full network and high-confidence interactions, resulting in 15,360 nodes with 170,244 edges for pigs and 16,793 proteins with 251,982 edges in humans.

2.2.6. Mapping of dysregulated proteins in the PPIs networks

For this aim, we selected those proteins with adjusted p-value ≤ 0.05 and fold-change ≥ 1.5 and mapped them on the pig- and human-specific protein–protein interactions (PPI). For each network, we calculated the percentage coverage and the network connectivity distinguishing between up-regulated, down-regulated, and total differentially abundant proteins (Supplementary Figs. 1A–D). Network connectivity was calculated by computing a z-score of the largest connected component for each group of proteins and comparing it against 10,000 randomly selected protein sets of the same size.

2.2.7. Identification and biological characterization of dysregulated proteins core

We checked whether each connected component among the up-regulated and down-regulated proteins would be statistically significant in pigs and in humans. Once we extracted the main cores among the up- and down-regulated proteins, we identified expanded networks that would connect at least 90% of the up- and down-regulated proteins respectively, including their interacting proteins. For this purpose, we have used a random walk with restart algorithm, setting the restarting parameter, alpha, equal to 0.9, ensuring that the propagation would remain close to the original set of seed genes. We expanded the seed genes (up- and down-regulated proteins) until 90% would be connected. The biological characterization of the protein cores and the expanded networks was performed by enrichment analyses for the three main branches of the gene ontology (GO) [28] biological processes (BP), molecular functions (MF), and cellular components (CC), and for Kyoto Encyclopedia of Genes and Genomes (KEGG) pathway [29] using GSEAPY [30].

2.2.8. Disease relationship

Disease gene associations were retrieved from DisGeNet [31] which represents the largest publicly available collections of genes and variants associated with human diseases, including expert-curated

associations from genome-wide association studies (GWAS) catalogues, animal models and scientific literature. Depending on the accuracy of the type of information, each gene–disease association is attributed with a gene–disease association (GDA) score that ranges from 0 to 1. We selected associations with a GDA score >0.3 , retrieving information for 11,099 diseases. The relationship between each set of differentially abundant proteins (s1) and set of disease proteins (s2) was then computed in two different ways: 1) by calculating their Jaccard index ($\text{intersection}(s1,s2)/\text{union}(s1,s2)$), and by network proximity of the two sets [32]. Network proximity computes the closest distance between two sets of proteins in a network and by comparing it against 10,000 random sets of similar topological features. In this way, we considered and corrected for interactome biases such as the heavy-tail degree distribution and the discretization of other common network distances like the shortest path.

2.3. Targeted metabolomics

Targeted metabolomics measurements were performed using liquid chromatography- and flow injection-electrospray ionization-tandem mass spectrometry (LC- and FIA-ESI-MS/MS) and the Absolute/*IQ*TM p180 Kit (BIOCRATES Life Sciences AG, Innsbruck, Austria). The assay allows simultaneous quantification of 188 metabolites. For the LC-part, compounds were identified and quantified based on scheduled multiple reaction monitoring measurements (sMRM), for the FIA-part on MRM. The complete assay procedures as well as the tissue extraction have been previously published [33]. In brief, tissue homogenates were always prepared freshly as follows: frozen porcine liver tissue samples were weighed into homogenization tubes with ceramic beads (1.4 mm). For metabolite extraction, to each 1 mg of frozen porcine liver tissue 3 μ L of a cooled mixture (4 °C) of ethanol/phosphate buffer (85/15 v/v) were added. Tissue samples were homogenized using a Precellys24 homogenizer (PEQLAB Biotechnology GmbH, Germany) three times for 30 s at 5,500 rpm and -4 °C, with 30 s pause intervals to ensure constant temperature, followed by centrifugation at $10,000 \times g$ for 5 min. Subsequently, 10 μ L of the supernatants were analyzed with the p180 assay. Data evaluation for quantification of metabolite concentrations and quality assessment were performed with the software MultiQuant 3.0.1 (SCIEX) and the Met/*IQ*TM software package, which is an integral part of the Absolute/*IQ*TM Kit. Metabolite concentrations were calculated using internal standards and reported as pmol/mg for wet tissue.

2.4. Shotgun lipidomics

All standards were purchased from Avanti Polar Lipids: Ultimate SplashOne (#330820), dFA 18:1 (#861809), dFA 20:4 (#861810), dCer d18:0/13:0 (#330726), Glu Cer(d18:1-d7/15:0) (#330729), dLacCer d18:1/15:0 (#330727), 15:0-18:1-d7-PA (#791642), EquiSPLASH (#330731).

2.4.1. Lipidomic sample extraction

15 μ L (equivalent to 5 mg) of the liver homogenates (see 2.3 for procedure) were transferred into 1.5-mL glass vials together with 85 μ L of MilliQ water (H₂O). For accurate quantification, 25 μ L of a mix of 77 deuterated internal standards were then added to the samples (Ultimate SplashOne, dFA 18:1, dFA 20:4, dCer d18:0/13:0, Glu Cer(d18:1-d7/15:0), dLacCer d18:1/15:0, 15:0-18:1-d7-PA). For lipid extraction, 160 μ L of methanol (MeOH, Optigrade, Thermofisher) and 575 μ L methyl tert-butyl ether (MTBE) were added followed by incubation for 30 min on an orbital shaker DOS-10L (Neolabline, Heidelberg, Germany) at 300 rpm. For phase separation, 200 μ L of H₂O was added to each vial and were centrifuged at $5,000 \times g$ for 10 min at

room temperature with a Sigma 4-5C centrifuge (Qiagen, Hilden, Germany). The upper (organic) phase was evaporated with nitrogen gas using a Barkey evaporator (Barkey, Leopoldshoehe, Germany). The aqueous phase was again extracted with 100 μ L MeOH and 300 μ L MTBE. After addition of 100 μ L H₂O, the samples were incubated for 5 min at room temperature at 300 rpm and then centrifuged for 10 min at 5,000 \times g. The organic phase was transferred into the respective vial from the first extraction step and evaporated to dryness with gaseous nitrogen. Samples were reconstituted in 275 μ L running solvent (10 mM ammonium acetate in Dichloromethane:MeOH (50:50, v/v)) and 267 μ L were subsequently transferred into new vials with insert. For quality control purposes (QC-pool samples), 10 μ L of each study sample were pooled. 15 μ L aliquots were created and extracted with the above-described procedure. Additionally, 3 blank samples consisting of 15 μ L EtOH/phosphate buffer were prepared and extracted.

2.4.2. Shotgun lipidomics measurements

The DMS-SLA shotgun lipidomics assay is based on the method published by Baolong Su et al. [34]. All samples were measured with a SCIEX Exion UHPLC-system coupled to a SCIEX QTRAP 6500+ mass spectrometer equipped with a SelexION differential ion mobility interface (SCIEX, Darmstadt, Germany) operated with Analyst 1.6.3. 75 μ L of the re-dissolved sample were injected using the running solvent (10 mM ammonium acetate in Dichloromethane:MeOH (50:50, v/v)) at an isocratic flow rate of 8 μ L/min. After 9 min the flowrate was ramped to 30 μ L/min for 2 min to allow washing. Each sample was analyzed using multiple reaction monitoring (MRM) in two consecutive flow injection analysis (FIA) runs. In the first run, phosphatidylcholines (PC), phosphatidylethanolamines (PE), phosphatidylglycerols (PG), phosphatidylinositols (PI), phosphatidylserines (PS), and sphingomyelins (SM) were separated with the SelexION DMS cell using field asymmetric ion mobility mass spectrometry (FAIMS) prior to analysis in the Turbo Spray IonDrive source of the mass spectrometer. To enhance the separation of the lipid classes, 1-propanol was used as a chemical modifier. In the second run, cholesteryl esters (CE), ceramides (Cer d18:1), dihydroceramides (Cer d18:0), lactosylceramides (LacCER), hexosylceramides (HexCER), phosphatidic acid (PA), lysophosphatidylcholines (LPC), lysophosphatidylethanolamines (LPE), lysophosphatidylglycerols (LPG), lysophosphatidylinositols (LPI), lysophosphatidylserines (LPS), free fatty acids (FFA), diglycerides (DG), and triglycerides (TG) were measured with the DMS-cell switched off. Lipids were quantified with the Shotgun Lipidomics Assistant (SLA) software (v1.3) by calculating the area ratio between the analyte and the respective internal standard [34]. Lipid concentrations (nmol/g) were corrected for isobaric overlap with SLA. The mass spectrometer was operated with the following conditions: curtain gas 20 psi, ion source gas 1 14 psi, ion source gas 2 20 psi, Collision gas medium, temperature 150 $^{\circ}$ C, separation voltage +3500 V, ion spray voltage +4200 and +4500 V in ESI+ mode and -4400 and -3300 V in ESI- mode for run 01 and 02, respectively. Prior to each batch, the DMS cell was tuned, and the stability and sensitivity of the instrument was checked with the EquiSPLASH mixture.

2.4.3. Lipidomics data processing

The shotgun lipidomics raw data set contained 1,204 individual lipid species. Data were subsequently pre-processed using R (version 4.2.1). To assure high data quality, a multi-step procedure was applied: in the first step of this quality control (QC) procedure, lipids with missing values in more than 35% in the pool samples were discarded from the data set ($n = 136$). In the second step, the group-specific missingness was evaluated i.e., whether a specific lipid is

observed in only one of the biological groups. Lipids exhibiting a group-wise missingness of 50% in all groups were discarded from the data set ($n = 7$). Next, lipids with a coefficient of variation $>25\%$, determined by the QC-pool samples, were removed from the data set ($n = 22$). The last quality control step comprised the calculation of the dispersion ratio (D-ratio) for each lipid [35]:

$$\frac{\sigma_{tech}}{\sqrt{\sigma_{biol}^2 + \sigma_{tech}^2}}$$

where σ_{tech}^2 is the technical variance determined by the variance of the QC-pool samples and σ_{biol}^2 is the biological variance given by the variance of the biological samples within the study. We used a D-ratio threshold of 50%, as this implies that the technical variance is higher than the biological variance ($n = 43$ lipids were removed). After quality control, 996 lipid species remained in the liver data set, which contained 445 missing values (equivalent to 2% of the data set). Missing values were imputed using the k-nearest-neighbor obs-sel approach with $k = 10$ nearest-neighbors [36].

2.5. Multi-omics data integration

Co-inertia analysis (CIA) was performed using R package *omicade4* [37], to estimate the co-variability of proteomics and metabolomics datasets. Before CIA, each dataset was log₂ transformed and Pareto scaled. The similarity between the two datasets was estimated with the RV parameter, which is a multivariate extension of the Pearson correlation coefficients. RV value close to 1 indicates a high degree of co-structure in datasets. The permutation test with 200 iterations was used to assess the significance of the RV coefficient.

2.6. Oil red O staining

Liver tissue samples of 3-day-old piglets were fixed in PBS-buffered 4% PFA for 48 h, immersed in sucrose (each 2 h in 7.5% and 15% sucrose at room temperature, followed by 30% sucrose over night at 4 $^{\circ}$ C), embedded in Tissue-Tek[®] O.C.T.[™] compound, frozen on dry ice, and stored at -80 $^{\circ}$ C till cryosectioning. 4 μ m thick cryosections were stained with oil red O stain and embedded in Kaiser's glycerin gelatin.

2.7. Clinical chemistry and determination of HOMA-IR and QUICKI index

For clinical-chemical analysis, frozen plasma samples derived from non-fasted 3-day-old piglets were thawed for 1 h at room temperature, mixed thoroughly and then centrifuged (10 min, 5000 \times g at 8 $^{\circ}$ C) and afterwards analyzed immediately using an AU480 clinical chemistry analyzer (Beckman Coulter) and adapted reagent kits from Beckman Coulter, Randox (Glycerol) or FUJIFILM Wako Chemicals GmbH (NEFA) as described previously [38]. Insulin concentration was determined with ultrasensitive insulin ELISA from EDTA plasma (#10-1132-01, Mercodia) collected from newborn piglets before first milk intake. The homeostatic model assessment for insulin resistance index (HOMA-IR) [39] for estimating insulin resistance at fasting conditions was calculated using the formula: HOMA-IR = fasting plasma insulin (μ U/mL) \times fasting plasma glucose (mg/dL)/405. The 'Quantitative Insulin sensitivity Check' (QUICKI) index [40] was calculated with the formula: QUICKI = 1/[log(insulin (mU/L)) + log(glucose (mg/dL))].

2.8. Statistical analysis

All statistical analysis and data visualization were performed in R (<https://www.r-project.org/>). Statistical significance of proteome,

Original Article

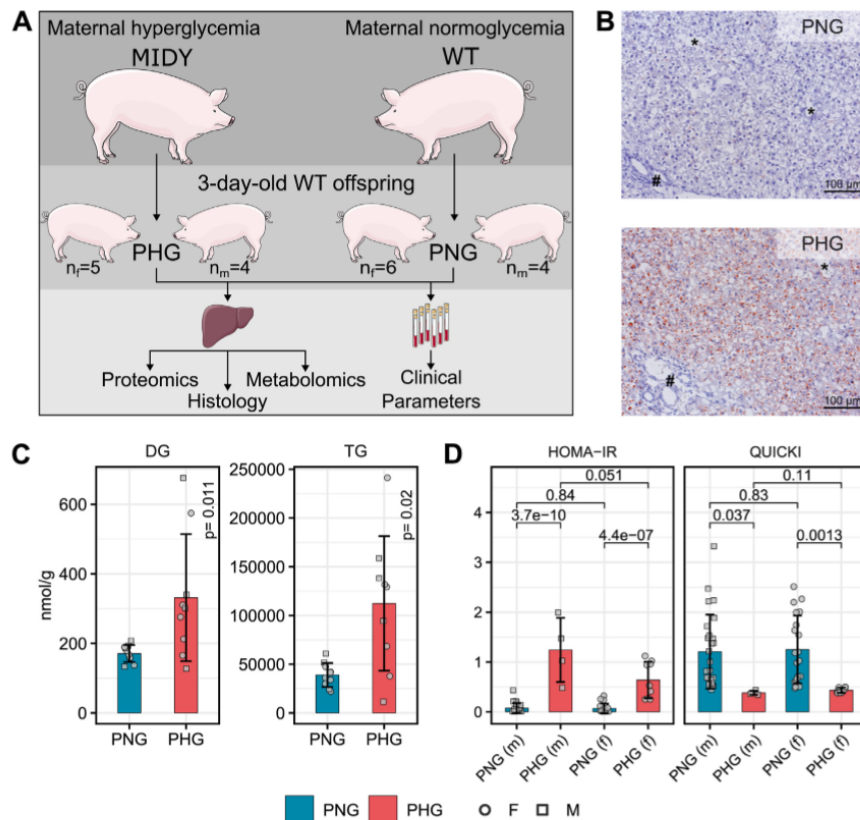


Figure 1: Experimental design, Oil red O stains of liver and assessment of insulin sensitivity. **A:** Proteomics, metabolomics and histological evaluation of liver samples alongside serum clinical chemical parameters from PHG (n = 5 female, n = 4 male) and PNG (n = 6 female, n = 4 male). PHG, piglets born to hyperglycemic mothers; PNG, piglets born to normoglycemic mothers; MIDY, mutant *INS* gene induced diabetes of youth; WT, wild-type. **B:** Oil Red O stains of liver cryosections of 3-day-old piglets show mediovesselicular lipid accumulation in hepatocytes in PHG. #, portal triad; *, central vein. **C:** Total diglyceride (DG) and triglyceride (TG) levels in PHG and PNG. P-values are from two-way ANOVA (group effect). **D:** Homeostatic model assessment of insulin resistance (HOMA-IR) and the 'QUantitative Insulin sensitivity Check' (QUICKI) index of PHG (n = 9 female, n = 4 male) and PNG (n = 20 female, n = 26 male) at birth. Statistical significance of the pair-wise differences was assessed using the Student's *t*-test. Bar diagrams show means and standard deviations.

metabolome, lipidome and clinical parameter changes was evaluated using two-way analysis of variance (ANOVA) considering the effect of the group (PHG/PNG), sex (female/male) and interaction between group and sex (group*sex). All resulting p-values (group, sex and group*sex) were pooled and adjusted for multiple-hypothesis testing with the Benjamini-Hochberg procedure. Biomolecules with a significant interaction effect were further followed by Tukey's honest significant difference (HSD) post-hoc test. Principal component analysis (PCA) was performed on log₂ transformed data using `prcomp()` function in R. Hierarchical clustering was performed using the R package *ComplexHeatmap* [41] with Ward's method as the clustering method and the Euclidean as a distance measure. Supervised clustering method, orthogonal projection to latent structures discriminant analysis (OPLS-DA), according to the class information (PHG versus PNG), was performed using the R package *ropls* [42]. Before the OPLS-DA, omics

datasets were log₂ transformed and subsequently Pareto scaled (mean-centered and divided by the square root of standard deviation). The leave-one-out cross-validation (LOOCV) of all models was used to select the best fitted OPLS-DA model. LOOCV is advantageous for small datasets as it maximizes the size of the training set. R2Y and Q2Y were used to assess the fitting validity and predictive performance of the OPLS-DA model, respectively. A 200-step permutation test was employed to estimate whether the supervised classification according to the known class (PHG versus PNG) is significantly better than any other random classification. Variance importance in projection (VIP) scores of the selected OPLS-DA model were used to rank the metabolites based on their discriminating ability of PHG and the PNG. Over-representation analysis (ORA) based on significantly changed proteins was performed using the R package *webgestaltR* [43] with the functional category "GO Biological Process nonredundant". The false-

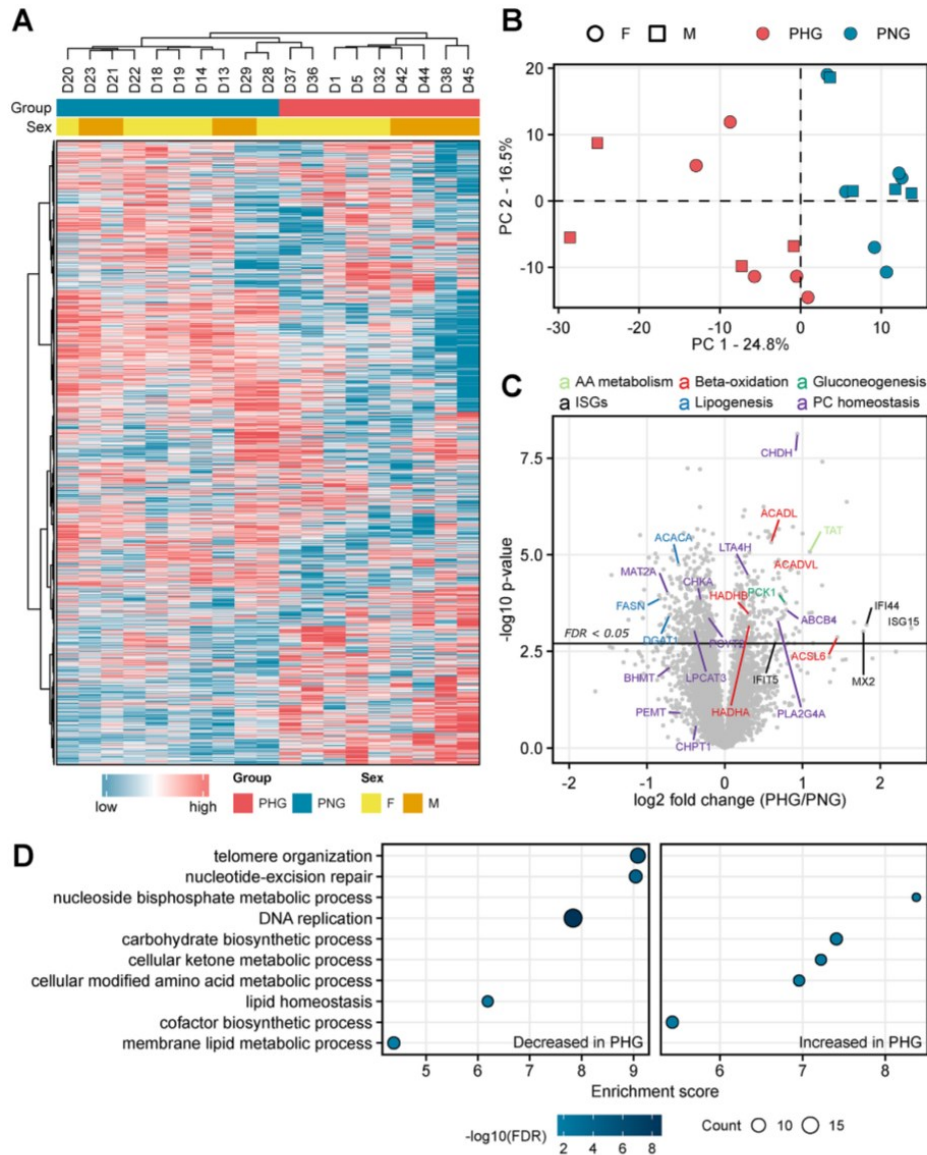


Figure 2: Overview of proteome differences in the liver from hyperglycemia exposed and control offspring. **A:** Unsupervised hierarchical clustering of standardized LFQ intensity values of liver proteomes leads to clustering of each sample according to the maternal glycemic status. The color code shows standardized abundance values. **B:** Principal component analysis of log₂-transformed data reveals maternal glycemic status as the strongest contributor to the inter-sample variation of the liver proteomes. The shape of each spot corresponds to the sex, and the color to the mother's genotype. **C:** Volcano plot comparing the protein abundance change between conditions (PHG/PNG). The x and y axis show the log₂ fold-change in protein levels and the log₁₀ two-way ANOVA group p-value, respectively. Selected proteins are annotated with gene names and color coded according to the corresponding biological processes. Proteins changed in abundance with false-discovery rate of 0.05 are above the vertical solid line. ISGs, interferon stimulated genes; FDR, false discovery-rate **D:** Enrichment analysis results of liver proteins less abundant in PHG (left column) and more abundant in PHG liver (right column). The size of each dot indicates the number of differentially abundant proteins involved in the corresponding GO biological process (referred to as count in the figure) and colors the significance (Benjamini-Hochberg adjusted p-value) of enrichment. Enrichment score is the magnitude of over-representation.

Original Article

discovery rate was controlled using the Benjamini-Hochberg method. Western blot signal intensities, the homeostatic model assessment-insulin resistance index (HOMA-IR) and the 'Quantitative Insulin Sensitivity Check' (QUICKI) index were compared using two-tailed Student's *t*-test.

3. RESULTS

3.1. General aspects

This study aimed to investigate the effect of maternal diabetes on non-diabetic offspring. For this purpose, as a translational model for human research, we used a non-obese genetically diabetic (*INS*^{C94Y} transgenic) pig model characterized by severe hyperglycemia [19], mimicking severe insulin deficient diabetes (SIDD) [44]. In this study, the hepatic proteome, metabolome as well as serum clinical parameters from 3-day-old wild-type (WT) piglets born to hyperglycemic mothers (PHG) were compared to the profiles of WT controls born to normoglycemic mothers (PNG). To complement the molecular findings, a histomorphological evaluation of the liver was performed (Figure 1A). Oil red O staining showed that PHG livers contained an increased amount of microvesicular and mediovesicular lipid droplets in hepatocytes (Figure 1B). To gain further molecular insights into an elevated lipid droplet formation, hepatic triglyceride (TG) and diglyceride (DG) levels were quantified using targeted lipidomics. Results showed elevation of both TG and DG levels in PHG liver (Figure 1C, Supplementary Fig. 2B). A detailed overview of the lipidomics results can be found in Supplementary Tables 1A–G and Supplementary Figs. 2A–C. Furthermore, homeostatic model assessment of insulin resistance (HOMA-IR) index monitored shortly after birth was higher in PHG (mean [SD], male: 1.24 [0.65], female: 0.64 [0.37]) than in PNG (mean [SD], male: 0.08 [0.09], female: 0.07 [0.09]). Consistently, quantitative insulin sensitivity check index (QUICKI) was lower in PHG (mean [SD], male: 0.38 [0.04], female: 0.43 [0.05]) compared with PNG (mean [SD], male: 1.20 [0.74], female: 1.25 [0.68]). QUICKI in PHG was below the cut-off value of 0.45 indicative for decreased insulin sensitivity (Figure 1D). The body weight of PHG was significantly lower than PNG (Supplementary Fig. 3A). Liver mass, relative to body weight, was not significantly different between the groups (Supplementary Fig. 3B). Neither sex nor group*sex interaction-related differences were observed for these parameters.

3.2. Overview of proteome findings in the liver

To detect effects of maternal hyperglycemia on offspring's liver proteome, we performed a label-free liquid chromatography-tandem mass spectrometry analysis (LC-MS/MS) of liver tissue samples from PHG and PNG. To facilitate accurate and in-depth quantitative proteomics, a data-independent acquisition (DIA) approach was chosen. In the workflow, peptides were identified using an *in silico* predicted library, which was further refined by the project-specific chromatogram libraries generated with narrow-isolation window gasphase fractionation (GPF) DIA runs. The dataset has been submitted to the ProteomeXchange Consortium via the PRIDE [45] partner repository with the dataset identifier PXD040305. A total of 61,283 unique peptides from 6,313 protein groups were identified with high confidence (false-discovery-rate <0.01). Supplementary Table 2A contains a full list of all identified proteins and their abundance levels. In the unsupervised hierarchical clustering (Figure 2A) and principal component analysis (Figure 2B), the proteome profiles of liver tissue from PHG differed substantially from those of PNG, suggesting group-specific alterations in protein abundance.

To identify differentially abundant proteins, a two-way ANOVA was performed (Supplementary Table 2B). 123 proteins were found to be differentially abundant (Benjamini-Hochberg adjusted *p*-value ≤0.05 and *I*2fc ≥ 1.5) by the effect group (PHG/PNG), of which 62 were increased and 61 decreased in abundance (Supplementary Table 2C, Figure 2C). The protein with the highest increase in abundance in the PHG liver was ISG15 ubiquitin like modifier (ISG15) (5.3-fold). Likewise, the levels of other proteins involved in interferon signaling pathway such as interferon-induced GTP-binding protein Mx2 (MX2), interferon induced protein 44 (IF44), and interferon induced protein with tetratricopeptide repeats 5 (IFIT5) were elevated in PHG samples. Moreover, proteins involved in glucose metabolism, such as phosphoenolpyruvate carboxykinase (PCK1) and glucose-6-phosphate isomerase (GPI) were increased in abundance. Several proteins involved in retinol metabolism, such as retinol-binding protein 4 (RBP4) and dehydrogenase/reductase 7B (DHRS7), were also elevated. Further proteins with increased abundance in PHG liver were tyrosine aminotransferase (TAT), branched-chain-amino-acid aminotransferase (BCAT1), and aromatic-L-amino-acid decarboxylase (DDC), all known to be involved in amino acid metabolism. A large fraction of up-regulated proteins is known to be involved in lipid homeostasis, among which are acyl-CoA synthetase long chain family member 6 (ACSL6), long-chain specific acyl-CoA dehydrogenase (ACADL), mitochondrial acyl-CoA dehydrogenase very long chain (ACADVL), propionyl-CoA carboxylase alpha and beta chain (PCCA and PCCB), and others. Furthermore, proteins involved in glycerophospholipid metabolism (e.g. choline dehydrogenase (CHDH) and phospholipase A2 (PLA2G4A)) and transport (e.g. ATP-binding cassette 4 (ABC4)) were elevated in abundance. On the other hand, some of the down-regulated proteins are also known to be involved in lipid metabolism, among others fatty acid synthase (FASN), O-acyltransferase (DGAT1), acetyl-CoA carboxylase 1 (ACACA), ceramide synthase 4 (CERS4), and others. Furthermore, S-adenosylmethionine synthase (MAT2A), a protein involved in the methionine cycle, was decreased in abundance.

To get functional insights from proteome alterations between PHG and PNG, over-representation analysis (ORA) was performed using Web-Gestalt. The detailed results of the enrichment analysis are provided in Supplementary Table 2D and Figure 2D. Briefly, proteins involved in the nucleoside bisphosphate metabolic process, carbohydrate metabolic process, cellular ketone metabolic process, cellular modified amino acid metabolic process, and cofactor biosynthetic process were significantly overrepresented in the set of up-regulated proteins, while proteins involved in DNA replication, regulation of plasma lipoprotein particle levels, telomere organization, nucleotide-excision repair, DNA replication, lipid homeostasis, and membrane lipid metabolic process were overrepresented in the set of down-regulated proteins.

In terms of sex-related differences, only UDP-glucuronosyltransferase was changed significantly and was elevated in the liver of female compared to male offspring (Supplementary Table 2E). To explore proteins changed in the offspring's liver due to maternal glycemia in a sex-dependent manner, the group*sex interaction effect from the two-way ANOVA was used. This revealed only a few proteins that were significantly influenced by the group*sex interaction effect (Supplementary Fig. 4, Supplementary Table 2F). The proteins most significantly affected by the interaction effect were vacuolar protein sorting-associated protein 41 homolog (VPS41) and 60S ribosomal protein L26-like 1 isoform X1 (RPL26L1), both increased in female PHG (compared to female PNG) but decreased in male PHG (compared to male PNG). A similar regulation pattern was observed for further

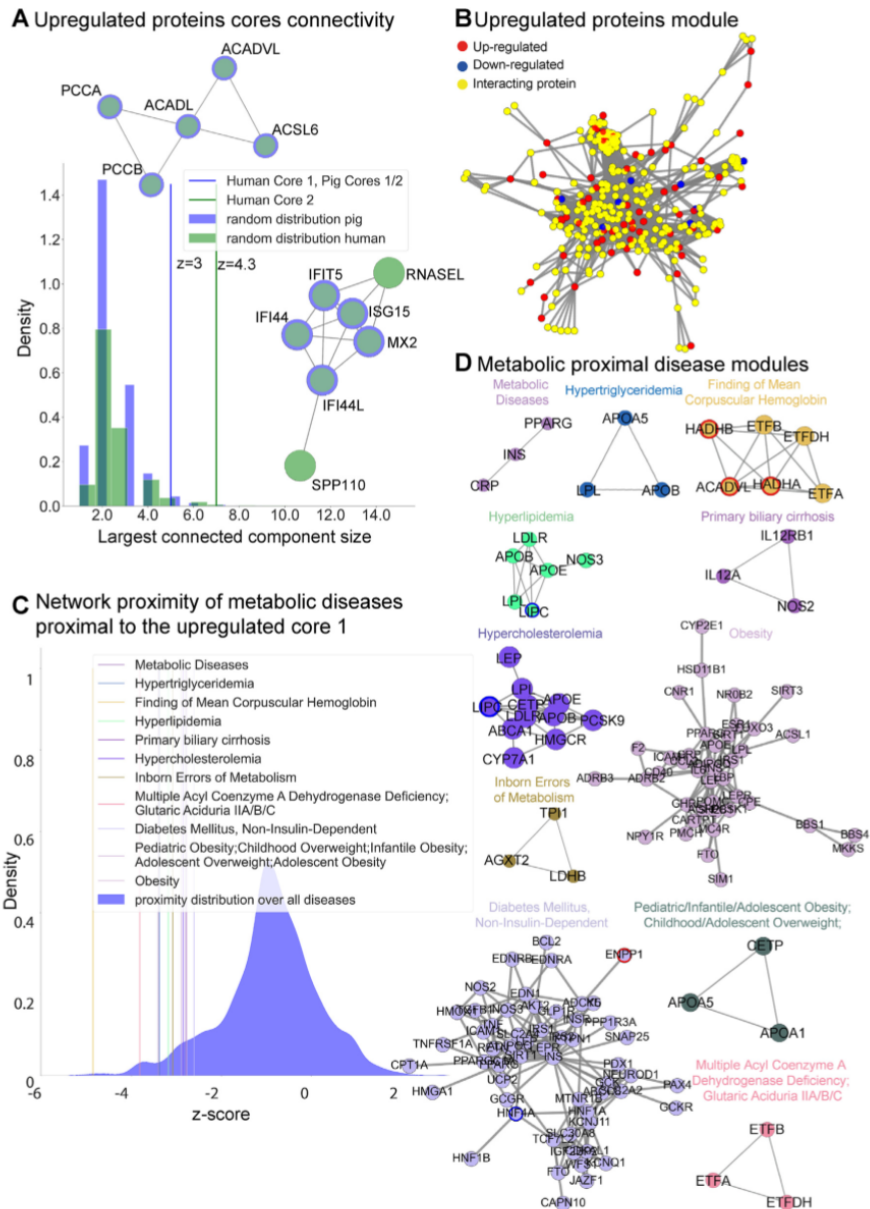


Figure 3: Network analysis of differentially abundant proteins and their relationships with human diseases. **A:** Identification of two up-regulated core proteins that deviate from random expectation (10,000 random sets of proteins of equal size) based on their connectivity ($z\text{-score}_{\text{core1}} = 3$, $z\text{-score}_{\text{core2}} = 4.3$). The green color refers to the human PPI, and the blue color to the pig PPI. **B:** Up-regulated expanded network which contains all up-regulated proteins and their interacting partners. This subnetwork is formed by 312 proteins colored in: red if up-regulated in PHG, blue if down-regulated in PHG, and yellow if not detected but interacting with differentially abundant proteins. **C:** Network proximity z-score distribution for all diseases ($N = 11,099$). With vertical, colored lines are highlighted 15 metabolic diseases that have been observed to be particularly proximal (related) to the up-regulated core 1. **D:** Diseases network modules (network size > 2 nodes) for proximal metabolic disorders to up-regulated core 1. Each node color reflects each specific disease, and a red outline is marked if a protein was identified as overly abundant in PHG, or a blue outline if it was down-regulated in PHG.

Original Article

proteins like glutaredoxin 5 (GLRX5) and complement component 1 Q subcomponent-binding protein, mitochondrial (C1QBPF).

Furthermore, to confirm quantitative changes detected by mass spectrometry by other means of quantification, we selected three candidates where working porcine-specific antibodies were available and quantified them using Western blot. [Supplementary Fig. 5](#) shows the abundance change of formyltetrahydrofolate dehydrogenase (ALDH1L2), Ras-related protein Rab-3 (RAB3D) and claudin (CLDN15) between PHG and PNG and they are in line with our mass spectrometry-based quantitative data.

3.3. Protein–protein interaction construction

Next, we evaluated whether among the differentially abundant proteins we could identify subsets of highly interacting proteins that participate in the same molecular mechanisms and tried to relate these mechanisms with human pathology. To do so, we first generated a pig-specific and a human-specific protein–protein interaction network (PPIs) compiled from the STRING database v11.5 (<https://string-db.org/>) [27], obtaining 15,360 nodes and 170,244 edges, and 16,793 proteins and 251,982 edges respectively. At this point, we compared the size of the connected components of the differentially abundant proteins against 10,000 random groups of proteins of equal size. In this way, we were able to identify two main cores among the up-regulated proteins in both pigs and humans ([Figure 3A](#)). The first module consists of five interacting proteins (ACADVL, ACADL, ACSL6, PCCB, PCCA) conserved in pig (p -value = 0.001) and in human (p -value = 0.003), which is responsible for lipid homeostasis ([Supplementary Table 3A](#) contains the full list of significantly enriched terms (adjusted p -value < 0.05)). The second up-regulated core is formed of five proteins in pig (MX2, IFIT5, IFI44, IFI44L, ISG15) (p -value = 0.001) and seven in human (MX2, IFIT5, IFI44, IFI44L, ISG15, SP110, RNASEL) (p -value = $1e-05$), which is related to an interferon type I response (full list of enriched terms [Supplementary Table 3B](#) for pig and [3C](#) for human). In both species, the down-regulated proteins form a connected core, 17 proteins in pigs (p -value = $1.7e-60$), and 22 in humans (p -value = $3e-74$) ([Supplementary Fig. 6A](#)).

Based on the fact and our observation that pigs and humans share similar core mechanisms on a network level, we decided to focus on the latter. Using a random walk with restart algorithm (see methods), we identified a network of 312 up-regulated proteins and their interactors ([Figure 3B](#)) and another network for 363 proteins which were down-regulated in PHG ([Supplementary Fig. 6B](#)). These two networks are very different as shown by their poor edge overlap (Jaccard index = 0.002), proving once again that they lay in two different parts of the PPI network contributing to different biological mechanisms. Their enrichment analysis resembles our previous findings ([Supplementary Tables 3D–E](#)) pointing to those interacting proteins that in tandem with the differentially abundant ones contribute to specific phenotypes (i.e. “fatty acid degradation”). Finally, to check the relationship of these dysregulated proteins with disease onset, we extracted disease–gene associations from DisGeNet [31], leading to a list of 11,099 diseases (after filtering). We computed two measures: the Jaccard index between the set of perturbed genes in diseases and the dysregulated proteins in our set-up and the network proximity [32] ([Supplementary Table 3F](#)). Since the Jaccard index does not make use of any network properties, these relationships can be driven even by a very small pool of genes. To address this, we decided to pursue our analyses by using network proximity and identified a plethora of related diseases (227, for the first up-regulated core, and 1,275, for the second one) (adjusted p -value < 0.05, [Supplementary Table 3G](#)). Among the 227 proximal diseases to the first up-regulated core, we

focused on those relevant to metabolic disorders and liver diseases ([Figure 3C](#)), observing very small z -scores compared to those of all diseases, standing for their closeness to the up-regulated core in the human PPI. The genes known to be responsible for these pathological conditions are strictly related to lipid metabolism, such as lipoprotein lipase (LPL), its receptor (LPLR), and hepatic triacylglycerol lipase (LIPC) ([Figure 3D](#)). This tight distance in the human PPI suggests that frequently reported susceptibility of GDM offspring to childhood and adolescence overweight may be caused by the network pathways that connect the up-regulated core genes (PCCA, PCCB, ACADL, ACADVL, ACSL6), to APOA5, CETP, and APOA1 ([Figure 3D](#)). Similar considerations can be applied to the second up-regulated core (related to the IFN pathway) and to the expanded unified up-regulated core ([Supplementary Table 3G](#)). After expansion, also by using the Jaccard index measure, we could observe among the most statistically significant associated diseases, primary and secondary biliary cholangitis (Benjamini-Hochberg adjusted p -value: 0.03), Glutaric Aciduria II (type A, B, C) (Benjamini-Hochberg adjusted p -value: 0.004), and Multiple Acyl Coenzyme A Dehydrogenase Deficiency (Benjamini-Hochberg adjusted p -value: 0.004), which could hint changes in bilirubin metabolism due to perturbations of the immediate neighbors in the human PPI of the up-regulated proteins.

3.4. Overview of metabolome findings in the liver

To gain further insights into the alteration of metabolic pathways as revealed by proteomics, quantitative readouts of relevant metabolite classes were performed. The results of the targeted metabolomics analysis are shown in [Supplementary Table 4A](#). Hierarchical clustering ([Figure 4A](#)) and principal component analysis ([Figure 4B](#)) separated samples of PHG and PNG. To reveal metabolites changed by the effects of group, sex, and group*sex, a two-way ANOVA was performed ([Supplementary Table 4B](#)). Metabolites with Benjamini-Hochberg adjusted p -value ≤ 0.05 and $I_2fc \geq 1.5$ were considered significant. 31 metabolites were changed by the effect group ([Supplementary Table 4C](#), [Figure 4C](#)). The supervised OPLS-DA method was used to evaluate to what extent metabolomics data can discriminate PHG from PNG. OPLS-DA clearly separated groups ([Figure 4D](#)). Statistical evaluation of the OPLS-DA indicated a robust model ($R2X = 0.58$, $R2Y = 0.99$, $Q2 = 0.93$). The permutation test with 200 iterations showed the significance of both predictive ($Q2Y$) and fitting ($R2Y$) components ($p = 0.002$). Variable importance in projection (VIP) plot ([Figure 4E](#)) revealed metabolites with the highest contribution to the separation of PHG from PNG animals on the OPLS-DA plot. [Figure 5](#) provides a detailed overview of differentially abundant metabolites. 24 different glycerophospholipids (specifically phosphatidylcholines (PC)) were changed in abundance of which 22 were increased and only two (PC ae C30:0 and PC aa C32:1) were decreased ([Figure 5A](#)). Furthermore, two sphingolipids (SM (OH) C14:1 and SM (OH) C16:1) were elevated ([Figure 5A](#)). In the PHG liver, enzymes and metabolites involved in the breakdown and removal (translocation from hepatocytes to bile) of the PC were elevated while those involved in biosynthesis were reduced ([Figure 5B–C](#)). Several members of biogenic amines were changed in abundance between PHG and PNG, of which total DMA (dimethylamine), SDMA (symmetric dimethylarginine) and ADMA (asymmetric dimethylarginine) were elevated while trans-4-hydroxyproline (t4-OH-Pro) was reduced. Furthermore, the amino acid proline was reduced by 1.7-fold ([Figure 5D](#)). Only one metabolite, PC ae C42:4, was affected by the effect sex (decreased in female offspring) ([Supplementary Table 4D](#)) and only two metabolites (PC ae C42:3 and SM C26:0) were affected by the interaction group*sex ([Supplementary Table 4E](#), [Supplementary Fig. 7](#)). Only three metabolite ratios, poly-

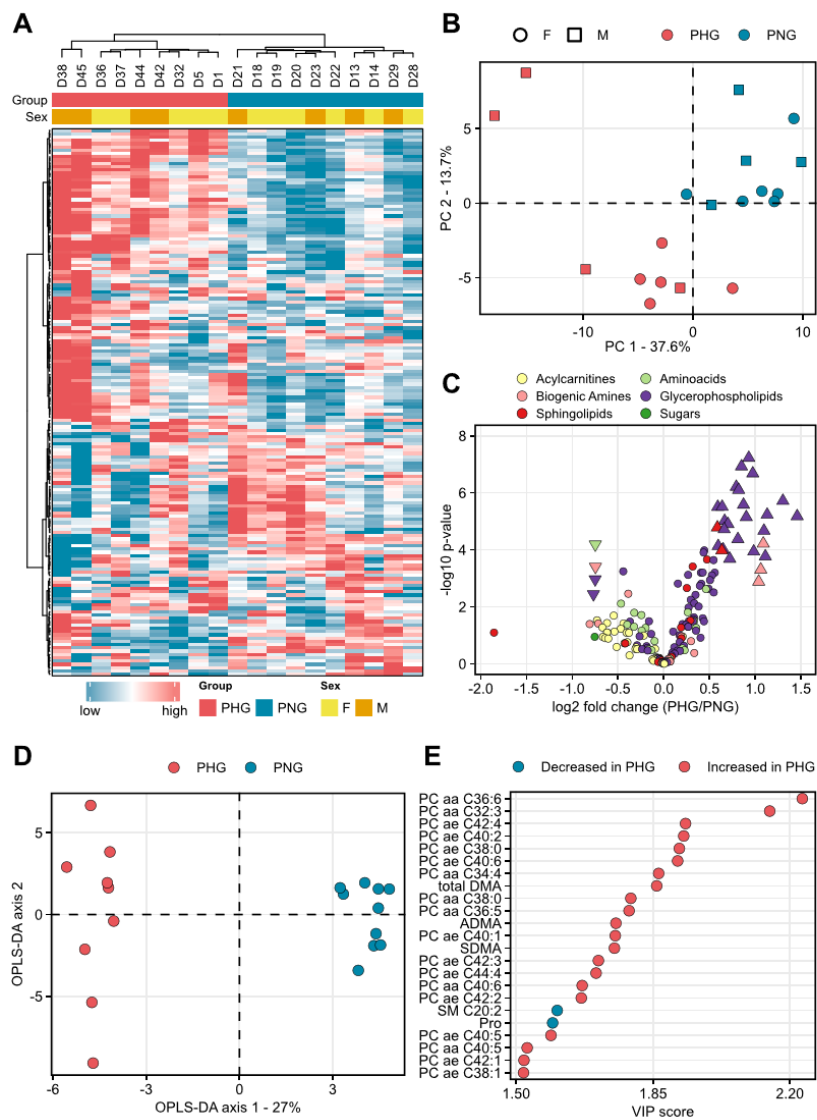


Figure 4: Overview of metabolome differences in the liver from hyperglycemia exposed and control offspring. **A:** Unsupervised hierarchical clustering of metabolite levels (pmol/mg tissue) leads to the clustering of each sample according to the maternal glycemic status. The color code shows standardized abundance values. **B:** Principal component analysis of \log_2 transformed and unit variance scaled data reveals maternal glycemic status as the strongest contributor to the inter-sample variation of the liver metabolome. The shape of each spot corresponds to the sex, and the color to the mother's genotype. **C:** Volcano plot comparing the metabolite abundance change between conditions (PHG/PNG). Significantly changed metabolites (Benjamini-Hochberg adjusted p-value ≤ 0.05 and fold change ≥ 1.5) are shown as up- and down-pointing triangles for increased and decreased abundance in PHG versus PNG, respectively. Circles correspond to non-significant changes. The x and y axis show the \log_2 fold-change in metabolite levels and the \log_{10} two-way ANOVA group p-value, respectively. Different metabolite classes are color-coded. **D:** Supervised classification of PHG from PNG samples using the cross-validated orthogonal partial least squares discriminant analysis (OPLS-DA). The x and y axis show the predictive (between class separation) and orthogonal component (within class separation), respectively. The best fitted OPLS-DA model was selected based on leave-one-out cross-validation followed by permutation test with a 200-step iteration which yielded $R^2X = 0.58$, $R^2Y = 0.99$, $Q^2 = 0.93$ ($R^2Y_p = 0.002$, $Q^2_p = 0.002$). **E:** Variance importance on projection (VIP) plot. Metabolites with the strongest impact on the supervised classification of PHG and PNG samples were extracted from the OPLS-DA model. Metabolites with $VIP > 1.5$ are shown.

Original Article

unsaturated to mono-unsaturated glycerophosphocholines (PUFA (PC)/MUFA (PC)), total PC ae and total sphingolipid (SM), were significantly changed between PHG and PNG (Benjamini-Hochberg adjusted p -value ≤ 0.05) and were elevated in PHG liver (Supplementary Tables 4F–G, Figure 5C). To check for similarities between the metabolic alterations in offspring and mother, plasma metabolomics data from this study was compared to a previously published set of plasma metabolite alterations from MIDY versus WT pigs [46] (Figure 5E). The mother of the offspring used in this study had the same insulin mutation as MIDY pigs published previously [19]. The majority of PCs changed in abundance in the offspring were also significantly changed in the same direction in the MIDY versus WT plasma. Total DMA was elevated in the offspring liver while it was significantly reduced in the MIDY plasma. Proline which was significantly increased in the offspring liver was not significantly changed in the MIDY plasma. The same is true for sphingolipids (SM (OH) C14:1 and SM (OH) C16:1) and biogenic amines (SDMA and ADMA, t4-OH-Pro).

3.5. Cross-omics correlation

Using a co-inertia analysis (CIA) [47], we investigated the complex association between proteomics and metabolomics datasets. CIA projects multiple omics datasets simultaneously onto the same plane. Representation of samples on a lower-dimensional space reveals global covariability between proteomics and metabolomics datasets (Figure 6A). CIA reveals that proteomics and metabolomics datasets are more similar within groups than between groups. The first component of the CIA (horizontal) accounted for 56% of the variance, and the second component (vertical) accounted for 25%. The CIA showed clear clustering of PHG and PNG samples. In line with this RV coefficient which represents the degree of association was 0.79 and was significant as revealed by 200-step permutation-based test ($p = 0.005$). The corresponding score plot shows the proteins and metabolites responsible for partitioning PHG and PNG samples on the CIA plot (Figure 6B). In the score plot, each quantified protein and metabolite is depicted by the black square and grey circles, respectively and some of the most informative biomolecules across datasets are labelled.

3.6. Overview of clinical-chemical findings in the serum

To clarify if maternal diabetes is associated with alteration of circulating biomarkers of liver damage, relevant clinical-chemical parameters were measured in the serum of PHG and PNG. The detailed clinical-chemical data and the results of the two-way ANOVA analysis are shown in Supplementary Table 5A and Supplementary Table 5B, respectively. Clinical-chemical parameters with statistically significant (p -value ≤ 0.05) changes between PHG and PNG serum samples were bilirubin (increased in PHG), non-esterified free fatty acids (NEFA) (increased in PHG), and albumin (increased in PHG) (Supplementary Table 5C). Glycerol (decreased in PHG, $p = 0.06$) and triglycerides (decreased in PHG, $p = 0.07$) levels were changed as a trend (Figure 7). High-density lipoprotein levels were significant for the effect of sex (increased in female offspring) (Supplementary Table 5D). Alanine transaminase (ALT) showed a significant interaction effect, with significantly higher levels in male PHG versus male PNG (Supplementary Table 5E, Supplementary Fig. 8).

4. DISCUSSION

To investigate to what extent maternal hyperglycemia affects the offspring's liver metabolism, a multi-omics analysis combining data-independent acquisition proteomics and targeted metabolomics was

performed. Additionally, relevant clinical-chemical parameters that reflect the liver state were measured in the serum. In this work, the liver and serum samples were collected from offspring born to a genetically engineered diabetic pig model for mutant *INS* gene-induced diabetes of youth (MIDY) [19] (PHG) and from offspring born to WT littermate controls (PNG), according to the principles of systematic random sampling [6]. The body weight of PHG was significantly lower than PNG. Similarly, in human studies, neonates of mothers with severe diabetic complications tended to have a lower birthweight (SGA) [48,49]. Like macrosomia, SGA is a risk factor for a variety of diseases in future life (reviewed in [50]). To clarify if hepatic damage in the offspring due to maternal glycemia is apparent already in the neonatal period, we investigated livers from 3-day-old piglets. To our knowledge, this is the first holistic multi-omics study from a clinically relevant large animal model addressing the molecular derangements in the offspring liver caused by maternal hyperglycemia.

Circulating bilirubin was significantly elevated in the offspring born to hyperglycemic mothers which was also observed previously in human offspring studies [51,52], underlining the clinical relevance of our finding. A higher level of bilirubin may reflect different types of liver or bile duct complications [53]. In line, disease–gene association revealed several diseases associated with disturbed bilirubin metabolism. One of the primary constituents of bile are phospholipids (predominantly phosphatidylcholines (PC)) [54]. PC excretion into bile is mediated by the PC-specific floppase ABCB4 [53,55]. Our targeted metabolomics revealed consistent elevation of multiple PC (with mainly one acyl- and one alkyl-bound fatty acids (PC ae), and a higher proportion of poly-unsaturated PCs), while proteomics showed significantly elevated levels of ABCB4, suggesting an active translocation of PCs to bile. Translocation of PCs is considered to have hepatoprotective properties as PCs inactivate the detergent activity of bile salts to prevent damage to cell membranes [56]. Besides translocation to bile, hydrolysis of PCs by phospholipase A2 to produce fatty acids and a lysoPC is an important step in PC homeostasis [57]. The products of PC hydrolysis are important precursors for generating key inflammatory mediators, oxylipins [58]. In our data, phospholipase A2 was significantly elevated while one of the downstream enzymes leukotriene a4 hydrolase (LTA4H) was moderately increased (LTA4H, I2fc = 0.31, adjusted p -value = 0.006), suggesting a breakdown of PC molecules and generation of leukotrienes in PHG liver. Finally, PC homeostasis in the liver is achieved via the metabolic pathways involved in its biosynthesis, predominantly from choline via the CDP-choline pathway (also known as the Kennedy pathway) [59]. Choline kinase (CHKA), the initial enzyme in the sequence, catalyzes the transfer of a phosphate group from adenosine triphosphate (ATP) to choline to form phosphocholine. Subsequently, the key regulatory enzyme in this process, CTP:phosphocholine cytidyltransferase (PCYT2, alias CCT) catalyzes the transfer of a cytidyl group to phosphocholine to form CDP-choline, which then forms PC (catalyzed by choline phosphotransferase 1 (CHPT1 alias CPT1)). Although with a moderate fold change (CHKA, I2fc = -0.31 ; PCYT2, I2fc = -0.22), CHKA and PCYT2 were reduced significantly (adjusted p -value < 0.05). CHPT1 levels were also reduced but did not reach statistical significance. CDP-choline is the major pathway of PC synthesis, however, in the hepatocytes where PC demand is high, it can also be synthesized by sequential methylations of phosphatidylethanolamine (PE) where MAT2A-catalyzed S-adenosyl-methionine (SAM) transformation to S-adenosylhomocysteine (SAH) donates the methyl groups. We found significantly reduced levels of MAT2A together with non-significantly reduced levels of other enzymes involved in this pathway. Additionally, LPCAT3, which catalyzes the third mechanism of PC synthesis -

Section A: Investigation of the effect of maternal hyperglycaemia on neonatal offspring liver metabolism 60

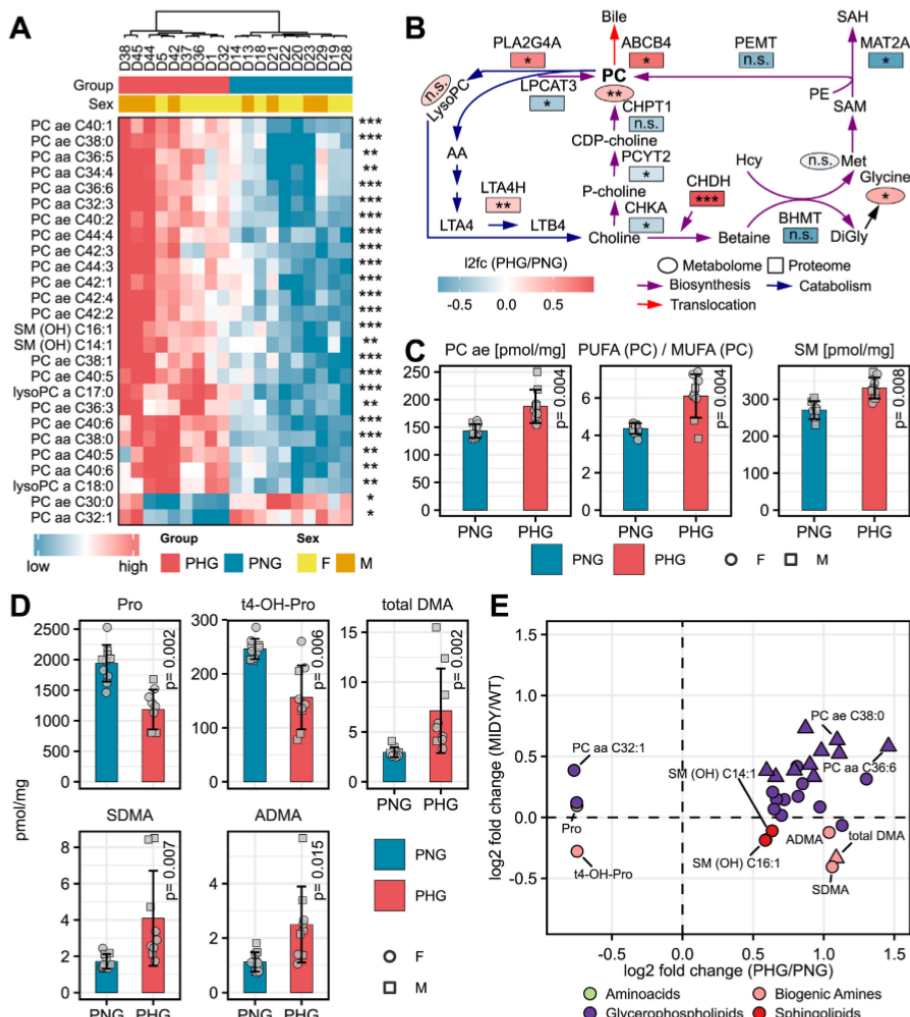


Figure 5: Overview of significantly changed metabolites between PHG and PNG. **A:** Levels of the significantly changed glycerophospholipids and sphingolipids in PHG and PNG samples. **B:** Scheme of PC synthesis (violet arrows), breakdown (dark blue arrows) and removal (translocation to bile, red arrow). Metabolites and enzymes are depicted as ellipses and rectangles, respectively. LysoPC, lysophosphatidylcholine; PLA2G4A, phospholipase A2 group IVA; LPCAT3, lysophosphatidylcholine acyltransferase 3; SM, sphingolipid; AA, arachidonic acid; LTA4, leukotriene A4; LTA4H, leukotriene A4 hydrolase; LTB4, leukotriene B4; CHKA, choline kinase alpha; PCYT2, phosphate cytidylyltransferase 2, ethanolamine; CDP, cytidine 5'-diphosphocholine; PC, phosphatidylcholine; CHDH, choline dehydrogenase; CHPT1, choline phosphotransferase 1; ABCB4, ATP-binding cassette 4; BHMT, betaine-homocysteine S-methyltransferase; DiGly, diglycine; Hcy, homocysteine; Met, methionine; SAM, S-adenosyl methionine; SAH, S-adenosylhomocysteine; PEMT, phosphatidylethanolamine n-methyltransferase; MAT2A, methionine adenosyltransferase 2A; PE, phosphatidylethanolamine; n.s., not significant. **C:** Levels of the significantly changed (Benjamini-Hochberg adjusted p-value ≤ 0.05) metabolite ratios. PUFA, polyunsaturated fatty acid; MUFA, monounsaturated fatty acid. **D:** Bar diagram of amino acids and biogenic amines significantly changed between groups. The bar diagrams show means and standard deviations. P-values are from two-way ANOVA (group effect) after the Benjamini-Hochberg correction. **E:** Scatter plot of log₂ fold-change of significantly altered metabolites (PHG/PNG) in offspring liver versus the changes of the same metabolites in the insulin-deficient diabetes (MIDY) versus WT pig plasma [46]. The mother of the offspring used in this study has the same insulin mutation as MIDY pigs published previously [19]. Different metabolite classes are color-coded. Metabolites which were changed in abundance between MIDY versus WT with a p-value <0.05 are shown as triangles. Benjamini-Hochberg adjusted significant p-values are labelled with asterisks in A and B, *p <0.05 ; **p <0.01 ; ***p <0.001 .

Original Article

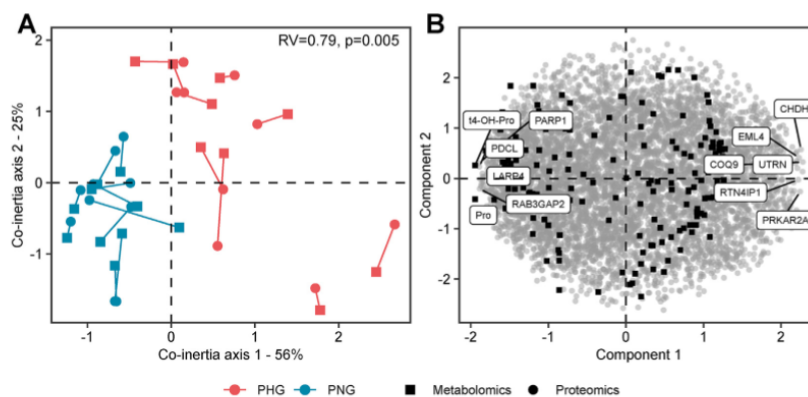


Figure 6: Proteomics and metabolomics data integration. (A, B) Multiple co-inertia analysis of proteome (circle) and metabolome (square) data from the PHG and PNG liver samples showing the first two components in the sample (A) and variable (B) space. The line length in the sample space (A) reflects the strength of the cross-omics correlation for each sample. The RV coefficient (RV = 0.79, 200 permutations, $p = 0.005$) shows the correlation between the two datasets. An RV close to 1 indicates a strong correlation. Proteins and metabolites with the highest values in component 1 are labelled in a variable space (B).

recylation of lysoPC to PC [60] - was moderately reduced ($I2fc = -0.4$, adjusted p -value = 0.03). Collectively, our data show reduced levels of enzymes involved in PC synthesis, but elevated levels of enzymes and

downstream products involved in its elimination and breakdown. Elevated PC levels in the PHG, despite reduced biosynthesis, may be explained by increased transplacental transfer from the hyperglycemic mother and subsequent hepatic uptake. This is in line with the previous data where PC levels were shown to be elevated in the serum of hyperglycemic pigs [46]. We suggest that the feedback loop mechanism by which increased PC levels downregulate enzymes involved in its biosynthesis is plausible. Supporting our hypothesis, previous reports showed a correlation of maternal and fetal metabolites during both the peripartum period [61] and even several years postpartum [62]. In line with increased lipid species as revealed by targeted metabolomics and targeted lipidomics, higher total hepatic lipid content was detected using Oil red O staining. Accumulation of liver fat is recognized as a risk factor for non-alcoholic fatty liver disease (NAFLD) [63], cardiometabolic disease [64,65] and other complications. Although the presence of liver steatosis in the offspring born to a diabetic mother is supported by several recent human [13,17,66,67] and rodent studies [68], another human study found that in predicting infant hepatic fat content, maternal diabetes may be less important than the presence of maternal obesity [14]. Authors of two systematic reviews proposed that the evidence for an association between maternal diabetes and offspring adiposity, which is strongly associated with NAFLD, remains inconclusive due to the attenuation of the association when adjusting for maternal pre-pregnancy BMI [69,70]. Lipogenesis as well as availability of plasma fatty acids are considered as important contributors to hepatic steatosis [71]. The initial rate-limiting step of hepatic *de novo* lipogenesis (DNL) is acetyl-CoA carboxylation to malonyl-CoA by the action of acetyl-CoA carboxylase (ACACA) [72]. Subsequent conversion of malonyl-CoA into palmitic or various other fatty acids is catalyzed by fatty acid synthase (FASN) which plays a central role in hepatic DNL [73]. The terminal step of triglyceride (TG) synthesis - the acylation of diglyceride - is catalyzed by diacylglycerol O-acyltransferase 1 (DGAT1) [74]. Despite increased hepatic fat content, levels of ACACA, FASN and DGAT1 were significantly reduced. Decreased circulating TG levels in PHG may be explained by an elevated hepatic TG accumulation and reduced release in the serum. This is in line with the downregulation of DGAT1 in PHG, as DGAT1 overexpression is associated with higher rates of very-low-density

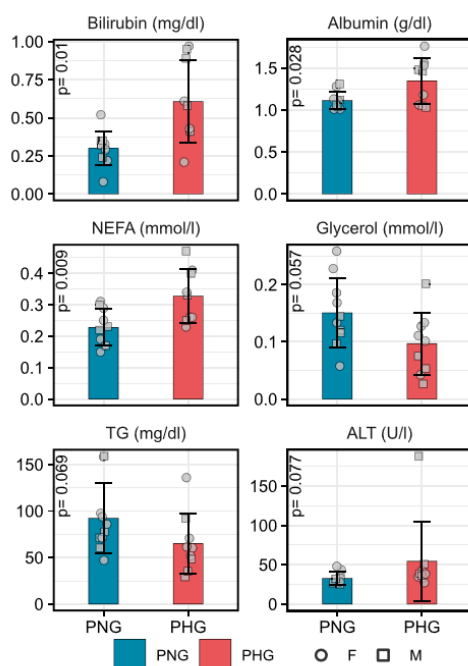


Figure 7: Changes in selected clinical-chemical parameters in the PNG and PHG blood. Bar diagrams show the mean and standard deviation. P-values are from two-way ANOVA (group effect). NEFA, non-esterified fatty acid; TG, triglyceride; ALT, alanine transaminase.

lipoprotein-TG complex secretion from rat hepatoma cells [75]. Conversely, inhibition of DGAT1 in mouse liver and isolated hepatocytes resulted in an increased transfer of fatty acids into mitochondria for beta-oxidation [76–78]. In PHG beta-oxidation markers such as ACSL6, ACADL and ACADVL were elevated suggesting active degradation of long-chain and very long-chain fatty acids. Furthermore, although with a moderate fold-change ($I2fc = 0.32$) both HADHA and HADHB which catalyze the last three steps of beta-oxidation were increased in abundance (adjusted p -value < 0.05). Decreased lipogenic enzymes in the liver suggests that elevated hepatic lipid content in PHG is not linked to DNL. This is in line with the observation that limited capacity for DNL exists in human fetus, and the drivers of fetal fat accumulation are primarily supplied transplacentally [79]. Shifting the balance of lipid metabolism away from *de novo* synthesis to favor lipid breakdown via beta-oxidation, mechanistically resembles the observation made for PC (see above). Decreased DNL together with increased beta-oxidation might be a way of adaptation developed in offspring to slow down or prevent the progression of increased fat content into liver steatosis, which is especially relevant in pigs as they seem to be protected against steatosis even in morbid obesity [80]. In line, previous studies reported protection against steatosis through pharmaceutical inhibition of DNL enzymes [81,82]. The resistance of pigs to hypertriglyceridemia is not well understood but extrahepatic lipogenesis has been proposed as a potential mechanism [83]. Another key driver of reduced lipogenesis might be PC which were elevated in PHG (see above). An elevated lipogenesis and steatosis in early stages of fatty liver disease was shown in the setting of reduced PC [84]. Additionally, several clinical studies observed the attenuation of steatosis after treatment with PC (reviewed in [85]).

Besides lipid metabolism, the homeostasis of other key biomolecules such as amino acids and glucose is a pivotal function of the liver. Under normal circumstances, the fetus is dependent on a continuous supply of glucose from the mother, and no significant production of glucose (gluconeogenesis) by the fetus has been demonstrated [86]. Conversely, a rapid rise of hepatic gluconeogenesis is observed in newborn mammals in parallel with the appearance of PCK1, the key enzyme of this pathway [87]. Specifically, in humans, gluconeogenesis is apparent soon after birth in healthy newborns and it contributes 30% of the total glucose produced [88]. Our proteomics data revealed significantly higher levels of PCK1 in PHG liver. Increased levels of gluconeogenic precursors were observed in the plasma of piglets born to diabetic mothers [18], and was explained by reduced insulin sensitivity. Impaired insulin sensitivity was also observed in offspring exposed to hyperglycemia *in utero* due to maternal GDM or type 1 diabetes compared with offspring from the background population [89]. It was proposed that increased rates of gluconeogenesis in the offspring born to diabetic mothers may be predictive of the increased risk of glucose intolerance in later life [89]. Interestingly, PCK1 was elevated in the liver of the male but not in female offspring born to streptozotocin (STZ)-induced diabetic mice [90]. Similarly, in our study increase in PCK1 levels were almost three times higher in male than in female PHG when compared to PNG. We also observed significantly elevated circulating levels of ALT in the PHG male but not in female offspring. ALT catalyzes conversion of the main gluconeogenic precursor alanine into pyruvate for glucose production and thus plays an important role in gluconeogenesis [91]. An ALT blood test is used to diagnose liver disorders [92] and it has been shown that ALT activities are increased in gluconeogenic conditions and may be implicated in the development of diabetes. Higher rates of gluconeogenesis in PHG may be explained by a

failure of insulin to inhibit gluconeogenesis in the setting of decreased insulin sensitivity [93]. Indeed, as revealed by QUICKI and HOMA-IR index, PHG had reduced insulin sensitivity with a more pronounced effect in male offspring. In line with this observation, notable sex-specific differences with regard to glucose metabolism were reported and females were shown to have higher whole-body insulin sensitivity than males [94]. The exact mechanism responsible for sex-specific differences in insulin sensitivity is not well understood, however, sex hormones or adipokines were proposed as potential contributors [95]. TAT which catalyzes the conversion of tyrosine to 4-hydroxyphenylpyruvate was another transaminase elevated in the PHG liver. In line, metabolomics showed near significance of reduced levels of tyrosine ($I2fc = -0.47$, adjusted p -value $= 0.06$), suggesting an active tyrosine catabolism. TAT is a gluconeogenic enzyme which is activated in the liver shortly after birth [96]. A potential mediator of decreased insulin sensitivity in PHG might be elevated NEFA levels [97]. Even slight elevation in plasma NEFA, whose flux is high, can significantly increase hepatic uptake [98]. Interestingly, higher expression of interferon-stimulated genes (ISGs) was observed in insulin resistant human patients [99]. ISG15 was positively correlated with insulin sensitivity and glucose homeostasis in humans and mice [100]. ISGs are a group of genes that are stimulated in response to interferon, thus their upregulation may hint towards inflammation due to an immune response [99]. Low-grade chronic inflammation may be a potential driver of insulin resistance in obesity and NAFLD [101]. A recent study reported the enrichment of ISGs, including IF44, in GDM human amniocytes [102]. Besides, the metabolic-inflammatory circuit that links perturbations in lipid homeostasis with the activation of innate immunity was suggested [103]. Taken together, upregulation of gluconeogenic precursors and related enzymes suggests higher rates of gluconeogenesis in PHG liver which may be associated with impaired insulin sensitivity and glucose intolerance in later life. In conclusion, using a clinically relevant large animal model we showed that maternal hyperglycemia without confounding obesity results in profound metabolic alterations in the neonatal offspring's liver. Specifically, maternal hyperglycemia was related with increased rates of hepatic gluconeogenesis, amino acid metabolism and beta-oxidation but decreased rates of lipogenesis in PHG. Additionally, we found that hepatic PC biosynthesis was reduced while catabolism and translocation to bile was increased in PHG. We hypothesize that elevated PC levels despite reduced biosynthesis may be due to increased transplacental transfer and subsequent downregulation of enzymes involved in its synthesis via a feedback loop mechanism. In this study protein abundance changes alongside with quantitative data of metabolites were used as a proxy for the state of biochemical processes, however, our comprehensive dataset would greatly benefit from future studies assessing further measures of protein activity such as protein interactions and post-translational modifications. The generated datasets provide an important resource for future comparative or meta-analysis studies on the progression of hepatic complications and other associated comorbidities in neonatal offspring due to isolated maternal hyperglycemia.

FUNDING

This study was supported by the German Center for Diabetes Research (DZD e.V.). This project has received funding from the European Union's Horizon 2020 research and innovation programme under the Marie Skłodowska-Curie grant agreement No 812660 (DohART-NET).

Original Article

AUTHOR CONTRIBUTIONS

B.S., L.V., E.W., E.K. and T.F.: Conceptualization; B.S.: Methodology, Software, Data curation and analysis, Writing- Original draft; B.S., L.V., S.D.L., C.P., M.H., F.R., R.E., B.R., J.M. and M.H.d.A.: Investigation; L.V., S.D.L., J.B.S., S.R., E.W., E.K. and T.F.: Writing- Reviewing and Editing; E.W., E.K. and T.F.: Supervision, Resources, Funding acquisition

DATA AND RESOURCE AVAILABILITY

The mass spectrometry proteomics data generated and analyzed in this study have been deposited to the ProteomeXchange Consortium via the PRIDE [45] partner repository, <http://proteomecentral.proteomexchange.org>; PXD040305. The metabolomics and clinical parameters results are included in the article/Supplementary Materials. Code to reproduce statistical analysis and visualization is available at: <https://github.com/bshashikadze/maternaldiabetes-offspring-liver-omics-paper>

DECLARATION OF COMPETING INTEREST

The authors declare that they have no known competing financial interests or personal relationships that could have appeared to influence the work reported in this paper.

DATA AVAILABILITY

Datasets and codes used for the analysis and visualization have been deposited in dedicated repositories and the links are included in the manuscript

ACKNOWLEDGMENTS

We acknowledge Christina Blechinger, Florentine Stotz, Tatiana Schröter, Silke Becker, Birgit Lange, Dr. Alexander Cecil, Michelle Kozubiak and Florian Schleicher for excellent technical assistance. Parts of the graphical abstract and Figure 1A were drawn by using pictures from Servier Medical Art. Servier Medical Art by Servier is licensed under a Creative Commons Attribution 3.0 Unported License (<https://creativecommons.org/licenses/by/3.0/>).

APPENDIX A. SUPPLEMENTARY DATA

Supplementary data to this article can be found online at <https://doi.org/10.1016/j.molmet.2023.101768>.

REFERENCES

- [1] Kwon EJ, Kim YJ. What is fetal programming?: a lifetime health is under the control of in utero health. *Obstet Gynecol Sci* 2017;60(6):506–19.
- [2] Parretti S, Caroli A, Torlone E. Nutrition and metabolic adaptations in physiological and complicated pregnancy: focus on obesity and gestational diabetes. *Front Endocrinol* 2020;11:611929.
- [3] Franzago M, Fraticelli F, Stuppia L, Vitacolonna E. Nutrigenetics, epigenetics and gestational diabetes: consequences in mother and child. *Epigenetics* 2019;14(3):215–35.
- [4] Shashikadze B, Flenkenthaler F, Stöckl J, Valla L, Renner S, Kemter E, et al. Developmental effects of (Pre-)Gestational diabetes on offspring: systematic screening using omics approaches. *Genes* 2021;12:1991.

- [5] Clausen TD, Mathiesen ER, Hansen T, Pedersen O, Jensen DM, Lauenborg J, et al. Overweight and the metabolic syndrome in adult offspring of women with diet-treated gestational diabetes mellitus or type 1 diabetes. *J Clin Endocrinol Metab* 2009;94(7):2464–70.
- [6] Albl B, Haesner S, Braun-Reichhart C, Streckel E, Renner S, Seeliger F, et al. Tissue sampling guides for porcine biomedical models. *Toxicol Pathol* 2016;44(3):414–20.
- [7] Zettler S, Renner S, Kemter E, Hinrichs A, Klymiuk N, Backman M, et al. A decade of experience with genetically tailored pig models for diabetes and metabolic research. *Anim Reprod* 2020;17(3):e20200064.
- [8] Wolf E, Braun-Reichhart C, Streckel E, Renner S. Genetically engineered pig models for diabetes research. *Transgenic Res* 2013;23.
- [9] Renner S, Blutke A, Clauss S, Deeg CA, Kemter E, Merkus D, et al. Porcine models for studying complications and organ crosstalk in diabetes mellitus. *Cell Tissue Res* 2020;380(2):341–78.
- [10] Litten-Brown JC, Corson AM, Clarke L. Porcine models for the metabolic syndrome, digestive and bone disorders: a general overview. *Animal* 2010;4(6):899–920.
- [11] Mota-Rojas D, Orozco-Gregorio H, Villanueva-García D, Bonilla-Jaime H, Suarez-Bonilla X, Hernández-González R, et al. Foetal and neonatal energy metabolism in pigs and humans: a review. *Vet Med* 2018;56:215–25.
- [12] Yu YH, Ginsberg HN. Adipocyte signaling and lipid homeostasis: sequelae of insulin-resistant adipose tissue. *Circ Res* 2005;96(10):1042–52.
- [13] Patel S, Lawlor DA, Callaway M, Macdonald-Wallis C, Sattar N, Fraser A. Association of maternal diabetes/glycosuria and pre-pregnancy body mass index with offspring indicators of non-alcoholic fatty liver disease. *BMC Pediatr* 2016;16:47.
- [14] Brumbaugh DE, Tearse P, Cree-Green M, Fenton LZ, Brown M, Scherzinger A, et al. Intrahepatic fat is increased in the neonatal offspring of obese women with gestational diabetes. *J Pediatr* 2013;162(5):930–936.e1.
- [15] Oben JA, Mouralidarane A, Samuelsson AM, Matthews PJ, Morgan ML, McKee C, et al. Maternal obesity during pregnancy and lactation programs the development of offspring non-alcoholic fatty liver disease in mice. *J Hepatol* 2010;52(6):913–20.
- [16] Mouralidarane A, Soeda J, Visconti-Pugmire C, Samuelsson AM, Pombo J, Maragkoudaki X, et al. Maternal obesity programs offspring nonalcoholic fatty liver disease by innate immune dysfunction in mice. *Hepatology* 2013;58(1):128–38.
- [17] Geurtsen ML, Wahab RJ, Felix JF, Gaillard R, Jaddoe VWV. Maternal early-pregnancy glucose concentrations and liver fat among school-age children. *Hepatology* 2021;74(4):1902–13.
- [18] Renner S, Martins AS, Streckel E, Braun-Reichhart C, Backman M, Prehn C, et al. Mild maternal hyperglycemia in INS (C93S) transgenic pigs causes impaired glucose tolerance and metabolic alterations in neonatal offspring. *Dis Model Mech* 2019;12(8).
- [19] Renner S, Braun-Reichhart C, Blutke A, Herbach N, Emrich D, Streckel E, et al. Permanent neonatal diabetes in INS(C94Y) transgenic pigs. *Diabetes* 2013;62(5):1505–11.
- [20] Searle BC, Pino LK, Egertson JD, Ting YS, Lawrence RT, MacLean BX, et al. Chromatogram libraries improve peptide detection and quantification by data independent acquisition mass spectrometry. *Nat Commun* 2018;9(1):5128. 5128.
- [21] Pino LK, Just SC, MacCoss MJ, Searle BC. Acquiring and analyzing data independent acquisition proteomics experiments without spectrum libraries. *Mol Cell Proteomics* 2020;19(7):1088–103.
- [22] Amodei D, Egertson J, MacLean BX, Johnson R, Merrihew GE, Keller A, et al. Improving precursor selectivity in data-independent acquisition using overlapping windows. *J Am Soc Mass Spectrom* 2019;30(4):669–84.

- [23] MacLean B, Tomazela DM, Shulman N, Chambers M, Finney GL, Frewen B, et al. Skyline: an open source document editor for creating and analyzing targeted proteomics experiments. *Bioinformatics* 2010;26(7):966–8.
- [24] Tyanova S, Temu T, Cox J. The MaxQuant computational platform for mass spectrometry-based shotgun proteomics. *Nat Protoc* 2016;11(12):2301–19.
- [25] Cox J, Hein MY, Luber CA, Paron I, Nagaraj N, Mann M. Accurate proteome-wide label-free quantification by delayed normalization and maximal peptide ratio extraction, termed MaxLFQ. *Mol Cell Proteomics* 2014;13(9):2513–26.
- [26] Stekhoven DJ, Bühlmann P. MissForest—non-parametric missing value imputation for mixed-type data. *Bioinformatics* 2011;28(1):112–8.
- [27] Szklarczyk D, Gable AL, Lyon D, Junge A, Wyder S, Huerta-Cepas J, et al. STRING v11: protein–protein association networks with increased coverage, supporting functional discovery in genome-wide experimental datasets. *Nucleic Acids Res* 2018;47(D1):D607–13.
- [28] Ashburner M, Ball CA, Blake JA, Botstein D, Butler H, Cherry JM, et al. Gene Ontology: tool for the unification of biology. *Nat Genet* 2000;25(1):25–9.
- [29] Kanehisa M, Goto S. KEGG: kyoto encyclopedia of genes and genomes. *Nucleic Acids Res* 2000;28(1):27–30.
- [30] Fang Z, Liu X, Peltz G. GSEAPy: a comprehensive package for performing gene set enrichment analysis in Python. *Bioinformatics* 2022;39(1).
- [31] Piñero J, Queralt-Rosinach N, Bravo A, Deu-Pons J, Bauer-Mehren A, Baron M, et al. DisGeNET: a discovery platform for the dynamical exploration of human diseases and their genes. *Oxford: Database*; 2015, bav028. 2015.
- [32] Guney E, Menche J, Vidal M, Barabasi A-L. Network-based in silico drug efficacy screening. *Nat Commun* 2016;7(1):10331.
- [33] Zukunif S, Prehn C, Röhring C, Möller G, Hrabě de Angelis M, Adamski J, et al. High-throughput extraction and quantification method for targeted metabolomics in murine tissues. *Metabolomics* 2018;14(1):18.
- [34] Su B, Bettcher LF, Hsieh WY, Hornburg D, Pearson MJ, Blomberg N, et al. A DMS shotgun lipidomics workflow application to facilitate high-throughput, comprehensive lipidomics. *J Am Soc Mass Spectrom* 2021;32(11):2655–63.
- [35] Broadhurst D, Goodacre R, Reinke SN, Kuligowski J, Wilson ID, Lewis MR, et al. Guidelines and considerations for the use of system suitability and quality control samples in mass spectrometry assays applied in untargeted clinical metabolomic studies. *Metabolomics* 2018;14(6):72.
- [36] Do KT, Wahl S, Raffler J, Molnos S, Laimighofer M, Adamski J, et al. Characterization of missing values in untargeted MS-based metabolomics data and evaluation of missing data handling strategies. *Metabolomics* 2018;14(10):128.
- [37] Meng C, Kuster B, Culhane AC, Gholami AM. A multivariate approach to the integration of multi-omics datasets. *BMC Bioinf* 2014;15(1):162.
- [38] Rathkolb B, Hans W, Prehn C, Fuchs H, Gailus-Dürner V, Aigner B, et al. Clinical chemistry and other laboratory tests on mouse plasma or serum. *Curr Protoc Mol Biol* 2013;3(2):69–100.
- [39] Matthews DR, Hosker JP, Rudenski AS, Naylor BA, Treacher DF, Turner RC. Homeostasis model assessment: insulin resistance and beta-cell function from fasting plasma glucose and insulin concentrations in man. *Diabetologia* 1985;28(7):412–9.
- [40] Katz A, Nambi SS, Mather K, Baron AD, Follmann DA, Sullivan G, et al. Quantitative insulin sensitivity check index: a simple, accurate method for assessing insulin sensitivity in humans. *J Clin Endocrinol Metab* 2000;85(7):2402–10.
- [41] Gu Z, Eils R, Schlesner M. Complex heatmaps reveal patterns and correlations in multidimensional genomic data. *Bioinformatics* 2016;32(18):2847–9.
- [42] Thévenot E, Roux A, Xu Y, Ezan E, Junot C. Analysis of the human adult urinary metabolome variations with age, body mass index, and gender by implementing a comprehensive workflow for univariate and OPLS statistical analyses. *J Proteome Res* 2015;14.
- [43] Liao Y, Wang J, Jaehnig EJ, Shi Z, Zhang B. WebGestalt 2019: gene set analysis toolkit with revamped UIs and APIs. *Nucleic Acids Res* 2019;47(W1):W199–205.
- [44] Ahlqvist E, Storm P, Käräjämäki A, Martinell M, Dorkhan M, Carlsson A, et al. Novel subgroups of adult-onset diabetes and their association with outcomes: a data-driven cluster analysis of six variables. *Lancet Diabetes Endocrinol* 2018;6(5):361–9.
- [45] Perez-Riverol Y, Bai J, Bandla C, García-Seisdedos D, Hewapathirana S, Kamatchinathan S, et al. The PRIDE database resources in 2022: a hub for mass spectrometry-based proteomics evidences. *Nucleic Acids Res* 2022;50(D1):D543–52.
- [46] Blütke A, Renner S, Flenkenthaler F, Backman M, Haesner S, Kemter E, et al. The Munich MIDY Pig Biobank - a unique resource for studying organ crosstalk in diabetes. *Mol Metabol* 2017;6(8):931–40.
- [47] Dolédec S, Chessel D. Co-inertia analysis: an alternative method for studying species–environment relationships. *Freshw Biol* 1994;31(3):277–94.
- [48] Samii L, Kallas-Koeman M, Donovan LE, Lodha A, Crawford S, Butalia S. The association between vascular complications during pregnancy in women with Type 1 diabetes and congenital malformations. *Diabet Med* 2019;36(2):237–42.
- [49] Biesenbach G, Grafinger P, Zazgornik J, Stöger H. Perinatal complications and three-year follow up of infants of diabetic mothers with diabetic nephropathy stage IV. *Ren Fail* 2000;22(5):573–80.
- [50] Ormoy A, Becker M, Weinstein-Fudim L, Ergaz Z. Diabetes during pregnancy: a maternal disease complicating the course of pregnancy with long-term deleterious effects on the offspring. A clinical review. *Int J Mol Sci* 2021;22(6).
- [51] Young BC, Ecker JL. Fetal macrosomia and shoulder dystocia in women with gestational diabetes: risks amenable to treatment? *Curr Diabetes Rep* 2013;13(1):12–8.
- [52] He J, Song J, Zou Z, Fan X, Tian R, Xu J, et al. Association between neonatal hyperbilirubinemia and hypoglycemia in Chinese women with diabetes in pregnancy and influence factors. *Sci Rep* 2022;12(1):16975.
- [53] Hochrath K, Krawczyk M, Goebel R, Langhirt M, Rathkolb B, Micklich K, et al. The hepatic phosphatidylcholine transporter ABCB4 as modulator of glucose homeostasis. *Faseb J* 2012;26(12):5081–91.
- [54] Ikeda Y, Morita S-y, Terada T. Cholesterol attenuates cytoprotective effects of phosphatidylcholine against bile salts. *Sci Rep* 2017;7(1):306.
- [55] Nosol K, Bang-Sørensen R, Irobalieva R, Erramilli S, Stieger B, Kossiakoff A, et al. Structures of ABCB4 provide insight into phosphatidylcholine translocation. *Proc Natl Acad Sci USA* 2021;118:e2106702118.
- [56] Oude Elferink RP, Paulusma CC. Function and pathophysiological importance of ABCB4 (MDR3 P-glycoprotein). *Pflügers Archiv* 2007;453(5):601–10.
- [57] Li Z, Agellon LB, Vance DE. Phosphatidylcholine homeostasis and liver failure. *J Biol Chem* 2005;280(45):37798–802.
- [58] Gabbs M, Leng S, Devassy JG, Monirujjaman M, Aukema HM. Advances in our understanding of oxylipins derived from dietary PUFAs. *Advances in nutrition (Bethesda, Md)* 2015;6(5):513–40.
- [59] Fagone P, Jackowski S. Phosphatidylcholine and the CDP-choline cycle. *Biochim Biophys Acta* 2013;1831(3):523–32.
- [60] Zhang Q, Yao D, Rao B, Jian L, Chen Y, Hu K, et al. The structural basis for the phospholipid remodeling by lysophosphatidylcholine acyltransferase 3. *Nat Commun* 2021;12(1):6869.
- [61] Lowe Jr WL, Bain JR, Nodzinski M, Reissetter AC, Muehlbauer MJ, Stevens RD, et al. Maternal BMI and glycemia impact the fetal metabolome. *Diabetes Care* 2017;40(7):902–10.
- [62] Ott R, Pawlow X, Weiss A, Hofelich A, Herbst M, Hummel N, et al. Inter-generational metabolomic analysis of mothers with a history of gestational diabetes mellitus and their offspring. *Int J Mol Sci* 2020;21(24).
- [63] Nassir F, Rector RS, Hammoud GM, Ibdah JA. Pathogenesis and prevention of hepatic steatosis. *Gastroenterol Hepatol* 2015;11(3):167–75.

Original Article

- [64] Geurtsen ML, Santos S, Felix JF, Duijts L, Vermooij MW, Gaillard R, et al. Liver fat and cardiometabolic risk factors among school-age children. *Hepatology* 2020;72(1):119–29.
- [65] Britton KA, Fox CS. Ectopic fat depots and cardiovascular disease. *Circulation* 2011;124(24):e837–41.
- [66] Patel KR, White FV, Deutsch GH. Hepatic steatosis is prevalent in stillborns delivered to women with diabetes mellitus. *J Pediatr Gastroenterol Nutr* 2015;60(2):152–8.
- [67] Knorr S, Bytøft B, Lohse Z, Boisen AB, Clausen TD, Jensen RB, et al. Fatty liver among adolescent offspring of women with type 1 diabetes (the EPICOM study). *Diabetes Care* 2019;42(8):1560–8.
- [68] Pereira TJ, Fonseca MA, Campbell KE, Moyce BL, Cole LK, Hatch GM, et al. Maternal obesity characterized by gestational diabetes increases the susceptibility of rat offspring to hepatic steatosis via a disrupted liver metabolome. *J Physiol* 2015;593(14):3181–97.
- [69] Philipps LH, Santhakumaran S, Gale C, Prior E, Logan KM, Hyde MJ, et al. The diabetic pregnancy and offspring BMI in childhood: a systematic review and meta-analysis. *Diabetologia* 2011;54(8):1957–66.
- [70] Kim SY, England JL, Sharma JA, Njoroge T. Gestational diabetes mellitus and risk of childhood overweight and obesity in offspring: a systematic review. *Exp Diabetes Res* 2011;2011:541308.
- [71] Ferré P, Foufelle F. Hepatic steatosis: a role for de novo lipogenesis and the transcription factor SREBP-1c. *Diabetes Obes Metabol* 2010;12(Suppl 2):83–92.
- [72] Kim CW, Moon YA, Park SW, Cheng D, Kwon HJ, Horton JD. Induced polymerization of mammalian acetyl-CoA carboxylase by MIG12 provides a tertiary level of regulation of fatty acid synthesis. *Proc Natl Acad Sci U S A* 2010;107(21):9626–31.
- [73] Radenne A, Akpa M, Martel C, Sawadogo S, Mauvoisin D, Mounier C. Hepatic regulation of fatty acid synthesis by insulin and T3: evidence for T3 genomic and nongenomic actions. *Am J Physiol Endocrinol Metab* 2008;295(4):E884–94.
- [74] Orland MD, Anwar K, Cromley D, Chu CH, Chen L, Billheimer JT, et al. Acyl coenzyme A dependent retinol esterification by acyl coenzyme A: diacylglycerol acyltransferase 1. *Biochim Biophys Acta* 2005;1737(1):76–82.
- [75] Liang JJ, Oelkers P, Guo C, Chu P-C, Dixon JL, Ginsberg HN, et al. Overexpression of human diacylglycerol acyltransferase 1, acyl-CoA:cholesterol acyltransferase 1, or acyl-CoA:cholesterol acyltransferase 2 stimulates secretion of apolipoprotein B-containing lipoproteins in McA-RH7777 cells*. *J Biol Chem* 2004;279(43):44938–44.
- [76] Yamaguchi K, Yang L, McCall S, Huang J, Yu XX, Pandey SK, et al. Diacylglycerol acyltransferase 1 anti-sense oligonucleotides reduce hepatic fibrosis in mice with nonalcoholic steatohepatitis. *Hepatology* 2008;47(2):625–35.
- [77] Cheng X, Gong F, Pan M, Wu X, Zhong Y, Wang C, et al. Targeting DGAT1 ameliorates glioblastoma by increasing fat catabolism and oxidative stress. *Cell Metabol* 2020;32(2):229–242.e8.
- [78] Yang W, Wang S, Looor JJ, Lopes MG, Zhao Y, Ma X, et al. Role of diacylglycerol O-acyltransferase (DGAT) isoforms in bovine hepatic fatty acid metabolism. *J Dairy Sci* 2022;105(4):3588–600.
- [79] Friedman JE. Developmental programming of obesity and diabetes in mouse, monkey, and man in 2018: where are we headed? *Diabetes* 2018;67(11):2137–51.
- [80] Renner S, Blütke A, Dobenecker B, Dhom G, Müller TD, Finan B, et al. Metabolic syndrome and extensive adipose tissue inflammation in morbidly obese Göttingen minipigs. *Mol Metabol* 2018;16:180–90.
- [81] Villanueva CJ, Monetti M, Shih M, Zhou P, Watkins SM, Bhanot S, et al. Specific role for acyl CoA:Diacylglycerol acyltransferase 1 (Dgat1) in hepatic steatosis due to exogenous fatty acids. *Hepatology* 2009;50(2):434–42.
- [82] O'Farrell M, Duke G, Crowley R, Buckley D, Martins EB, Bhattacharya D, et al. FASN inhibition targets multiple drivers of NASH by reducing steatosis, inflammation and fibrosis in preclinical models. *Sci Rep* 2022;12(1):15661.
- [83] Bergen WG, Mersmann HJ. Comparative aspects of lipid metabolism: impact on contemporary research and use of animal models. *J Nutr* 2005;135(11):2499–502.
- [84] Walker Amy K, René L, Jacobs Jennifer L, Watts V, Jiang Rottiers K, Deirdre M Finnegan, et al. A conserved SREBP-1/phosphatidylcholine feedback circuit regulates lipogenesis in metazoans. *Cell* 2011;147(4):840–52.
- [85] Osipova D, Kokoreva K, Lazebnik L, Golovanova E, Pavlov C, Dukhanin A, et al. Regression of liver steatosis following phosphatidylcholine administration: a review of molecular and metabolic pathways involved. *Front Pharmacol* 2022;13:797923.
- [86] Kalhan S, Parimi P. Gluconeogenesis in the fetus and neonate. *Semin Perinatol* 2000;24(2):94–106.
- [87] Girard J. Gluconeogenesis in late fetal and early neonatal life. *Biol Neonate* 1986;50(5):237–58.
- [88] Kalhan SC, Parimi P, Van Beek R, Gillilan C, Saker F, Gruca L, et al. Estimation of gluconeogenesis in newborn infants. *Am J Physiol Endocrinol Metab* 2001;281(5):E991–7.
- [89] Kelstrup L, Damm P, Mathiesen ER, Hansen T, Vaag AA, Pedersen O, et al. Insulin resistance and impaired pancreatic β -cell function in adult offspring of women with diabetes in pregnancy. *J Clin Endocrinol Metab* 2013;98(9):3793–801.
- [90] Inoguchi Y, Ichiyanagi K, Ohishi H, Maeda Y, Sonoda N, Ogawa Y, et al. Poorly controlled diabetes during pregnancy and lactation activates the Foxo1 pathway and causes glucose intolerance in adult offspring. *Sci Rep* 2019;9(1):10181.
- [91] Zhang X, Yang S, Chen J, Su Z. Unraveling the regulation of hepatic gluconeogenesis. *Front Endocrinol* 2019;9.
- [92] Hall P, Cash J. What is the real function of the liver 'function' tests? *Ulster Med J* 2012;81(1):30–6.
- [93] Hatting M, Tavares CDJ, Sharabi K, Rines AK, Puigserver P. Insulin regulation of gluconeogenesis. *Ann N Y Acad Sci* 2018;1411(1):21–35.
- [94] Varlamov O, Bethea CL, Roberts Jr CT. Sex-specific differences in lipid and glucose metabolism. *Front Endocrinol* 2014;5:241.
- [95] Geer EB, Shen W. Gender differences in insulin resistance, body composition, and energy balance. *Genet Med* 2009;6(Suppl 1):60–75.
- [96] Cole TJ, Blendy JA, Monaghan AP, Schmid W, Aguzzi A, Schütz G. Molecular genetic analysis of glucocorticoid signaling during mouse development. *Steroids* 1995;60(1):93–6.
- [97] Karpe F, Dickmann JR, Frayn KN. Fatty acids, obesity, and insulin resistance: time for a reevaluation. *Diabetes* 2011;60(10):2441–9.
- [98] Santos-Baez LS, Ginsberg HN. Nonalcohol fatty liver disease: balancing supply and utilization of triglycerides. *Curr Opin Lipidol* 2021;32(3):200–6.
- [99] Kalafati M, Kutmon M, Evelo CT, van der Kallen CJH, Schalkwijk CG, Stehouwer CDA, et al. An interferon-related signature characterizes the whole blood transcriptome profile of insulin-resistant individuals—the CODAM study. *Genes & Nutrition* 2021;16(1):22.
- [100] Yan S, Kumari M, Xiao H, Jacobs C, Kochumon S, Jedrychowski M, et al. IRF3 reduces adipose thermogenesis via ISG15-mediated reprogramming of glycolysis. *J Clin Invest* 2021;131(7).
- [101] Wieser V, Adolph TE, Grander C, Grabherr F, Enrich B, Moser P, et al. Adipose type I interferon signalling protects against metabolic dysfunction. *Gut* 2018;67(1):157–65.
- [102] Pinney SE, Joshi A, Yin V, Min SW, Rashid C, Condon DE, et al. Exposure to gestational diabetes enriches immune-related pathways in the transcriptome and methylome of human amniocytes. *J Clin Endocrinol Metab* 2020;105(10).
- [103] York AG, Williams KJ, Argus JP, Zhou QD, Brar G, Vergnes L, et al. Limiting cholesterol biosynthetic flux spontaneously engages type I IFN signaling. *Cell* 2015;163(7):1716–29.

3. Section B: Investigation of the effect of hyperglycaemia on lung

3.1. Literature review

3.1.1. Physiology and anatomy of lung – susceptibility to diabetes

Historically, the lung is not recognized as a major target organ of diabetic injury. Mechanistically, the effect of diabetes on lung tissue is multifactorial and not clearly understood. Additionally, pulmonary damage is mostly subclinical and thus difficult to detect [55]. The pulmonary system is prone to undergo microvascular damage and non-enzymatic glycation because of its large alveolar-capillary network and the abundance of connective tissue [56]. However, because of its large reserve, substantial loss of the microvascular bed can be tolerated without developing dyspnoea [57]. As a result, as mentioned above, pulmonary diabetic microangiopathy may be under-recognized clinically. The first study to suggest that the lung may be a target organ of diabetes was conducted nearly five decades ago [58], and investigated the lung function of young patients with type 1 diabetes. The study found a decrease in lung elastic recoil which was suggested to be a risk factor for developing chronic airflow obstruction. The effects of diabetes on the lung are reviewed in [55, 57, 59-62]. Hyperglycemia has been shown to lead to interstitial fibrosis (reviewed in [56]), and alveolar-capillary microangiopathy, it is associated with both restrictive and obstructive lung function impairment and was shown to contribute to an overproduction of mucus and surfactant associated with increased mortality rates [63].

Increased susceptibility to respiratory infections is frequently observed in the context of diabetes. Higher hospitalization and mortality rates were observed in diabetic patients with viral or bacterial infections such as influenza [64], COVID-19 [65], and others. A systematic review of the association between lung function and Type 2 diabetes mellitus concluded that systemic and local inflammation may play a major role and explain the associations between different conditions, including reduced lung function and Type 2 diabetes [57]. Additionally, diabetes significantly increases mortality rates in patients with idiopathic pulmonary fibrosis [66]. Furthermore, individuals with diabetes are at increased risk of developing further pulmonary conditions such as asthma, pulmonary fibrosis, and chronic obstructive pulmonary

disease (COPD) [67]. One report documented a fourfold increase in leukotriene B4 (proinflammatory mediator) in subjects with chronic obstructive pulmonary disease (COPD) who also had diabetes, compared with COPD patients and asthmatics without diabetes [68].

3.1.2. Pig lung – relevance to study human disease

The swine lung has become an excellent model for the normal human lung, for pathological abnormalities, for the development of therapies [69] and is even a promising option for lung xenotransplantation. For example, porcine lungs have been used to study lung development [70], lung transplantation [71], pulmonary artery hypertension [72], pulmonary vein hypertension [73], asthma [74], COPD [74], cystic fibrosis [75] and many other diseases. The morphological structure and distribution of the porcine airways are broadly similar to the human lung although they vary according to the age and breed of pig (extensive comparison between human and porcine lungs can be found in [69, 76]). The lungs of pigs and humans are highly lobulated, with well-defined pulmonary lobules distinguished by interlobular septae [76]. The porcine lung has two lobes on the left side and four lobes on the right side, conversely, humans have three right and two left lobes. Similar to other mammalian species pig and human lung have extensive interlobular and intralobular connective tissue, which is not true for the mice [77]. Anatomical similarities were also observed in the upper respiratory tract between humans and pigs [78]. Furthermore, similarities were observed between cellular lineages and composition [69]. Since the respiratory tract is constantly exposed to pathogens, the normal functioning of defence mechanisms is crucial to protect the lung. In this context, it is important that most proteins of the porcine immune system share structural and functional similarities with their human counterparts [79].

3.2. Article 3

This chapter contains a manuscript with the title:

Multi-omics analysis of diabetic pig lungs reveals molecular derangements underlying pulmonary complications of diabetes mellitus

Bachuki Shashikadze, Florian Flenkenthaler, Elisabeth Kemter, Sophie Franzmeier, Jan B. Stöckl, Mark Haid, Fabien Riols, Michael Rothe, Lisa Pichl, Simone Renner, Andreas Blutke, Eckhard Wolf, Thomas Fröhlich

Author contributions:

B.S., F.F., E.W., and T.F.: conceptualization; B.S.: Software, Data Curation, Formal Analysis, Investigation, Visualization, Writing – Original Draft; J.B.S., E.W. and T.F.: Reviewing and Editing. B.S., E.K., S.F., L.P. and A.B.: Investigation; M.R., F.R., M.H., Lipidomics measurements; S.R., A.B. and E.W.: Resources. E.W., T.F.: Supervision and Funding acquisition.

Multi-omics analysis of diabetic pig lungs reveals molecular derangements underlying pulmonary complications of diabetes mellitus

Bachuki Shashikadze¹, Florian Flenkenthaler^{1,2}, Elisabeth Kemter^{2,3,4}, Sophie Franzmeier⁵, Jan B. Stöckl¹, Mark Haid⁶, Fabien Riols⁶, Michael Rothe⁷, Lisa Pichl⁵, Simone Renner^{2,3,4}, Andreas Blutke⁵, Eckhard Wolf^{1,2,3,4,*}, Thomas Fröhlich^{1,*},⁸

¹Laboratory for Functional Genome Analysis (LAFUGA), Gene Center, LMU Munich, 81377 Munich, Germany;

²German Center for Diabetes Research (DZD), 85764 Neuherberg, Germany;

³Chair for Molecular Animal Breeding and Biotechnology, Gene Center and Department of Veterinary Sciences, LMU Munich, 81377 Munich, Germany

⁴Center for Innovative Medical Models (CiMM), LMU Munich, 85764 Oberschleißheim, Germany

⁵Institute for Veterinary Pathology, Center for Clinical Veterinary Medicine, LMU Munich, Germany

⁶Metabolomics and Proteomics Core (MPC), Helmholtz Zentrum München, 85764 Neuherberg, Germany

⁷Lipidomix GmbH, 13125 Berlin, Germany

* Corresponding author. Gene Center, LMU Munich, Feodor-Lynen-Str. 25, 81377 Munich, Germany. ORCID: <https://orcid.org/0000-0002-0430-9510>;

E-mail: ewolf@genzentrum.lmu.de (E. Wolf).

* Corresponding author. Gene Center, LMU Munich, Feodor-Lynen-Str. 25, 81377 Munich, Germany. ORCID: <https://orcid.org/0000-0002-4709-3211>;

E-mail: frohlich@genzentrum.lmu.de (T. Fröhlich).

⁸ Contributed equally

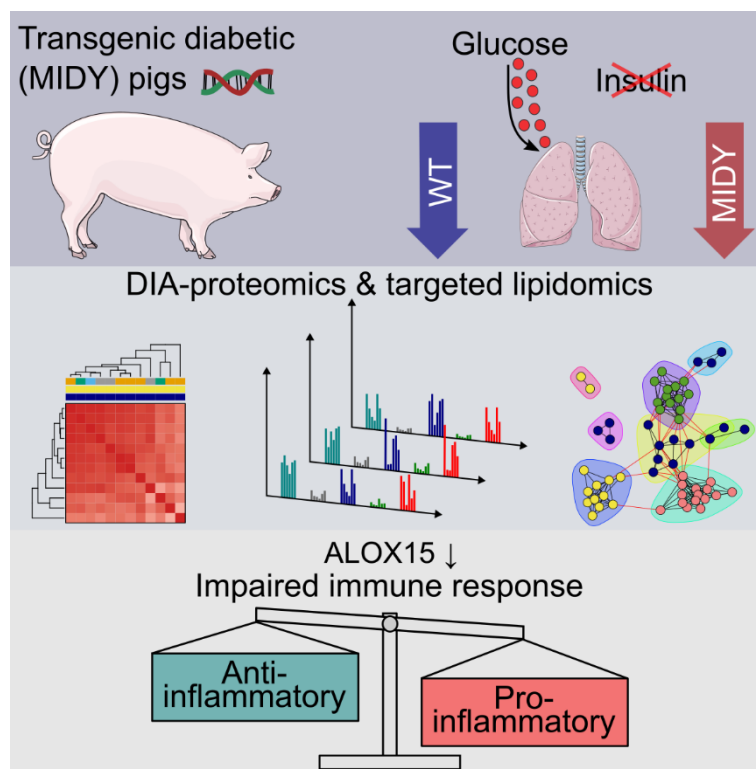
Highlights:

- Lung proteomes are affected by insulin deficiency and hyperglycemia
- Small leucine rich proteoglycans are increased in abundance in diabetic lung
- Proteins involved in immune system processes are reduced in diabetic lung
- Eicosanoid metabolism is impaired in diabetic lung
- Our study gives new insights into pathophysiological effects of diabetes in lung

In brief:

Data independent acquisition proteomics combined with lipidomics revealed alterations in the lipoxygenase metabolism in the diabetic lung from a clinically relevant large animal model. We observed a strong reduction of polyunsaturated fatty acid lipoxygenase (ALOX15) levels in the diabetic lung. Moreover, targeted lipidomics demonstrated reduced levels of inflammatory lipid mediators produced by ALOX15. This points to an imbalance in pro- and anti-inflammatory milieu in the diabetic lung which may contribute to frequently observed increased prevalence of infections in diabetic patients.

Graphical abstract:



ABSTRACT

Growing evidence shows that the lung is an organ prone to injury by diabetes mellitus. However, the molecular mechanisms of these pulmonary complications have not yet been characterized comprehensively. To systematically study the effects of insulin deficiency and hyperglycaemia on lung tissue, we combined proteomics and lipidomics with quantitative histomorphological analyses to compare lung tissue samples from a clinically relevant pig model for mutant *INS* gene induced diabetes of youth (MIDY) with samples from wild-type (WT) littermate controls. Among others, the level of pulmonary surfactant-associated protein A (SFTPA1), a biomarker of lung injury, was significantly elevated. Furthermore, key proteins related to humoral

immune response and extracellular matrix (ECM) organization were significantly altered in abundance. Importantly, a lipoxygenase pathway was dysregulated as indicated by a 2.5-fold reduction of polyunsaturated fatty acid lipoxygenase ALOX15 levels, associated with corresponding changes in the levels of lipids influenced by this enzyme. Our multi-omics study points to an involvement of reduced ALOX15 levels and an associated lack of eicosanoid switching as mechanisms contributing to a proinflammatory milieu in the lungs of subjects suffering from diabetes mellitus.

Keywords: Diabetes, biobank, insulin deficiency, lipidome, lipoxygenase, lung, pig model, proteome

ABBREVIATIONS

12-HETE, 12-hydroxyeicosatetraenoic acid; 14,15-DiHETE, 14,15-dihydroxyeicosatetraenoic; 14-HDHA, 14-hydroxydocosahexaenoic acid; 5,6-DiHETE, 5,6-dihydroxyeicosatetraenoic acid; AA, arachidonic acid; AGC, automatic gain control; ALOX15, polyunsaturated fatty acid lipoxygenase; APOA4, apolipoprotein A4; ASPN, asporin; C6, complement component C6; CES1, carboxylic ester hydrolase; CIA, co-inertia analysis; COPD, chronic obstructive pulmonary disease; CTGF, connective tissue growth factor; DAB, 3,3'-diaminobenzidine tetrahydrochloride dihydrate; DHA, docosahexaenoic acid; DIA, data-independent acquisition; ECHDC1, ethylmalonyl-CoA decarboxylase 1; ECM, extracellular matrix; EPA, eicosapentaenoic acid; FABP4, fatty acid-binding protein 4; LA, linoleic acid; LOOCV, leave-one-out cross-validation; LOX, lipoxygenase; LTA4, leukotriene A4; LTA4H, leukotriene A(4) hydrolase; LTB4, leukotriene B4; MIDY, mutant *INS* gene induced diabetes of youth; NCE normalized collision energy; PBS, phosphate-buffered saline; PCA, principal component analysis; PUFA, polyunsaturated fatty acid; SFTPA1, surfactant-associated protein A; SLRP, small-leucine-rich-proteoglycan; STZ, streptozotocin; SULT1E1, oestrogen sulfotransferase; TGFB1, transforming growth factor beta 1; WT, wild-type; α -LA, alpha-linolenic acid; γ -LA, gamma-linolenic acid.

INTRODUCTION

Diabetes mellitus alongside its associated complications has emerged as a global health problem whose prevalence has increased over the past decades. Diabetes causes profound long-term molecular effects on multiple tissues and organs. Traditionally, the chronic complications of diabetes are classified as macro- and microvascular complications [1]. The rich vascularization of the lungs and the abundance of connective tissue suggest that it may be affected by diabetic microvascular damage [2]. The pathophysiology of pulmonary symptoms in diabetes is complex and so far not clearly understood. In addition, pulmonary damage is mostly subclinical and therefore difficult to detect [2]. Multiple studies have pointed to various pulmonary complications in diabetes (reviewed in [2-4]). In particular, an increased susceptibility to respiratory infections is frequently observed in the context of diabetes. Since the respiratory tract is constantly exposed to pathogens, normal functioning of defence mechanisms is crucial to protect the lung. Higher hospitalization and mortality rates were observed in diabetic patients with viral or bacterial infections such as influenza [5], COVID-19 [6], and others. Additionally, diabetes significantly increases mortality rates in patients with idiopathic pulmonary fibrosis [7]. Furthermore, individuals with diabetes are at increased risk of developing further pulmonary conditions such as asthma, pulmonary fibrosis, and chronic obstructive pulmonary disease (COPD) [8].

So far, the research focus was mainly on epidemiological associations between diabetes and impaired lung function. However, for prevention and intervention strategies, understanding the underlying molecular mechanisms is crucial. Several rodent models have been established and provided valuable insights into the onset

and progression of diabetes [9]. Streptozotocin (STZ)-induced pancreatic injury in rodents is commonly used as a model of type 1 diabetes [10]. However, the confounding effects of STZ especially on the immune system [11] complicate the interpretation of the findings. Furthermore, rodents frequently lack clinical relevance due to fundamental physiological differences from humans. We thus investigated lung samples from *INS*^{C94Y} transgenic pigs, a tailored large animal model for mutant *INS* gene induced diabetes of youth (MIDY), characterized by impaired insulin secretion, β -cell loss, and chronic hyperglycaemia [12], and lung samples from wild-type (WT) littermate controls. Hyperglycaemia alone or the time of exposure to hyperglycaemia in MIDY pigs may not be sufficient to induce severe diabetic complications [13]. However, MIDY pigs develop diabetes-related alterations in various tissues including myocardium [14], retina [15], immune cells [16], liver [17], and adipose tissue [13, 18]. Although the full spectrum of complications as observed in humans is not described in porcine models, they are becoming increasingly important in diabetes research to bridge the gap between proof-of-concept studies in rodents and clinical trials [19, 20]. MIDY pigs exhibit a stable diabetic phenotype without further manipulation because of a specific clinically relevant impairment of β -cells [12, 21]. The pig is a valuable model in the context of respiratory medicine, as porcine and human lungs share many anatomic, histological, biochemical, and physiological characteristics [22]. Furthermore, functional similarities of the porcine host defence proteins with their human counterparts make the pig an excellent model to study the pathogenesis of respiratory inflammation [23].

In the present study, data-independent acquisition-based proteomics and targeted analysis of relevant lipid molecules were performed on lung tissue samples from the

Munich MIDY pig biobank [24] to systematically address pulmonary changes in response to chronic insulin deficiency and hyperglycaemia. Additional immunohistochemical and quantitative morphological analyses were carried out to localize differentially abundant key molecules in their pathophysiological context.

RESULTS

Overview of proteome differences

To investigate the molecular effects of chronic insulin deficiency and hyperglycaemia on the lung tissue proteome, we performed a label-free liquid chromatography-tandem mass spectrometry (LC-MS/MS) analysis of lung samples from MIDY and WT animals. Using a data-independent acquisition (DIA) (Figure 1A), we identified 45,411 distinct peptides from 5,465 protein groups with high confidence (false discovery rate < 0.01) (Tables S1-2). The dataset has been submitted to the ProteomeXchange Consortium via the PRIDE partner repository (PXD038014). Quantitative analysis using MS-EmpiRe workflow detected 265 proteins changed in abundance between MIDY versus WT with Benjamini–Hochberg corrected p-value ≤ 0.05 (Table S3), out of which 61 proteins were changed in abundance by at least 1.5-fold (Figure 1B).

The protein with the highest abundance increase (3.6-fold) in MIDY lung was ethylmalonyl-CoA decarboxylase 1 (ECHDC1). Likewise, other proteins involved in lipid catabolic processes, such as oestrogen sulfotransferase (SULT1E1), fatty acid-binding protein 4 (FABP4), apolipoprotein A4 (APOA4), and carboxylic ester hydrolase (CES1), were elevated. Furthermore, members of the small-leucine-rich proteoglycan (SLRP) family were more abundant in MIDY versus WT samples. The most prominent

was asporin (ASPN) with a 1.9-fold increase. In addition, SLRP levels were correlated significantly (Figure S1). Pulmonary surfactant-associated protein A (SFTPA1) was also elevated in MIDY lungs (Benjamini–Hochberg corrected p-value = 0.005).

One of the most prominently reduced proteins in MIDY lung (2.6-fold) was polyunsaturated fatty acid lipoxygenase ALOX15 (ALOX15). Several members of the complement and coagulation cascades were also reduced, of which complement component C6 (C6) was the most pronounced with a 1.8-fold decrease. A large fraction of differentially abundant proteins in MIDY compared to WT pigs were ECM proteins. We classified these proteins into the following groups: secreted factors, proteoglycans, ECM regulators, ECM glycoproteins, ECM-affiliated proteins, and collagens (Figure 1C). Similarly, proteins involved in the biological processes and pathways related to insulin homeostasis are visualized in Figure S2.

Furthermore, to functionally characterize proteome alterations between MIDY versus WT, a pre-ranked gene set enrichment analysis using STRING was performed. The detailed results of the enrichment analysis are provided in Table S4 and are visualized in Figure 1D. Gene sets, like acute-phase response, regulation of humoral immune response, blood coagulation, regulation of phagocytosis, platelet degranulation, cell killing, and humoral immune response, were enriched among the proteins decreased in abundance, whereas proteins related to keratan sulfate biosynthetic process, cornification, glycosaminoglycan biosynthetic process, and intermediate filament cytoskeleton organization were enriched among the upregulated proteins. An enrichment of proteins related to lipid storage, mucopolysaccharide metabolic process, and aminoglycan metabolic process was simultaneously found in the sets of more and less abundant proteins.

Protein localization studies and quantitative stereology

In lung tissue sections of MIDY and WT pigs, ALOX15 immunoreactivity was present in mononuclear cells within alveolar walls and inside the vascular lumina (Figure 2A, B). Confirming the significantly reduced ALOX15 protein levels in the MIDY lung tissue identified by proteomic analysis, quantitative stereological analysis revealed a significantly decreased volume density of ALOX15-positive cells within the lung tissue (Figure 2C). The volume density of interstitial connective tissue in the lung tissue (excluding air-filled spaces) of MIDY pigs was slightly increased (p-value = 0.19) as compared to WT animals (Figure S3).

Overview of lipidome differences

To clarify if the markedly reduced levels of ALOX15 in the MIDY animals affect the total level of eicosanoids, we used mass spectrometry-based targeted lipidomics and compared eicosanoid levels from MIDY and WT lungs. The results are shown in Table S5. A global correlation map of all quantified eicosanoids is shown in Figure 3A and in Table S6. Hierarchical clustering revealed several clusters of molecules that share the same biosynthetic pathway and show a similar regulation trend across animals. Hierarchical clustering revealed four homogenous regions, of which one, consisting of lipids produced mainly by a lipoxygenase (LOX) pathway, was particularly interesting. Magnification of this cluster (Figure 3A, right inset) shows a heatmap of lipids with strong correlation to each other, and some of these correlations remained significant after adjusting for all pairwise comparisons using the Benjamini-Hochberg method. Focusing on the hypothesis of eicosanoid co-regulation in the MIDY lung, we visualized highly correlated ($|\text{Rho}| > 0.8$) lipids as a network (Figure 3B, C). The community detection algorithm revealed several densely populated sub-networks. To

visualize whether distinct communities contain lipids that share the same biosynthetic pathway, we coloured the nodes according to the substrate (Figure 3B) and enzyme (Figure 3C). In agreement with Figure 3A, dense clusters with strong associations across biomolecule classes were apparent. Figure 3C further shows a network for the selected community with significantly ($Rho > 0.8$ and Benjamini–Hochberg corrected p -value < 0.05) correlated lipids. Figure 3D shows the trend of reduced eicosanoid levels in MIDY compared to WT lungs, from the selected cluster (1 in Figure 3A, 2 in Figure 3C). Next, a principal component analysis was performed on the entire data set (Figure 4A), which indicated moderate clustering of MIDY from the WT animals. Furthermore, some of the PUFA precursors in a free state were quantified (Figure 4C, Table S8).

Multi-omics data integration

For multi-omics data integration co-inertia analysis (CIA) [25] was used. Graphical representation of samples (Figure 5A) and variables (Figure 5B) on a lower-dimensional space allows interpretation of global variance structure and identification of the most informative biomolecules across datasets. CIA of proteome (circle) and lipidome (square) revealed a significant relationship ($RV = 0.78$, 500 permutation, $p = 0.041$). The corresponding score plot shows the proteins and lipids responsible for partitioning MIDY and WT samples on the CIA plot. Although not displaying clear clusters, the CIA showed trends towards separation of MIDY and WT samples.

DISCUSSION

To reveal biological processes and pathways altered by insulin-deficiency in the lung and to identify molecular key drivers of these alterations, a multi-omics analysis

combining in-depth data-independent acquisition proteomics, and quantitative readouts of relevant lipid molecules was performed.

The crucial lipid-protein mixture that reduces alveolar surface tension and facilitates breathing is pulmonary surfactant [26], which covers the entire alveolar surface of the lungs [27]. Defects in the stimulation of pulmonary surfactant production have been observed in various medical conditions such as COPD [28] and idiopathic pulmonary fibrosis [29]. These defects might also be contributing factors to airway dysfunction in diabetes [30]. Surfactant proteins leak from the alveolar space into the bloodstream, when the alveolar-capillary barrier is damaged, which makes them useful biomarkers for lung injury [31]. We detected a ~50% increase of the pulmonary surfactant-associated protein A (SFTPA1 alias SP-A) in MIDY compared to WT pig lungs (Benjamini-Hochberg-adjusted P-value 0.005). SP-A is the major protein component of surfactant and regulates surfactant phospholipid synthesis, secretion, and recycling [32]. Insulin is known to inhibit expression of the SP-A in the lung [33, 34], therefore increased abundance of SP-A in our study is in line with insulin deficiency in MIDY pigs. The clinical relevance of our finding is supported by a randomized population-based study revealing elevated circulating SP-A levels in the blood of patients with glucose intolerance and diabetes [35]. SP-A levels were also elevated in the lung of obese diabetic rats compared to lean nondiabetic control [30]. The observed increased abundance of SP-A in the MIDY model may reflect the diabetes-associated impairment of pulmonary diffusing capacity reported in children and adolescents with type 1 diabetes [2].

Besides pulmonary surfactant, the composition and function of lung ECM also become markedly deranged due to pathological tissue remodelling in diabetes mellitus [36].

Excessive production of ECM components and nonenzymatic glycation of ECM proteins due to hyperglycaemia lead to matrix stiffening, remodelling the lung tissue structure and promoting pulmonary fibrosis. Secreted factors such as transforming growth factor beta 1 (TGFB1) and connective tissue growth factor (CTGF alias CCN2) are the notorious pro-fibrotic agents involved in the initiation and progression of pulmonary fibrosis [37]. Elevated levels of TGFB1 were found in the lungs of STZ-induced diabetic rats and were associated with pulmonary fibrosis [38]. However, in the MIDY lung, the abundance of TGFB1 was not increased, and CTGF was even reduced by 1.7-fold (Benjamini–Hochberg corrected p-value = 0.01). The absence of a pro-fibrotic environment in the MIDY lung might be related to the elevated levels of small leucine-rich proteoglycans (SLRPs), which modulate the expression and activity of TGFB1 and CTGF and could therefore potentially protect the tissue against their deleterious effects [39]. Furthermore, SLRP levels were correlated significantly and together, SLRPs could counteract the vicious cycle observed previously in the diabetic lung, being characterized by elevated production of the pro-fibrotic growth factors and increased matrix deposition. In line with this, analysis of histological lung tissue sections from MIDY and WT pigs did not reveal evidence of fibrosis in the MIDY lung. Levels of different members of SLRP were also elevated in other diabetic conditions such as human diabetic nephropathy [40], diabetic foot ulceration [41], type 2 diabetes and obesity [42]. In the case-cohort study, decorin – one of the best characterized SLRP - was selected as one of the most important biomarkers for type 2 diabetes prediction [43]. Furthermore, the occurrence of sterile inflammation, characterized by a low-grade inflammatory response, is considered to contribute to pulmonary complications in hyperglycaemic conditions. Reduced complement system activity and humoral immunity associated with a reduced response of specialized immune cells

increase the risk of infections in diabetic patients [44]. In line with this, gene set enrichment analysis of proteomics data from the MIDY lung revealed proteins related to the regulation of the humoral immune response to be the most overrepresented in the set of downregulated proteins (among others, serpin family A members, complement and coagulation proteins). In line, a proteomics study of human type 1 diabetes serum revealed dysregulation of proteins involved in innate immune responses and in the activation cascade of complement [45]. Taken together, the humoral immune response seems to be compromised in the MIDY lung, potentially worsening the defence response.

A particularly novel and interesting finding of this investigation is a prominent, 2.5-fold downregulation of polyunsaturated fatty acid lipoxygenase ALOX15 in the MIDY lung. Alterations in ALOX15 regulation have been observed in various cardiovascular, renal, neurological, and metabolic disorders (reviewed in [46]). Although ALOX15 orthologues are known for several decades, their biological role is still under discussion. Like other lipoxygenases, ALOX15 is involved in the metabolism of polyunsaturated fatty acids (PUFAs) to form biologically active lipid mediators. The physiological substrates of ALOX15 are linoleic acid (LA), alpha-linolenic acid (α -LA), gamma-linolenic acid (γ -LA), arachidonic acid (AA), eicosapentaenoic acid (EPA), and docosahexaenoic acid (DHA). In the lung, ALOX15 products can stimulate or resolve inflammation and stimulate tissue repair [47]. A recent review highlighted the importance of ALOX15 in the formation of key lipid mediators to terminate inflammation during lung cancer in humans [48]. The strong downregulation of ALOX15 in the MIDY lung seems to be indicative of a disturbed immune response. Besides, leukotriene A(4) hydrolase (LTA4H) was moderately elevated in the MIDY

lung. LTA4H converts leukotriene A4 (LTA4) to leukotriene B4 (LTB4) and therefore plays an important role in the generation of pro-inflammatory leukotrienes. A shift from the leukotriene to the lipoxin production, also known as eicosanoid class switching, is necessary to resolve inflammation and to prevent the progression to chronic inflammation [49]. The inverse regulation of LTA4H and ALOX15 therefore possibly indicates the unbalanced production of pro-inflammatory lipid mediators. This agrees with the observed dysregulation of proteins related to humoral immune response in the MIDY lung discussed above. Furthermore, the lipidomics dataset showed a trend lower levels of lipoxygenase products in the MIDY lung, which is concordant with the strongly reduced protein levels of ALOX15. Eicosanoid levels derived from the lipoxygenase pathway were strongly correlated suggesting an orchestrated co-regulation of these molecules. The most pronounced from these molecules were downregulation of 14-HDHA and 12-HETE. 12-HETE, which can be produced by ALOX15, is known to have pro- and anti-inflammatory effects [50]. 14-HDHA, which was reduced by ~2.2-fold, is produced through the ALOX15-catalyzed oxygenation of docosahexaenoic acid (DHA) and is the key precursor of maresin, an anti-inflammatory lipid mediator [50]. Taken together, strongly reduced ALOX15 and associated eicosanoid levels reflect imbalanced production of pro- and anti-inflammatory mediators in the MIDY lung and provide molecular insights into the impoverished ability of inflammation resolution as a hallmark of diabetes lung disease.

In conclusion, this is the first multi-omics characterization of lung tissue in a clinically relevant large animal model of insulin-deficient diabetes mellitus. The fact that – for logistic reasons - only female pigs could be maintained for two years represents a limitation of this study. Another limitation of the study is the relatively small group size,

which may explain that some of the findings are trends close to the significance threshold. However, combination of multiple layers of molecular information with rigorous statistical and bioinformatic approaches revealed novel functional consequences of insulin deficiency for the lungs. The generated datasets further provide an important resource for future studies on the progression of pulmonary complications and other associated comorbidities in diabetes mellitus.

MATERIALS AND METHODS

Proteomics

Sample Preparation

Frozen lung tissue samples were washed briefly in ice-cold phosphate-buffered saline (PBS) supplemented with protease inhibitors (Roche Diagnostics, Mannheim, Germany). Samples were snap-frozen in liquid nitrogen and transferred into prechilled tubes and cryo-pulverized in a CP02 Automated Dry Pulverizer (Covaris, Woburn, MA, USA) using an impact level of five according to the manufacturer's instructions. Powdered tissue was lysed in 8 M urea/0.5 M NH_4HCO_3 supplemented with protease inhibitors (Roche Diagnostics, Mannheim, Germany) by ultrasonication (18 cycles of 10 s) using a Sonopuls HD3200 (Bandelin, Berlin, Germany). Pierce 660 nm Protein Assay (Thermo Fisher Scientific, Rockford, IL, USA) was used for protein quantification. 20 μl of lysate containing 50 μg of protein was processed for digestion. Briefly, disulfide bonds were reduced (45 mM dithiothreitol/20 mM tris(2-carboxyethyl) phosphine, 30 min, 56°C) and cysteine residues were alkylated (100 mM iodoacetamide, 30 min, room temperature), followed by quenching of excess iodoacetamide with dithiothreitol (90 mM, 15 min, room temperature). Proteins were then digested sequentially, firstly, with Lys-C (FUJIFILM Wako Chemicals Europe

GmbH, Neuss, Germany) for 4 h (1:50 enzyme to protein ratio) and subsequently with modified porcine trypsin (Promega, Madison, WI, USA) for 16 h at 37°C (1:50 enzyme to protein ratio). Peptides were then desalted using a Sep Pak C18 cartridge (Waters, Milford, MA) according to the manufacturer's instructions. The SepPak eluents were dried before analysis using a vacuum centrifuge.

Nano-liquid chromatography tandem mass spectrometry analysis

1 µg of the digest was injected on an UltiMate 3000 nano-LC system coupled online to a Q-Exactive HF-X instrument (Thermo Fisher Scientific) operated in the data-independent acquisition (DIA) mode. Peptides were transferred to a PepMap 100 C18 trap column (100 µm×2 cm, 5 µM particles, Thermo Fisher Scientific) and separated on an analytical column (PepMap RSLC C18, 75 µm×50 cm, 2 µm particles, Thermo Fisher Scientific) at 250 nL/min with an 80-min gradient of 5-20% of solvent B followed by a 9-min increase to 40%. After gradient, the column was washed with 85% solvent B for 9-min, followed by 10-min re-equilibration with 3% solvent B. Solvent A consisted of 0.1% formic acid in water and solvent B of 0.1% formic acid in acetonitrile. The Q-Exactive HF-X instrument was configured to acquire 50 x 12 m/z-wide (in the range of 400-1000 m/z) precursor isolation window DIA spectra (15,000 resolution, AGC target 1e6, maximum inject time 20 ms, NCE 27) as described in [51, 52] using a staggered window pattern [53] with window placements optimized by Skyline software (v. 21.1) [54]. Precursor spectra (in the range of 390-1010 m/z, 60,000 resolution, AGC target 1e6, max IIT 60 ms, +3H assumed charge state) were interspersed among every 50 ms/ms spectra. Chromatogram libraries using gas-phase fractionation [55] was built using the same LC settings. Six injections of pooled digest were performed with 25 X

4 m/z-wide DIA (30,000 resolution, AGC target 1e6 maximum inject time 55 ms, NCE 27, +3H assumed charge state) using a staggered window pattern with window placements optimized by Skyline software (v. 21.1) (i.e. 400.43-502.48, 500.48-602.52, 600.52-702.57, 700.57-802.61, 800.61-902.66, 900.66-1002.70), producing 300 x 2 m/z-wide windows spanning from 400 to 1000 m/z after deconvolution. Table S9 contains the actual windowing schemes.

Identification, quantification and bioinformatics

Raw data processing was carried out using DIA-NN (v1.8) [56]. Identification was based on predicted spectral libraries generated by DIA-NN's built-in deep-learning-based spectra and retention time predictor and further constrained by experimental data from project-specific gas-phase fractionation-based library (also generated by DIA-NN). For all searches, the *Sus scrofa* protein database (UniProt Reference Proteome – Taxonomy 9823 – Proteome ID UP000008227 – last modified June 16, 2021, 49,792 entries) alongside the MaxQuant contaminants fasta file [57] were used. The enzyme for digestion was set to trypsin and one missed cleavage was allowed. Only peptides with a charge state of +2, +3, and +4 were considered. Cysteine carbamidomethylation was set as a fixed modification. The precursors were filtered at 1 % false discovery rate. Retention time correction was performed automatically by DIA-NN and quantification strategy was set to Robust LC (high accuracy mode). Similarly, mass tolerance was determined automatically by DIA-NN as described in [56] and was set to 8 ppm and 20 ppm for MS1 and MS2, respectively. The top 6 fragments (based on their reference library intensities) were used to calculate raw intensities for precursors. The “Genes” column was used to count unique proteins (as

gene products identified and quantified using proteotypic peptides only). All other settings were left default. Table S10 contains detailed description of DIA-NN parameters used in this study. DIA-NN's main output containing precursor level data was used for the downstream analysis in R [58] using custom scripts. Briefly, the output was filtered at 1% false discovery rate, using experimental-wide q-values for protein groups and both experimental-wide and run-specific q-values for precursors. Non-proteotypic peptides, peptides with a low signal quality and peptides derived from potential contaminants were excluded from further analysis. Precursor intensities for different charge states were aggregated to peptide level by taking the sum of intensities. Peptide intensities were normalized and proteins with at least two unique peptides detected in at least three biological replicates of each condition were tested for differential abundance using the MS-Empire algorithm [59]. The STRING pre-ranked gene set enrichment analysis [60] was used to reveal biological pathways associated with differentially abundant proteins between MIDY and WT. Signed log-transformed p-values were used as ranking metrics and false discovery rate was controlled at 5%. To minimize redundancy, significant Gene Ontology (GO) biological processes were grouped into similar ontological terms with REVIGO [61] at an allowed similarity of 0.7.

Targeted lipidomics

Sample preparation for analysis of polyunsaturated fatty acid-derived lipid mediators and metabolites

An antioxidant cocktail consisting of BHT (CAS 128-37-0), Indomethacin (CAS 53-86-1) and TPPU (CAS 1222780-33-7) was added to 10-30 mg of the thawed tissue sample, to protect the sample from oxidation during sample preparation. Additionally,

an deuterated internal standard mix consisting of: 14,15-DHET-d₁₁, 15-HETE-d₈, 20-HETE-d₆, 8,9, EET-d₁₁, 9,10-DiHOME-d₄, 12(13)-EpOME-d₄, 13-HODE-d₄, PGB2-d₄, LTB4-d₄ 100 pg each (Cayman Chemical, Ann Arbor, USA) was spiked in. Methanol and sodium hydroxide were added for protein precipitation and alkaline hydrolysis at 60 °C for 30 minutes. After solid phase extraction, the eluate was evaporated [62] to obtain a solid residue which was dissolved in 100 µL methanol/water. The residues were analysed using an Agilent 1290 HPLC system with binary pump, multi-sampler and column thermostat with a Zorbax Eclipse plus C-18, 2.1 x 150 mm, 1.8 µm column using a gradient solvent system of aqueous acetic acid (0.05%) and acetonitrile / methanol 50:50. The flow rate was set at 0.3 mL/min, the injection volume was 20 µL. The HPLC was coupled with an Agilent 6495 triple quadrupole mass spectrometer (Agilent Technologies, Santa Clara, USA) with electrospray ionization source. Analysis was performed with Multiple Reaction Monitoring in negative mode with at least two mass transitions for each compound. All oxylipins were individually calibrated using authentic standards purchased from Cayman Chemical (Ann Arbor, USA) in relation to deuterated. Certified MaxSpec® quality was used if available. If not, the uncertified standards have been adapted to MaxSpec® standards of similar compounds.

Sample preparation for analysis of oxylipin precursors

All compounds were purchased from Cayman Chemicals.

Preparation of tissue samples and quality controls:

Porcine lung tissue samples were weighted into homogenization tubes with ceramic beads (1.4 mm) (Bertin P000933-LYSK0A tubes). To each 1 mg of frozen porcine lung tissue 3 µL of a cooled mixture (4 °C) of ethanol/phosphate buffer (85:15, v/v) were

added. Tissue samples were homogenized using a Precellys® 24 homogenizer (PEQLAB Biotechnology GmbH, Germany) three times for 30 s at 5,500 rpm and 4 °C, with 30 s pause intervals to ensure constant temperature. 30 µL (equivalent to 10 mg) of the lung homogenates were transferred into a 1.5 mL Eppendorf tube. QC pool samples were prepared in triplicates by taking out 20 µL from each study sample. The pool sample was subsequently mixed and 30 µL were transferred into 1.5 mL Eppendorf tubes.

QC reference samples were prepared in triplicates in 1.5 mL Eppendorf tubes by mixing 5 µL of the standard mixture (300 ng/mL) with 45 µL of water. Blank (triplicate) and zero (single) samples were prepared by transferring 30 µL of ethanol/phosphate buffer (85:15, v/v) into 1.5 mL Eppendorf tubes. Calibrators were prepared in 1.5 mL Eppendorf tubes by successive dilutions (factor 3) in water/MeOH (50:50, v/v) of the calibration mixture (2000 ng/mL) to reach 9 calibrator points (cal.): 666.67 ng/mL (cal. 09) to 0.102 ng/mL (cal. 01). 30 µL of each cal. was then transferred to a new 1.5 mL Eppendorf tube.

Every tube was pre-cooled in wet ice before starting sample preparation and kept on wet ice all along the extraction procedure.

For accurate quantification, 10 µL of ISTD mixture (50 ng/mL) were added to the samples, except zero sample.

Extraction procedure:

For lipid extraction, 150 µL of cold MeOH (-20 °C) were added to the samples followed by incubation for 10 min with vortexing every 3 min. Protein precipitation was performed by centrifugation of the samples at 10,000 x g for 15 min at 4 °C. The

supernatant (around 150 μ L) was transferred to a 1 mL NuncTM 96-well polypropylene plate (ThermoFisher), and the volume was adjusted with water to reach 1 ml (final MeOH concentration of 15%) and mixed up. Solid phase extraction was then performed with a Strata-X Micro 96-well plate, 33 μ m, 2 mL (Phenomenex) using a positive pressure-96 processor (Waters). After SPE plate conditioning with 2 x 0.5 mL MeOH and then 2 x 0.5 mL water, 2 x 0.5 mL of each sample were loaded on the SPE plate. After rinsing with 2 x 0.5 mL 10% MeOH in water (v/v) the analytes were eluted with 2 x 100 μ L MeOH into a new 1 mL 96-well plate. Samples were transferred to a select-a-vial 96-well plate with 300 μ L glass inserts (Analytical Services) and evaporated to dryness at 30 °C with nitrogen gas. Analytes were resuspended with 30 μ L 50% MeOH in water (v/v), vortexed, and centrifuged for some seconds at 1000 x g before direct injection into the analytical system.

LC-MS/MS analysis

All samples were measured with an Exion UHPLC-system coupled to a QTRAP 6500+ mass spectrometer (SCIEX, Darmstadt, Germany) operated with Analyst 1.6.3. Chromatographic separation was achieved using a Kinetex C18 reversed phase column (1.7 μ m, 100 \times 2.1 mm, Phenomenex) with a SecurityGuard Ultra Cartridge C18 (Phenomenex) precolumn, heated at 40 °C. Mobile phases A, water:ACN (70:30, v/v) + 100 μ L AA, and B, ACN/IPA (50:50, v/v) were used with gradient program with an isocratic flow rate of 500 μ L/min as follow: 0% B at 0 min, 70% B at 6.5 min, 100% B at 7.8 min, 100% B at 9.5 min, and 0% B at 11 min. The autosampler was operated at 4 °C with an injection volume of 10 μ L of sample.

The coupled mass spectrometer was equipped with an electrospray ionization (ESI) Turbo-VTM source set to negative mode. Source parameters were optimized to the

following values: source temperature 500 °C, curtain gas flow 40 psi, ionspray voltage –4000 V, ion source gas 1 50 psi, ion source gas 2 40 psi. Metabolites were analyzed via scheduled multiple reaction monitoring (sMRM) with nitrogen as collision gas. All MRM transitions were optimized for each compound, as well as the source parameters such as declustering potential, collision energy, cell exit potential and entrance potential. The sMRM detection window was set to 60 s. Acquisition time was about 8.5 min.

SciexOS software version 2.2.0.5738 (Sciex) was finally used for peak detection, integration and for quantitation of compounds (MQ4 algorithm). For quantification, linear calibration curves were generated from extracted calibrator samples for every compound via the IS method using the area ratio between the analyte and its ISTD, with a weighting factor of $1/x$.

Bioinformatics

Principal component analysis (PCA) was performed to discover natural grouping existing in the data. PCA was built on log-transformed data using `prcomp` function from R package *stats* [58]. To reveal eicosanoid subclasses with a similar regulation pattern, correlation analysis with rank-based approach (Spearman correlation) was employed. The significance of correlation (p-value) was corrected for all pairwise comparisons with Benjamini-Hochberg procedure using R package *psych* [63]. The correlation matrix was first subjected to hierarchical clustering using complete linkage-clustering as the clustering method and the Spearman correlation as the distance measure [64]. The resulting heatmap was partitioned into four different clusters using the k-means algorithm. A correlation matrix was also visualized as a network using R

package *igraph* [65]. Community detection was performed using the walktrap algorithm which attempts to find densely populated subnetworks by random walks [66]. Focusing on similarities between proteomics and lipidomics data, co-inertia analysis (CIA) was performed using R package *omicade4* [25], to assess global measures for the co-variability of two datasets. The similarity between the two datasets was evaluated with parameter RV, which is a multivariate extension of the Pearson correlation coefficient. The significance of the RV coefficient was assessed with a permutation test consisting of 500 iterations.

Histopathology, immunohistochemistry and quantitative morphological analyses

For qualitative and quantitative histomorphological analyses, paraffin sections stained with haematoxylin and eosin or Masson's trichrome stain (connective tissue stain) were examined. Immunohistochemical detection of ALOX15 was performed using following antibodies: mouse monoclonal anti ALOX15 (clone OT17H6, #TATA504358, origene), followed by biotinylated goat-anti-mouse secondary antibody (#115-065-146, Jackson ImmunoResearch) and horseradish peroxidase labelled avidin biotin complex (#PK-6100, Vector Laboratories). Immunoreactivity was visualized using 3,3'-diaminobenzidine tetrahydrochloride dihydrate (DAB). Sections stained with buffer instead of the primary antibody were used as negative control. The volume density of immunohistochemically ALOX15-positively labelled cells within the lung ($V_{V(\text{ALOX15-positive cells/lung})}$) was determined following the principle of Delesse and calculated as the sum of cross-sectional areas of ALOX15-positive cell profiles, divided by the sum of cross-sectional areas of lung tissue (excluding air-filled spaces) in 48 ± 2 systematically randomly sampled section areas per case. ALOX15-positive area densities were determined by differential point counting, using an automated

stereology system (VIS-Visiopharm Integrator System™ Version 3.4.1.0 with newCAST™ software, Visiopharm A/S, Denmark), as previously described [17, 67]. In each case, >100,000 points were counted. The volume density of interstitial connective tissue within the lung ($V_{V(\text{interstitial connective tissue/lung})}$), was determined analogously in Masson-trichrome stained lung tissue sections (counting > 10,000 points per case). All quantitative morphological analyses were performed in a blinded manner, i.e., without knowing the affiliation of the examined animals. Statistical significance of the difference in the volume density of immunohistochemically ALOX15-positively labelled cells and volume density of interstitial connective tissue in the lung between MIDY and WT were evaluated using two-sample Mann–Whitney U Test.

Statistical analysis

In this study, lung tissue samples collected by systematic random sampling [68] from two-year-old female MIDY pigs (n=4) and female WT littermates (n=5) were used. Tissues were shock-frozen on dry ice and stored at -80°C in the Munich MIDY Pig Biobank [24] until analysis. During analysis, all samples were processed in parallel to avoid possible bias related to different storage times. Histology and immunohistochemistry were performed on lung tissue samples taken from the exactly same locations as the proteomic and lipidomic analysis samples. All experiments were performed according to the German Animal Welfare Act and approved by the Government of Upper Bavaria, following the ARRIVE guidelines and Directive 2010/63/EU for animal experiments. All statistical analyses were performed in R [58]. Samples were analysed with a DIA method with MS1 spectra interspersed every 50 ms/ms scans. Identification was performed using DIA-NN [56] and its built-in deep

learning-based spectra and retention time predictor alongside project specific narrow-window gas-phase fractionation-based library. A false discovery-rate cut-off of 1% was applied on precursor and protein level. MS-EmpiRe workflow [59] followed by a Benjamini-Hochberg multiple testing correction was used to reveal differentially abundant proteins. Correlation between selected variables was evaluated using Spearman correlation and resulting p-values were corrected for all pairwise comparisons using Benjamini-Hochberg method.

ACKNOWLEDGMENTS

We acknowledge Vadim Demichev (Charité - Universitätsmedizin Berlin, Quantitative Proteomics) for his ongoing support on DIA data analysis. We also thank Tatiana Schröter for excellent technical assistance. Parts of the graphical abstract and Figure 1A were drawn by using pictures from Servier Medical Art. Servier Medical Art by Servier is licensed under a Creative Commons Attribution 3.0 Unported License (<https://creativecommons.org/licenses/by/3.0/>).

CONFLICTS OF INTERESTS

MR is owner of Lipidomix GmbH. This does not alter the author's adherence to all policies on sharing data and materials. All other authors report no potential conflicts of interest relevant to this article.

FUNDING

This study was supported by the German Center for Diabetes Research (DZD e.V.); This project has received funding from the European Union's Horizon 2020 research and innovation programme under the Marie Skłodowska-Curie grant agreement No 812660 (DohART-NET).

DATA AVAILABILITY

The mass spectrometry proteomics data generated and analysed in this study have been deposited to the ProteomeXchange Consortium via the PRIDE [69] partner repository, <http://proteomecentral.proteomexchange.org>; PXD038014. The lipidomics results are included in the article/Supplementary Materials. Code to reproduce statistical analysis and visualization is available at: <https://github.com/bshashikadze/diabetes-lung-omics-paper>

AUTHOR CONTRIBUTIONS

B.S., F.F., E.W., and T.F.: conceptualization; B.S.: Software, Data Curation, Formal Analysis, Investigation, Visualization, Writing – Original Draft; J.B.S., E.W. and T.F.: Reviewing and Editing. B.S., E.K., S.F., M.H., F.R., M.R., L.P. and A.B.: Investigation; S.R., A.B. and E.W.: Resources. E.W., T.F.: Supervision and Funding acquisition.

SUPPLEMENTAL DATA

This article contains supplemental data

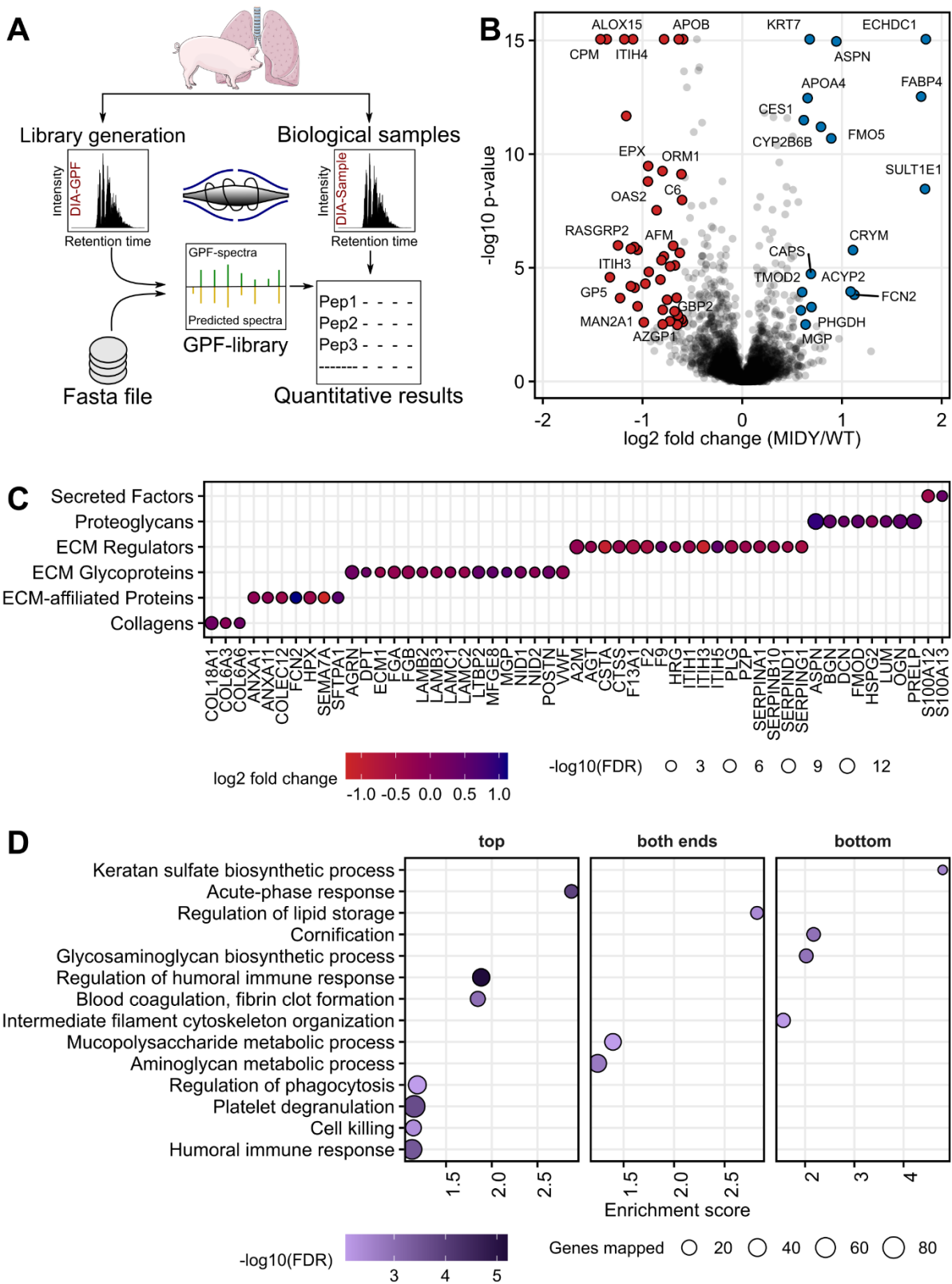


Figure 1. Quantitative proteome analysis of lung tissue from WT and MIDY pigs.

(A) Experimental design—lung tissue proteome from the MIDY and WT animals were analysed using a multi-injection gas-phase fractionation data-independent acquisition as described in [51, 56]. (B) Volcano plot visualization of proteome abundance changes between MIDY and WT. Protein abundance changes with Benjamini–Hochberg corrected p -value ≤ 0.05 , and fold-change ≥ 1.50 in MIDY lung are coloured in red and blue for downregulation and upregulation, respectively. (C) Abundance change of proteins that are part of the extracellular matrix according to [70]. The colour of the bubble corresponds to the \log_2 fold change of protein (red downregulation, blue upregulation) and the size of the bubble indicates the significance of the protein change. (D) Pre-ranked enrichment analysis using STRING with gene sets according to gene ontology (GO) biological process databases was used to reveal processes enriched in the top (downregulated) or bottom (upregulated) of a ranked list of genes. Significantly enriched GO biological processes (false discovery rate < 0.05) were summarized with REVIGO by grouping semantically similar ontology terms. Processes related to down-regulated proteins (left column), up-regulated proteins (right column), and simultaneously related to more and less abundant proteins (middle column) are shown. The size of the bubble indicates the corresponding number of the quantified proteins (referred genes mapped in the Figure) associated with the pathway, and colour the significance of enrichment. Fold enrichment represents the magnitude of over-representation.

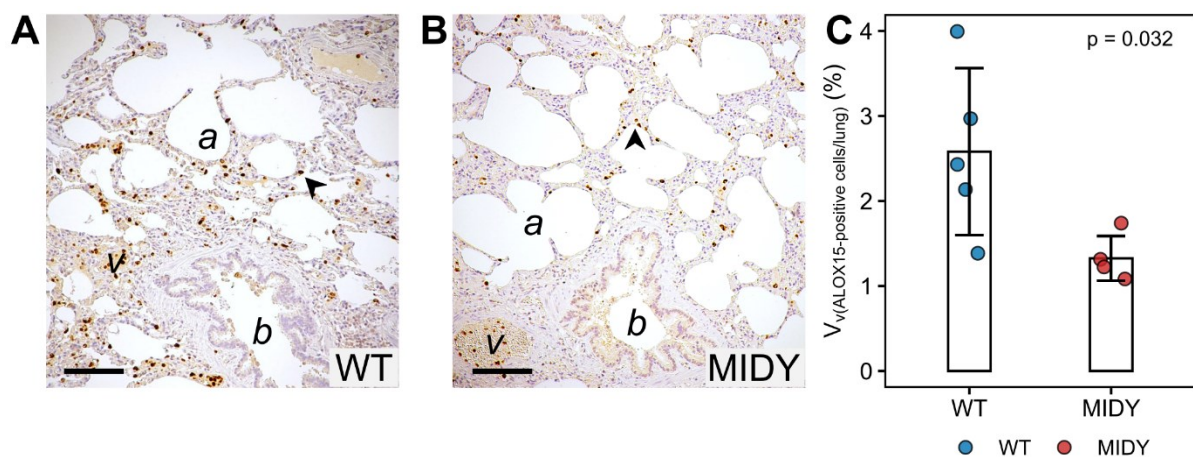


Figure 2. Immunohistochemical detection of ALOX15 in lung sections of WT (A) and MIDY pigs (B). Histological landmarks (alveoli (a), blood vessels (v), bronchioli (b)) are indicated. ALOX15-positive cells (dark brown colour) are present within alveolar septae (arrowheads) and inside vascular lumina. Paraffin sections. Chromogene: DAB, nuclear counterstain: haemalum. Size bar = 100 μm . (C) Volume densities of ALOX15-positive cells within the lung of WT and MIDY pigs. Statistical significance of the difference was assessed using the Mann-Whitney-U-test. The bar diagrams show means and standard deviations.

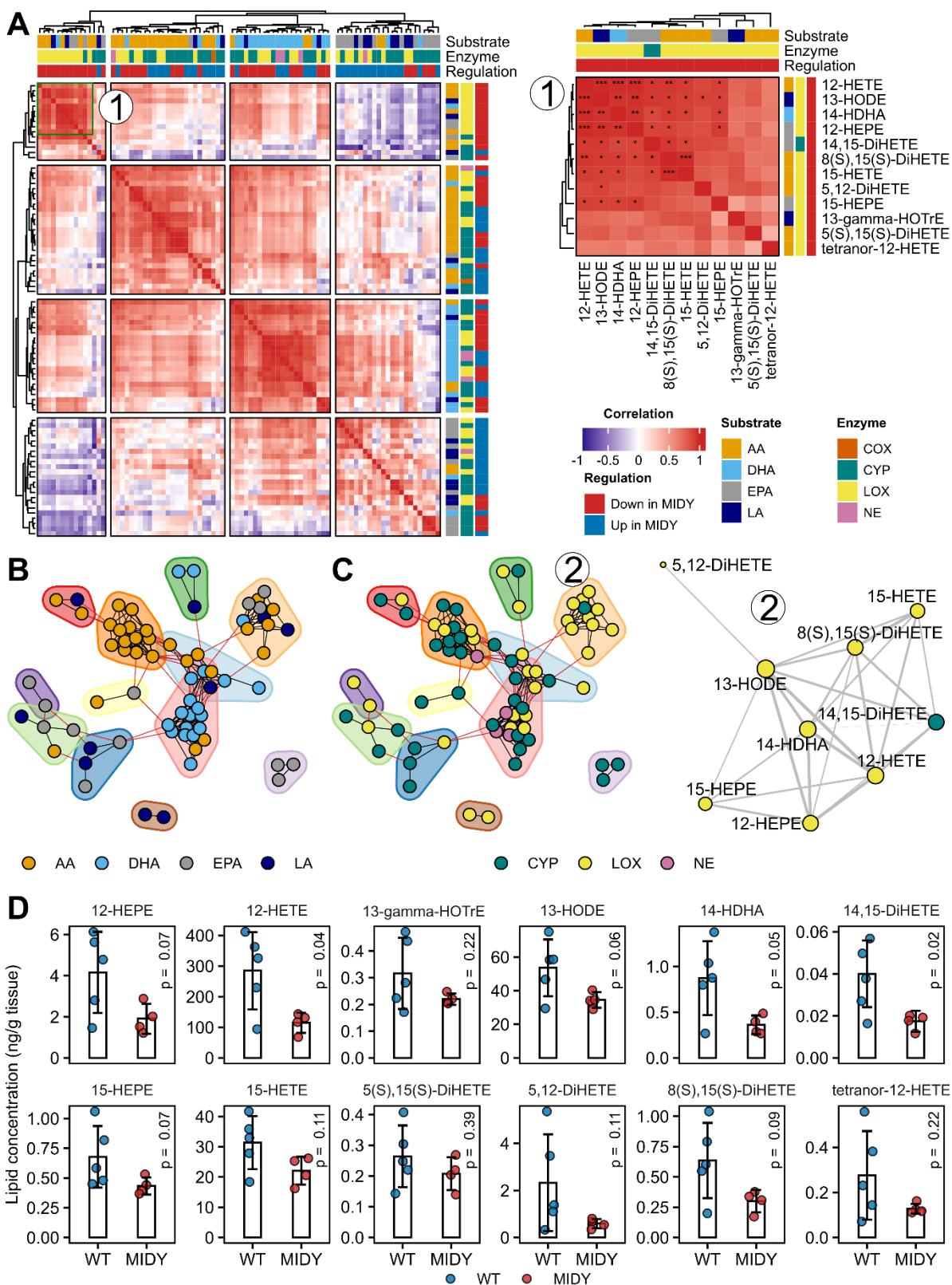


Figure 3. Correlation analysis of eicosanoid levels from WT and MIDY lung. (A)

Global correlation map of eicosanoid levels on the left with an inset of the selected cluster (1) on the right. The correlation was estimated using the non-parametric Spearman rank correlation coefficient. Red and blue patches in the correlation map indicate positive and negative correlations, respectively. Columns and rows of the heatmap are annotated for each lipid, based on the substrates and enzymes involved in their production. The regulation column indicates the abundance change of eicosanoids in MIDY versus WT. The correlation map was partitioned into homogenous regions using the k-means method ($k=4$). The correlation map on the right is labelled with an asterisk according to the significance (p -value) of the correlation after multiple testing correction for all pairwise comparisons using the Benjamini-Hochberg method. $*p < 0.05$; $**p < 0.01$; $***p < 0.001$. (B, C) Correlation between eicosanoid levels shown as a network. Each node corresponds to a single lipid and edges are drawn between highly correlated ($|\text{Rho}| > 0.8$) molecules. Nodes with dense connections were grouped using the random walk-based community detection algorithm (coloured drawings around the group of nodes). The network with nodes coloured based on a substrate (B) and enzyme (C), with an inset of the selected community network (2) on the right that was filtered for the significant correlations (Benjamini-Hochberg corrected p -value < 0.05). The edge thickness on the right cluster (2) corresponds to the magnitude of the correlation (Rho) and the size of the node to the number of its adjacent edges. AA, arachidonic acid; DHA, docosahexaenoic acid; EPA, eicosapentaenoic acid; LA, linoleic acid; COX, cyclooxygenase; CYP, cytochrome P450; LOX, lipoxygenase; NE, non-enzymatic. (D) Eicosanoid levels from the selected clusters (1 in Figure 3A, 2 in Figure 3B) in MIDY

versus WT. Statistical significance of the difference was assessed using the two-tailed Welch's t-test. The bar diagrams show means and standard deviations.

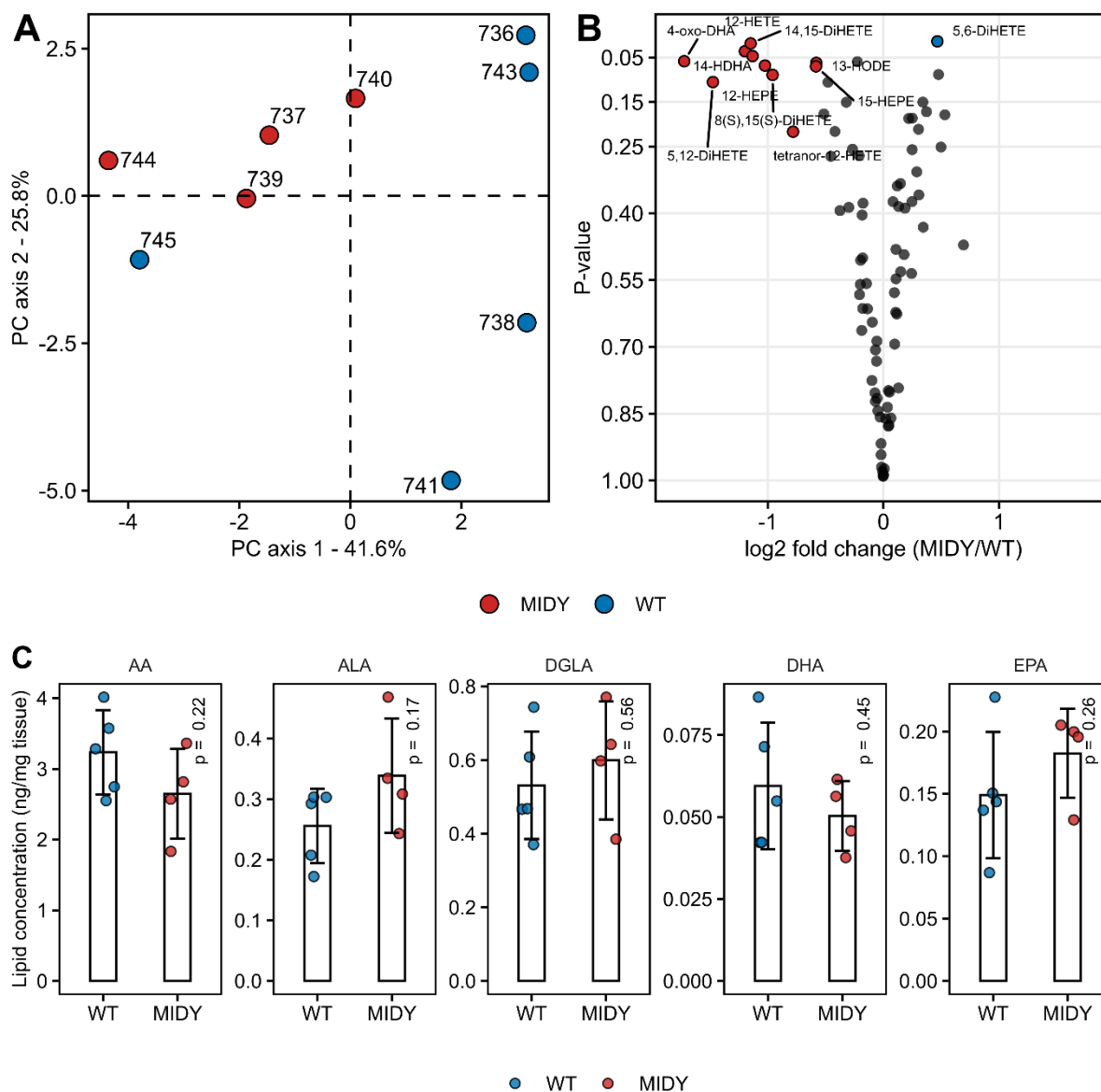


Figure 4. Eicosanoid levels in lung tissue from WT and MIDY pigs. (A) Unsupervised principal component analysis (PCA) based on log transformed lipid levels from MIDY and WT animals. The first two principal components explained 67.4% of the total variance. (B) Volcano plot obtained from the univariate statistics showing log₂ fold change and two-tailed Welch's t-test p-value. (C) PUFA precursor

levels in a free state from MIDY and WT lungs. Statistical significance of the difference was assessed using the two-tailed Welch's t-test. The bar diagrams show means and standard deviations.

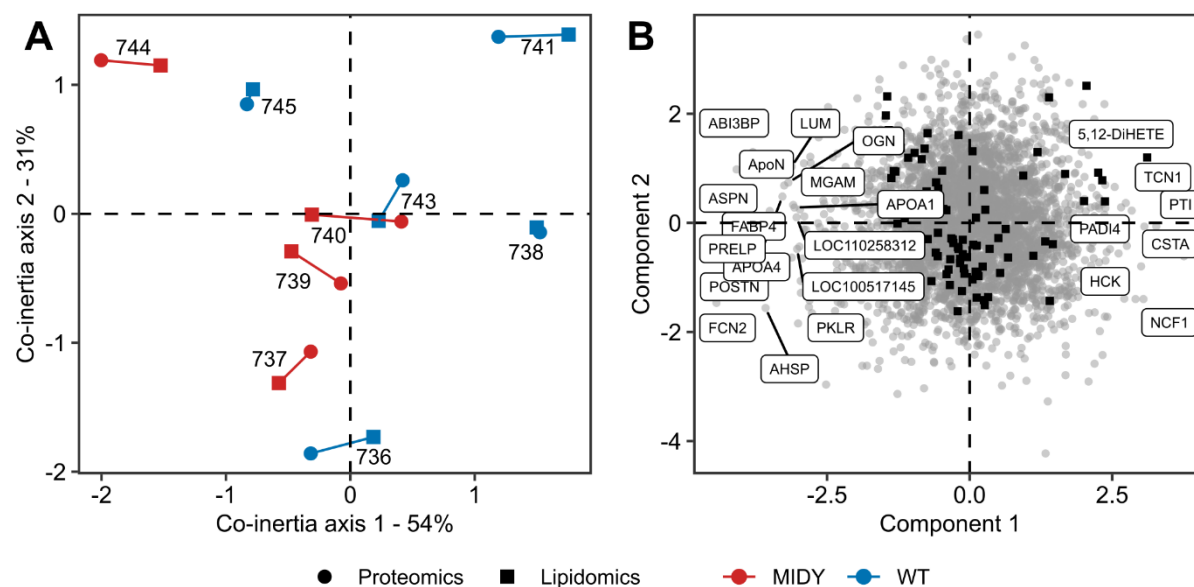


Figure 5. Omics data integration. (A, B) Multiple co-inertia analysis of lipidome and proteome data from the WT and MIDY lung showing the first two components in the sample (A) and variable (B) space. Circles and squares represent the proteome and lipidome data of a given animal, respectively. Short lines in the sample space (A) indicate a higher cross-omics correlation. The RV coefficient ($RV = 0.78$, 500 permutation, $p = 0.04$) shows the correlation of two datasets. A RV close to 1 indicates a strong correlation. Proteins and lipids with high scores in component 1 and component 2 are labelled in a variable space (B).

1. Vithian, K. and S. Hurel, *Microvascular complications: pathophysiology and management*. Clinical medicine (London, England), 2010. **10**(5): p. 505-509.
2. Mameli, C., M. Ghezzi, A. Mari, G. Cammi, M. Macedoni, F.C. Redaelli, V. Calcaterra, G. Zuccotti, and E. D'Auria, *The Diabetic Lung: Insights into Pulmonary Changes in Children and Adolescents with Type 1 Diabetes*. Metabolites, 2021. **11**(2).

3. Kolahian, S., V. Leiss, and B. Nurnberg, *Diabetic lung disease: fact or fiction?* Rev Endocr Metab Disord, 2019. **20**(3): p. 303-319.
4. Rajasurya, V., K. Gunasekaran, and S. Surani, *Interstitial lung disease and diabetes.* World J Diabetes, 2020. **11**(8): p. 351-357.
5. Klekotka, R., E. Mizgala, and W. Król, *The etiology of lower respiratory tract infections in people with diabetes.* Advances in Respiratory Medicine, 2015. **83**(5): p. 401-408.
6. Lim, S., J.H. Bae, H.-S. Kwon, and M.A. Nauck, *COVID-19 and diabetes mellitus: from pathophysiology to clinical management.* Nature Reviews Endocrinology, 2021. **17**(1): p. 11-30.
7. Hyldgaard, C., O. Hilberg, and E. Bendstrup, *How does comorbidity influence survival in idiopathic pulmonary fibrosis?* Respir Med, 2014. **108**(4): p. 647-53.
8. Ehrlich, S.F., C.P. Quesenberry, Jr., S.K. Van Den Eeden, J. Shan, and A. Ferrara, *Patients diagnosed with diabetes are at increased risk for asthma, chronic obstructive pulmonary disease, pulmonary fibrosis, and pneumonia but not lung cancer.* Diabetes Care, 2010. **33**(1): p. 55-60.
9. King, A.J.F., *The use of animal models in diabetes research.* British journal of pharmacology, 2012. **166**(3): p. 877-894.
10. Furman, B.L., *Streptozotocin-Induced Diabetic Models in Mice and Rats.* Current Protocols, 2021. **1**(4): p. e78.
11. Muller, Y.D., D. Golshayan, D. Ehrchiou, J.C. Wyss, L. Giovannoni, R. Meier, V. Serre-Beinier, G. Puga Yung, P. Morel, L.H. Bühler, and J.D. Seebach, *Immunosuppressive effects of streptozotocin-induced diabetes result in absolute lymphopenia and a relative increase of T regulatory cells.* Diabetes, 2011. **60**(9): p. 2331-40.
12. Renner, S., C. Braun-Reichhart, A. Blutke, N. Herbach, D. Emrich, E. Streckel, A. Wunsch, B. Kessler, M. Kurome, A. Bähr, N. Klymiuk, S. Krebs, O. Puk, H. Nagashima, J. Graw, H. Blum, R. Wanke, and E. Wolf, *Permanent neonatal diabetes in INS(C94Y) transgenic pigs.* Diabetes, 2013. **62**(5): p. 1505-11.
13. Renner, S., A. Blutke, S. Clauss, C.A. Deeg, E. Kemter, D. Merkus, R. Wanke, and E. Wolf, *Porcine models for studying complications and organ crosstalk in diabetes mellitus.* Cell Tissue Res, 2020. **380**(2): p. 341-378.
14. Hinkel, R., A. Howe, S. Renner, J. Ng, S. Lee, K. Klett, V. Kaczmarek, A. Moretti, K.L. Laugwitz, P. Skroblin, M. Mayr, H. Milting, A. Dendorfer, B. Reichart, E. Wolf, and C. Kupatt, *Diabetes Mellitus-Induced Microvascular Destabilization in the Myocardium.* J Am Coll Cardiol, 2017. **69**(2): p. 131-143.
15. Kleinwort, K.J.H., B. Amann, S.M. Hauck, S. Hirmer, A. Blutke, S. Renner, P.B. Uhl, K. Lutterberg, W. Sekundo, E. Wolf, and C.A. Deeg, *Retinopathy with central oedema in an INS (C94Y) transgenic pig model of long-term diabetes.* Diabetologia, 2017. **60**(8): p. 1541-1549.
16. Giese, I.M., M.C. Schilloks, R.L. Degroote, M. Weigand, S. Renner, E. Wolf, S.M. Hauck, and C.A. Deeg, *Chronic Hyperglycemia Drives Functional Impairment of Lymphocytes in Diabetic INS (C94Y) Transgenic Pigs.* Front Immunol, 2020. **11**: p. 607473.
17. Backman, M., F. Flenkenthaler, A. Blutke, M. Dahlhoff, E. Landstrom, S. Renner, J. Philippou-Massier, S. Krebs, B. Rathkolb, C. Prehn, M. Grzybek, U. Coskun, M. Rothe, J. Adamski, M.H. de Angelis, R. Wanke, T. Frohlich, G.J. Arnold, H. Blum, and E. Wolf,

-
- Multi-omics insights into functional alterations of the liver in insulin-deficient diabetes mellitus*. Mol Metab, 2019. **26**: p. 30-44.
18. Flenkenthaler, F., E. Ländström, B. Shashikadze, M. Backman, A. Blutke, J. Philippou-Massier, S. Renner, M. Hrabe de Angelis, R. Wanke, H. Blum, G.J. Arnold, E. Wolf, and T. Fröhlich, *Differential Effects of Insulin-Deficient Diabetes Mellitus on Visceral vs. Subcutaneous Adipose Tissue-Multi-omics Insights From the Munich MIDY Pig Model*. Frontiers in medicine, 2021. **8**: p. 751277-751277.
 19. Renner, S., B. Dobenecker, A. Blutke, S. Zöls, R. Wanke, M. Ritzmann, and E. Wolf, *Comparative aspects of rodent and nonrodent animal models for mechanistic and translational diabetes research*. Theriogenology, 2016. **86**(1): p. 406-21.
 20. Kleinert, M., C. Clemmensen, S.M. Hofmann, M.C. Moore, S. Renner, S.C. Woods, P. Huypens, J. Beckers, M.H. de Angelis, A. Schürmann, M. Bakhti, M. Klingenspor, M. Heiman, A.D. Cherrington, M. Ristow, H. Lickert, E. Wolf, P.J. Havel, T.D. Müller, and M.H. Tschöp, *Animal models of obesity and diabetes mellitus*. Nature reviews. Endocrinology, 2018. **14**(3): p. 140-162.
 21. Wolf, E., C. Braun-Reichhart, E. Streckel, and S. Renner, *Genetically engineered pig models for diabetes research*. Transgenic research, 2013. **23**.
 22. Judge, E.P., J.M. Hughes, J.J. Egan, M. Maguire, E.L. Molloy, and S. O'Dea, *Anatomy and bronchoscopy of the porcine lung. A model for translational respiratory medicine*. Am J Respir Cell Mol Biol, 2014. **51**(3): p. 334-43.
 23. Rogers, C.S., W.M. Abraham, K.A. Brogden, J.F. Engelhardt, J.T. Fisher, P.B. McCray, Jr., G. McLennan, D.K. Meyerholz, E. Namati, L.S. Ostedgaard, R.S. Prather, J.R. Sabater, D.A. Stoltz, J. Zabner, and M.J. Welsh, *The porcine lung as a potential model for cystic fibrosis*. Am J Physiol Lung Cell Mol Physiol, 2008. **295**(2): p. L240-63.
 24. Blutke, A., S. Renner, F. Flenkenthaler, M. Backman, S. Haesner, E. Kemter, E. Ländström, C. Braun-Reichhart, B. Albl, E. Streckel, B. Rathkolb, C. Prehn, A. Palladini, M. Grzybek, S. Krebs, S. Bauersachs, A. Bähr, A. Brühshwein, C.A. Deeg, E. De Monte, M. Dmochewitz, C. Eberle, D. Emrich, R. Fux, F. Groth, S. Gumbert, A. Heitmann, A. Hinrichs, B. Keßler, M. Kurome, M. Leipzig-Rudolph, K. Matiasek, H. Öztürk, C. Otzdorff, M. Reichenbach, H.D. Reichenbach, A. Rieger, B. Rieseberg, M. Rosati, M.N. Saucedo, A. Schleicher, M.R. Schneider, K. Simmet, J. Steinmetz, N. Übel, P. Zehetmaier, A. Jung, J. Adamski, Ü. Coskun, M. Hrabě de Angelis, C. Simmet, M. Ritzmann, A. Meyer-Lindenberg, H. Blum, G.J. Arnold, T. Fröhlich, R. Wanke, and E. Wolf, *The Munich MIDY Pig Biobank - A unique resource for studying organ crosstalk in diabetes*. Molecular metabolism, 2017. **6**(8): p. 931-940.
 25. Meng, C., B. Kuster, A.C. Culhane, and A.M. Gholami, *A multivariate approach to the integration of multi-omics datasets*. BMC Bioinformatics, 2014. **15**(1): p. 162.
 26. Milad, N. and M.C. Morissette, *Revisiting the role of pulmonary surfactant in chronic inflammatory lung diseases and environmental exposure*. European Respiratory Review, 2021. **30**(162): p. 210077.
 27. Zuo, Y.Y., R.A.W. Veldhuizen, A.W. Neumann, N.O. Petersen, and F. Possmayer, *Current perspectives in pulmonary surfactant — Inhibition, enhancement and evaluation*. Biochimica et Biophysica Acta (BBA) - Biomembranes, 2008. **1778**(10): p. 1947-1977.
 28. Obeidat, M., en, X. Li, S. Burgess, G. Zhou, N. Fishbane, N.N. Hansel, Y. Bossé, P. Joubert, K. Hao, D.C. Nickle, M. van den Berge, W. Timens, M.H. Cho, B.D. Hobbs, K. de Jong, M. Boezen, R.J. Hung, N. Rafaels, R. Mathias, I. Ruczinski, T.H. Beaty, K.C. Barnes, P.D. Paré, and D.D. Sin, *Surfactant protein D is a causal risk factor for*

-
- COPD: results of Mendelian randomisation*. *European Respiratory Journal*, 2017. **50**(5): p. 1700657.
29. Beike, L., C. Wrede, J. Hegermann, E. Lopez-Rodriguez, C. Kloth, J. Gaudie, M. Kolb, U.A. Maus, M. Ochs, and L. Knudsen, *Surfactant dysfunction and alveolar collapse are linked with fibrotic septal wall remodeling in the TGF- β 1-induced mouse model of pulmonary fibrosis*. *Laboratory Investigation*, 2019. **99**(6): p. 830-852.
 30. Foster, D.J., P. Ravikumar, D.J. Bellotto, R.H. Unger, and C.C. Hsia, *Fatty diabetic lung: altered alveolar structure and surfactant protein expression*. *Am J Physiol Lung Cell Mol Physiol*, 2010. **298**(3): p. L392-403.
 31. López-Cano, C., A. Ciudin, E. Sánchez, F.J. Tinahones, F. Barbé, M. Dalmases, M. García-Ramírez, A. Soto, A.M. Gaeta, S. Pellitero, R. Martí, C. Hernández, R. Simó, and A. Lecube, *Liraglutide Improves Forced Vital Capacity in Individuals With Type 2 Diabetes: Data From the Randomized Crossover LIRALUNG Study*. *Diabetes*, 2022. **71**(2): p. 315-320.
 32. Aswani, K. and J. Snyder, *Surfactant protein A (SP-A): The alveolus beyond*. *FASEB journal : official publication of the Federation of American Societies for Experimental Biology*, 2001. **15**: p. 59-69.
 33. Rucka, Z., P. Vanhara, I. Koutna, L. Tesarova, M. Potesilova, S. Stejskal, P. Simara, J. Dolezel, V. Zvonicek, O. Coufal, and I. Capov, *Differential effects of insulin and dexamethasone on pulmonary surfactant-associated genes and proteins in A549 and H441 cells and lung tissue*. *Int J Mol Med*, 2013. **32**(1): p. 211-8.
 34. Miakotina, O.L., K.L. Goss, and J.M. Snyder, *Insulin utilizes the PI 3-kinase pathway to inhibit SP-A gene expression in lung epithelial cells*. *Respiratory Research*, 2002. **3**(1): p. 26.
 35. Fernández-Real, J.M., B. Chico, M. Shiratori, Y. Nara, H. Takahashi, and W. Ricart, *Circulating surfactant protein A (SP-A), a marker of lung injury, is associated with insulin resistance*. *Diabetes Care*, 2008. **31**(5): p. 958-63.
 36. Zhou, Y., J.C. Horowitz, A. Naba, N. Ambalavanan, K. Atabai, J. Balestrini, P.B. Bitterman, R.A. Corley, B.S. Ding, A.J. Engler, K.C. Hansen, J.S. Hagood, F. Kheradmand, Q.S. Lin, E. Neptune, L. Niklason, L.A. Ortiz, W.C. Parks, D.J. Tschumperlin, E.S. White, H.A. Chapman, and V.J. Thannickal, *Extracellular matrix in lung development, homeostasis and disease*. *Matrix Biol*, 2018. **73**: p. 77-104.
 37. Tam, A.Y.Y., A.L. Horwell, S.L. Trinder, K. Khan, S. Xu, V. Ong, C.P. Denton, J.T. Norman, A.M. Holmes, G. Bou-Gharios, and D.J. Abraham, *Selective deletion of connective tissue growth factor attenuates experimentally-induced pulmonary fibrosis and pulmonary arterial hypertension*. *The international journal of biochemistry & cell biology*, 2021. **134**: p. 105961-105961.
 38. Talakatta, G., M. Sarikhani, J. Muhamed, K. Dhanya, B.S. Somashekar, P.A. Mahesh, N. Sundaresan, and P.V. Ravindra, *Diabetes induces fibrotic changes in the lung through the activation of TGF-beta signaling pathways*. *Sci Rep*, 2018. **8**(1): p. 11920.
 39. Nastase, M.V., R.V. Iozzo, and L. Schaefer, *Key roles for the small leucine-rich proteoglycans in renal and pulmonary pathophysiology*. *Biochim Biophys Acta*, 2014. **1840**(8): p. 2460-70.
 40. Schaefer, L., I. Raslik, H.-J. Gröne, E. Schönherr, K. Macakova, J. Ugorcakova, S. Budny, R.M. Schaefer, and H. Kresse, *Small proteoglycans in human diabetic nephropathy: discrepancy between glomerular expression and protein accumulation*

-
- of decorin, biglycan, lumican, and fibromodulin*. The FASEB Journal, 2001. **15**(3): p. 559-561.
41. Theocharidis, G., B.E. Thomas, D. Sarkar, H.L. Mumme, W.J.R. Pilcher, B. Dwivedi, T. Sandoval-Schaefer, R.F. Sîrbulescu, A. Kafanas, I. Mezghani, P. Wang, A. Lobao, I.S. Vlachos, B. Dash, H.C. Hsia, V. Horsley, S.S. Bhasin, A. Veves, and M. Bhasin, *Single cell transcriptomic landscape of diabetic foot ulcers*. Nature Communications, 2022. **13**(1): p. 181.
 42. Bolton, K., D. Segal, and K. Walder, *The small leucine-rich proteoglycan, biglycan, is highly expressed in adipose tissue of Psammomys obesus and is associated with obesity and type 2 diabetes*. Biologics, 2012. **6**: p. 67-72.
 43. Thorand, B., A. Zierer, M. Büyüközkan, J. Krumsiek, A. Bauer, F. Schederecker, J. Sudduth-Klinger, C. Meisinger, H. Grallert, W. Rathmann, M. Roden, A. Peters, W. Koenig, C. Herder, and C. Huth, *A Panel of 6 Biomarkers Significantly Improves the Prediction of Type 2 Diabetes in the MONICA/KORA Study Population*. J Clin Endocrinol Metab, 2021. **106**(4): p. e1647-e1659.
 44. Muller, L.M., K.J. Gorter, E. Hak, W.L. Goudzwaard, F.G. Schellevis, A.I. Hoepelman, and G.E. Rutten, *Increased risk of common infections in patients with type 1 and type 2 diabetes mellitus*. Clin Infect Dis, 2005. **41**(3): p. 281-8.
 45. Zhang, Q., T.L. Fillmore, A.A. Schepmoes, T.R. Clauss, M.A. Gritsenko, P.W. Mueller, M. Rewers, M.A. Atkinson, R.D. Smith, and T.O. Metz, *Serum proteomics reveals systemic dysregulation of innate immunity in type 1 diabetes*. J Exp Med, 2013. **210**(1): p. 191-203.
 46. Singh, N.K. and G.N. Rao, *Emerging role of 12/15-Lipoxygenase (ALOX15) in human pathologies*. Prog Lipid Res, 2019. **73**: p. 28-45.
 47. Abrial, C., S. Grassin-Delyle, H. Salvator, M. Brollo, E. Naline, and P. Devillier, *15-Lipoxygenases regulate the production of chemokines in human lung macrophages*. Br J Pharmacol, 2015. **172**(17): p. 4319-30.
 48. Tian, R., X. Zuo, J. Jaoude, F. Mao, J. Colby, and I. Shureiqi, *ALOX15 as a suppressor of inflammation and cancer: Lost in the link*. Prostaglandins & other lipid mediators, 2017. **132**: p. 77-83.
 49. Ringholz, F.C., P.J. Buchanan, D.T. Clarke, R.G. Millar, M. McDermott, B. Linnane, B.J. Harvey, P. McNally, and V. Urbach, *Reduced 15-lipoxygenase 2 and lipoxin A4/leukotriene B4 ratio in children with cystic fibrosis*. Eur Respir J, 2014. **44**(2): p. 394-404.
 50. Snodgrass, R.G. and B. Brüne, *Regulation and Functions of 15-Lipoxygenases in Human Macrophages*. Front Pharmacol, 2019. **10**: p. 719.
 51. Pino, L.K., S.C. Just, M.J. MacCoss, and B.C. Searle, *Acquiring and Analyzing Data Independent Acquisition Proteomics Experiments without Spectrum Libraries*. Mol Cell Proteomics, 2020. **19**(7): p. 1088-1103.
 52. Shashikadze, B., L. Valla, S.D. Lombardo, C. Prehn, M. Haid, F. Riols, J.B. Stockl, R. Elkhateib, S. Renner, B. Rathkolb, J. Menche, M. Hrabe de Angelis, E. Wolf, E. Kemter, and T. Frohlich, *Maternal hyperglycemia induces alterations in hepatic amino acid, glucose and lipid metabolism of neonatal offspring: Multi-omics insights from a diabetic pig model*. Mol Metab, 2023. **75**: p. 101768.
 53. Amodei, D., J. Egertson, B.X. MacLean, R. Johnson, G.E. Merrihew, A. Keller, D. Marsh, O. Vitek, P. Mallick, and M.J. MacCoss, *Improving Precursor Selectivity in*

-
- Data-Independent Acquisition Using Overlapping Windows*. J Am Soc Mass Spectrom, 2019. **30**(4): p. 669-684.
54. MacLean, B., D.M. Tomazela, N. Shulman, M. Chambers, G.L. Finney, B. Frewen, R. Kern, D.L. Tabb, D.C. Liebler, and M.J. MacCoss, *Skyline: an open source document editor for creating and analyzing targeted proteomics experiments*. Bioinformatics, 2010. **26**(7): p. 966-8.
 55. Searle, B.C., L.K. Pino, J.D. Egertson, Y.S. Ting, R.T. Lawrence, B.X. MacLean, J. Villén, and M.J. MacCoss, *Chromatogram libraries improve peptide detection and quantification by data independent acquisition mass spectrometry*. Nature communications, 2018. **9**(1): p. 5128-5128.
 56. Demichev, V., C.B. Messner, S.I. Vernardis, K.S. Lilley, and M. Ralser, *DIA-NN: neural networks and interference correction enable deep proteome coverage in high throughput*. Nat Methods, 2020. **17**(1): p. 41-44.
 57. Tyanova, S., T. Temu, and J. Cox, *The MaxQuant computational platform for mass spectrometry-based shotgun proteomics*. Nat Protoc, 2016. **11**(12): p. 2301-2319.
 58. R Core Team (2021), *R: A language and environment for statistical computing*. 2021: Vienna, Austria.
 59. Ammar, C., M. Gruber, G. Csaba, and R. Zimmer, *MS-EmpiRe Utilizes Peptide-level Noise Distributions for Ultra-sensitive Detection of Differentially Expressed Proteins*. Mol Cell Proteomics, 2019. **18**(9): p. 1880-1892.
 60. Szklarczyk, D., A.L. Gable, D. Lyon, A. Junge, S. Wyder, J. Huerta-Cepas, M. Simonovic, N.T. Doncheva, J.H. Morris, P. Bork, L.J. Jensen, and C.V. Mering, *STRING v11: protein-protein association networks with increased coverage, supporting functional discovery in genome-wide experimental datasets*. Nucleic Acids Res, 2019. **47**(D1): p. D607-d613.
 61. Supek, F., M. Bošnjak, N. Škunca, and T. Šmuc, *REVIGO Summarizes and Visualizes Long Lists of Gene Ontology Terms*. PLOS ONE, 2011. **6**(7): p. e21800.
 62. Rivera, J., N. Ward, J. Hodgson, I.B. Puddey, J.R. Falck, and K.D. Croft, *Measurement of 20-Hydroxyeicosatetraenoic Acid in Human Urine by Gas Chromatography–Mass Spectrometry*. Clinical Chemistry, 2004. **50**(1): p. 224-226.
 63. Revelle, W.R., *psych: Procedures for personality and psychological research*. 2017.
 64. Gu, Z., R. Eils, and M. Schlesner, *Complex heatmaps reveal patterns and correlations in multidimensional genomic data*. Bioinformatics, 2016. **32**(18): p. 2847-9.
 65. Csárdi, G. and T. Nepusz. *The igraph software package for complex network research*. 2006.
 66. Pons, P. and M. Latapy, *Computing Communities in Large Networks Using Random Walks*. J. Graph Algorithms Appl., 2006. **10**: p. 191-218.
 67. Vyvyan Howard, M.R., *Unbiased Stereology: Three-Dimensional Measurement in Microscopy* Vol. 2nd Edition. 2004, London: Garland Science. 277.
 68. Albl, B., S. Haesner, C. Braun-Reichhart, E. Streckel, S. Renner, F. Seeliger, E. Wolf, R. Wanke, and A. Blutke, *Tissue Sampling Guides for Porcine Biomedical Models*. Toxicol Pathol, 2016. **44**(3): p. 414-20.
 69. Perez-Riverol, Y., J. Bai, C. Bandla, D. García-Seisdedos, S. Hewapathirana, S. Kamatchinathan, D.J. Kundu, A. Prakash, A. Frericks-Zipper, M. Eisenacher, M. Walzer, S. Wang, A. Brazma, and J.A. Vizcaino, *The PRIDE database resources in*

2022: *a hub for mass spectrometry-based proteomics evidences*. Nucleic Acids Res, 2022. **50**(D1): p. D543-d552.

70. Naba, A., K.R. Clauser, S. Hoersch, H. Liu, S.A. Carr, and R.O. Hynes, *The matrisome: in silico definition and in vivo characterization by proteomics of normal and tumor extracellular matrices*. Mol Cell Proteomics, 2012. **11**(4): p. M111.014647.

Supplemental data

Table of Contents

(Excel) Table S1: Peptides identified and quantified by nano-LC-MS/MS-based DIA proteomics

(Excel) Table S2: Protein groups identified by nano-LC-MS/MS-based DIA proteomics

(Excel) Table S3: Results of MS-EmpiRe-based quantitative proteomics of MIDY vs. WT pigs. Proteins with BH adjusted p-value < 0.05 are shown. Positive log₂ fold change means more abundant in the MIDY group

(Excel) Table S4: STRING Functional Enrichment Analysis of MIDY vs. WT. Gene Ontology (GO) biological processes with direction "top" are enriched for proteins less abundant and with direction "bottom" are enriched for proteins more abundant in MIDY vs. WT. Processes with "both ends" are simultaneously enriched for proteins more and less abundant

(Excel) Table S5: Results of quantitative targeted lipidomics of MIDY vs. WT pig (shown as ng/g tissue)

(Excel) Table S6: Global correlation matrix of quantified eicosanoid levels. The correlations were estimated using the non-parametric Spearman correlation method. Color gradient corresponds to the magnitude of the correlation

(Excel) Table S7: Statistical analysis of targeted lipidomics data. Positive log₂ fold changes means more abundant in the MIDY group. P-values are calculated using two-tailed Welch's t-test. Variance importance in projection (VIP) scores are from the orthogonal partial least squares discriminant analysis (OPLS-DA) model

(Excel) Table S8: Window placements optimized by Skyline software (v.21.1) for the single-injection DIA runs and gas-phase fractionation (GPF) DIA runs

(Excel) Table S9: Detailed description of DIA-NN parameters

Supplemental Figures

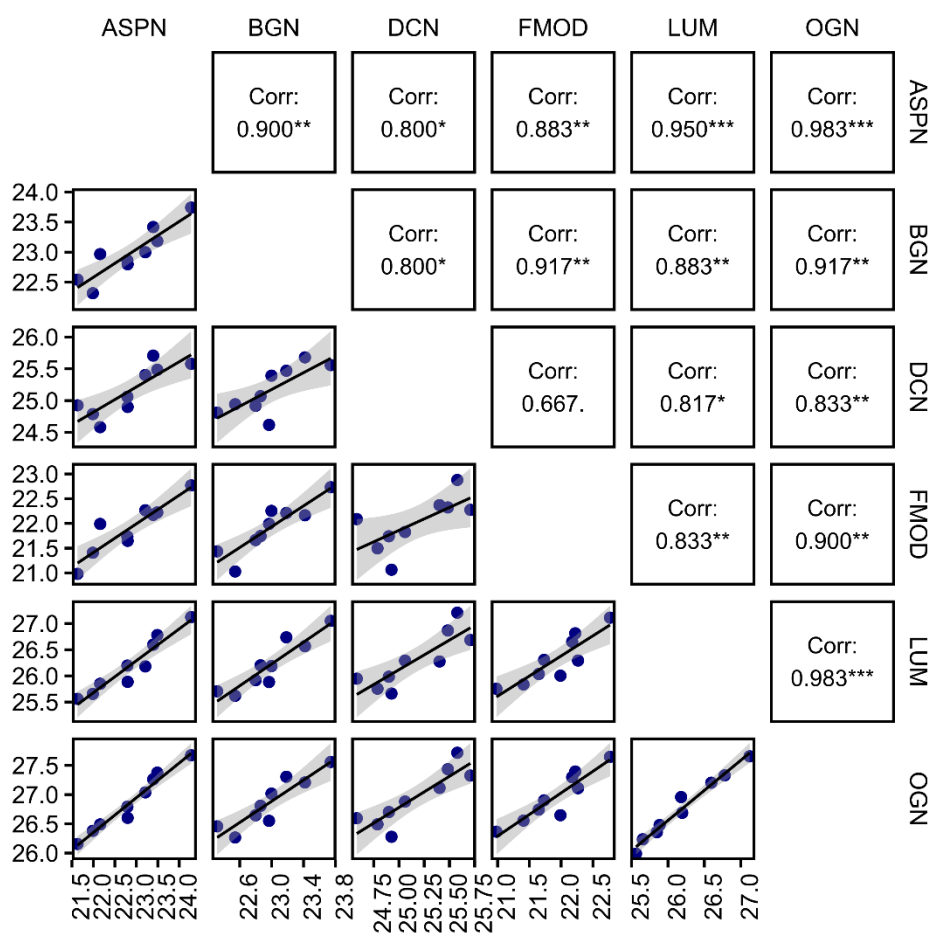


Figure S1. Multi-scatter plot of small-leucine rich proteoglycan levels in all animals with regression line (black solid line) and confidence interval (grey area) (lower triangle). Spearman correlation coefficient and the significance of the correlation (p-value) is shown in the upper triangle. * $p < 0.05$; ** $p < 0.01$; *** $p < 0.001$

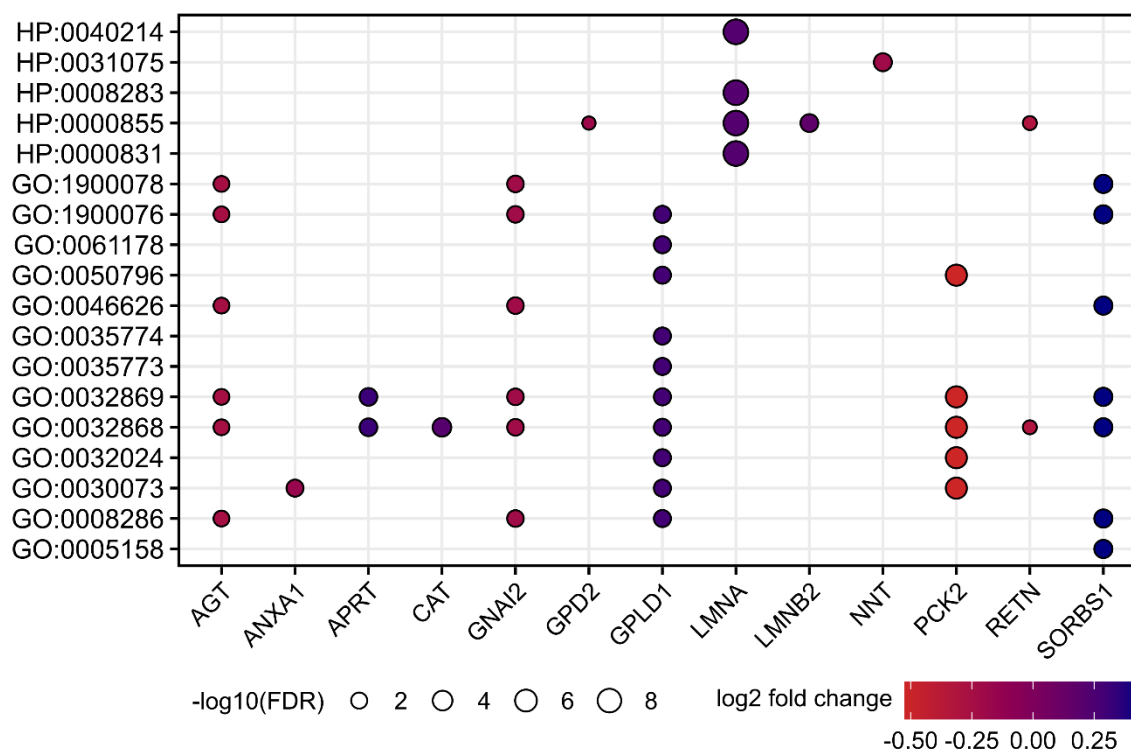


Figure S2. Abundance change of proteins (adjusted p-value < 0.05) related to HP:0040214 (abnormal insulin level), HP:0031075 (abnormal response to insulin tolerance test), HP:0008283 (fasting hyperinsulinemia), HP:0000855 (insulin resistance), HP:0000831 (insulin resistant diabetes mellitus), GO:1900078 (positive regulation of cellular response to insulin stimulus), GO:1900076 (regulation of cellular response to insulin stimulus), GO:0061178 (regulation of insulin secretion involved in cellular response to glucose stimulus), GO:0050796 (regulation of insulin secretion), GO:0046626 (regulation of insulin receptor signaling pathway), GO:0035774 (positive regulation of insulin secretion involved in cellular response to glucose stimulus), GO:0035773 (insulin secretion involved in cellular response to glucose stimulus), GO:0032869 (cellular response to insulin stimulus), GO:0032868 (response to insulin), GO:0032024 (positive regulation of insulin secretion), GO:0030073 (insulin secretion), GO:0008286 (insulin receptor signaling pathway), GO:0005158 (insulin receptor binding). The color of the bubble corresponds to the log2 fold change of protein (red downregulation, blue upregulation) and the size of the bubble indicates the significance of the protein change. AGT, angiotensin 1-10; ANXA1, annexin; APRT, adenine phosphoribosyltransferase; CAT, catalase; GNAI2, G protein subunit alpha i2; GPD2, glycerol-3-phosphate dehydrogenase; GPLD1, glycosyl-

phosphatidylinositol-specific phospholipase D; LMNA, prelamin-A/C; LMNB2, lamin B2; NNT, proton-translocating NAD(P)(+) transhydrogenase; PCK2, phosphoenolpyruvate carboxykinase (GTP); RETN, resistin; SORBS1, sorbin and SH3 domain containing 1.

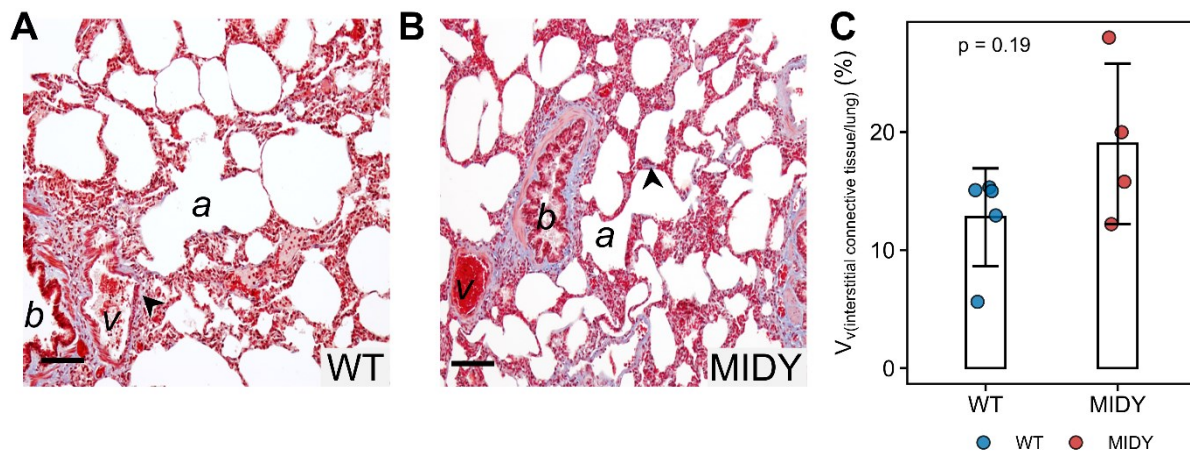


Figure S3. Detection and quantification of interstitial connective tissue in the WT and MIDY lung. Masson's trichrome-stained lung sections of MIDY (A) and WT (B) pigs. Histological landmarks (alveoli (a), blood vessels (v), and bronchioli (b)) are indicated. Connective tissue stains blue. Size bars: 100 μ m. (C) Volume densities (in %) of interstitial connective tissue in the lung (excluding air-filled alveolar spaces). Statistical significance was assessed by the two-sample Mann–Whitney U Test. The bar diagrams show means and standard deviations.

4. Appendix

4.1. Presentations, and conference contributions

i. **Gene Center retreat (Munich, June 2022)**

Bachuki Shashikadze, Florian Flenkenthaler, Elisabeth Kemter, Jan B. Stöckl, Andreas Blutke, Simone Renner, Eckhard Wolf, Thomas Fröhlich

Differential effects of insulin-deficient diabetes mellitus on lung tissue: Multi-omics insights

ii. **International Mass Spectrometry Conference (Maastricht, IMSC 2022)**

Bachuki Shashikadze, Florian Flenkenthaler, Elisabeth Kemter, Jan B. Stöckl, Andreas Blutke, Simone Renner, Eckhard Wolf, Thomas Fröhlich

Data-independent acquisition proteomics combined with targeted lipidomics reveals unique molecular signatures of the lung in insulin-deficient diabetes mellitus

iii. **DZD Workshop (Dresden, October 2022)**

Bachuki Shashikadze, Evamaria O. Riedel, Florian Flenkenthaler, Simone Renner, Dominik Schüttler, Sebastian Clauß, Eckhard Wolf, Thomas Fröhlich

Proteomic signatures of the heart in insulin-deficient diabetes mellitus

Bachuki Shashikadze, Libera Valla, Elisabeth Kemter, Simone Renner, Birgit Rathkolb, Cornelia Prehn, Eckhard Wolf, Thomas Fröhlich

Maternal hyperglycemia causes metabolic alterations in the liver of neonatal offspring

iv. **Risk management, prevention and interventions in adversely affected pregnancies (Rotterdam, December 2022)**

Maternal hyperglycemia causes metabolic alterations in the liver of neonatal offspring

v. **Gene Center seminar (Munich, June 2022)**

Is the lung a target in diabetes? Proteomics insights from a transgenic pig model

5. Acknowledgements

This work would not have been possible without the support of many people, many of whom have also become close friends. I would like to thank my supervisor, Dr. Thomas Fröhlich for his trust in me, and his patience and support while I was taking my first steps in proteomics. He consistently created opportunities for me to present my research, collaborate with experts in the field and publish my work. Also, I could not thank him enough for guiding me through the complex administrative matters during the first weeks after my arrival in Germany. Special thanks to Prof. Dr. Eckhard Wolf for his vast knowledge, but also for being phenomenally enthusiastic and encouraging which had a pivotal role in making me a better writer, presenter, scientist and has been an endless source of inspiration for learning. Thanks to Florian Flenkenthaler for becoming like a supervisor to me both in scientific aspects and in professional development.

I thank my lab/office mates, for a wonderful time together. Thanks to Lena who had an incredible ability to sense when I needed encouragement, whether it was during a challenging experiment or when I was struggling to find motivation for writing a paper. Special thanks to my dear friend Karolina. Our daily lunch breaks (which we never missed), where we discussed everything from science to our personal lives, created a bond that I value deeply. Thanks to Jan for convincing me to learn coding – advice that has profoundly shaped my career path. I also want to thank all students I mentored during last three years, I learned so much from each of them.

I would like to thank the DohART-NET consortium for funding my research and introducing me to incredible researchers. Special thanks to Alex, Fede, and Libera for the great time in Budapest and Munich. Thanks to the QBM graduate school, and especially to Markus Hohle, for organizing excellent courses. Also, many wonderful collaborators from the Chair for Molecular Animal Breeding for interesting research projects, as well as for their friendship outside of academia.

I also want to thank many teachers from the early stages of my academic career who fueled my curiosity and pushed me to become a better researcher. I am forever grateful to my childhood friends from Georgia for their support and regular calls, during which we shared jokes and revisited the countless times we spent together.

Finally, heartfelt thanks to my parents, my dear sister, grandparents and other family members for placing a high value on my education even when it came at personal expense, and for your patience and support while I am following my dreams.

6. References

1. Sinha, A. and M. Mann, *A beginner's guide to mass spectrometry-based proteomics*. The Biochemist, 2020. **42**(5): p. 64-69.
2. Ong, S.E. and M. Mann, *Mass spectrometry-based proteomics turns quantitative*. Nat Chem Biol, 2005. **1**(5): p. 252-62.
3. Smith, R., A.D. Mathis, D. Ventura, and J.T. Prince, *Proteomics, lipidomics, metabolomics: a mass spectrometry tutorial from a computer scientist's point of view*. BMC Bioinformatics, 2014. **15 Suppl 7**(Suppl 7): p. S9.
4. Ludwig, C., L. Gillet, G. Rosenberger, S. Amon, B.C. Collins, and R. Aebersold, *Data-independent acquisition-based SWATH-MS for quantitative proteomics: a tutorial*. Mol Syst Biol, 2018. **14**(8): p. e8126.
5. Xu, L.L., A. Young, A. Zhou, and H.L. Rost, *Machine Learning in Mass Spectrometric Analysis of DIA Data*. Proteomics, 2020. **20**(21-22): p. e1900352.
6. Vogel, C. and E.M. Marcotte, *Insights into the regulation of protein abundance from proteomic and transcriptomic analyses*. Nature reviews. Genetics, 2012. **13**(4): p. 227-232.
7. Liu, Y., A. Beyer, and R. Aebersold, *On the Dependency of Cellular Protein Levels on mRNA Abundance*. Cell, 2016. **165**(3): p. 535-550.
8. Paulo, J.A., V. Kadiyala, P.A. Banks, H. Steen, and D.L. Conwell, *Mass spectrometry-based proteomics for translational research: a technical overview*. Yale J Biol Med, 2012. **85**(1): p. 59-73.
9. Bouatra, S., F. Aziat, R. Mandal, A.C. Guo, M.R. Wilson, C. Knox, T.C. Bjorndahl, R. Krishnamurthy, F. Saleem, P. Liu, Z.T. Dame, J. Poelzer, J. Huynh, F.S. Yallou, N. Psychogios, E. Dong, R. Bogumil, C. Roehring, and D.S. Wishart, *The human urine metabolome*. PLoS One, 2013. **8**(9): p. e73076.
10. Johnson, C.H., J. Ivanisevic, and G. Siuzdak, *Metabolomics: beyond biomarkers and towards mechanisms*. Nat Rev Mol Cell Biol, 2016. **17**(7): p. 451-9.
11. Zapalska-Sozoniuk, M., L. Chrobak, K. Kowalczyk, and M. Kankofer, *Is it useful to use several "omics" for obtaining valuable results?* Mol Biol Rep, 2019. **46**(3): p. 3597-3606.
12. Nakayasu, E.S., C.D. Nicora, A.C. Sims, K.E. Burnum-Johnson, Y.M. Kim, J.E. Kyle, M.M. Matzke, A.K. Shukla, R.K. Chu, A.A. Schepmoes, J.M. Jacobs, R.S. Baric, B.J. Webb-Robertson, R.D. Smith, and T.O. Metz, *MPLEx: a Robust and Universal Protocol for Single-Sample Integrative Proteomic, Metabolomic, and Lipidomic Analyses*. mSystems, 2016. **1**(3).

13. Krassowski, M., V. Das, S.K. Sahu, and B.B. Misra, *State of the Field in Multi-Omics Research: From Computational Needs to Data Mining and Sharing*. Front Genet, 2020. **11**: p. 610798.
14. Wolf, E., C. Braun-Reichhart, E. Streckel, and S. Renner, *Genetically engineered pig models for diabetes research*. Transgenic Res, 2014. **23**(1): p. 27-38.
15. Ahlqvist, E., P. Storm, A. Käräjämäki, M. Martinell, M. Dorkhan, A. Carlsson, P. Vikman, R.B. Prasad, D.M. Aly, P. Almgren, Y. Wessman, N. Shaat, P. Spégel, H. Mulder, E. Lindholm, O. Melander, O. Hansson, U. Malmqvist, Å. Lernmark, K. Lahti, T. Forsén, T. Tuomi, A.H. Rosengren, and L. Groop, *Novel subgroups of adult-onset diabetes and their association with outcomes: a data-driven cluster analysis of six variables*. Lancet Diabetes Endocrinol, 2018. **6**(5): p. 361-369.
16. Phillips, K.A., S. Van Bebber, and A.M. Issa, *Diagnostics and biomarker development: priming the pipeline*. Nat Rev Drug Discov, 2006. **5**(6): p. 463-9.
17. Perleberg, C., A. Kind, and A. Schnieke, *Genetically engineered pigs as models for human disease*. Dis Model Mech, 2018. **11**(1).
18. Larsen, M.O. and B. Rolin, *Use of the Göttingen minipig as a model of diabetes, with special focus on type 1 diabetes research*. Ilar j, 2004. **45**(3): p. 303-13.
19. Bryda, E.C., *The Mighty Mouse: the impact of rodents on advances in biomedical research*. Mo Med, 2013. **110**(3): p. 207-11.
20. Renner, S., B. Dobenecker, A. Blutke, S. Zöls, R. Wanke, M. Ritzmann, and E. Wolf, *Comparative aspects of rodent and nonrodent animal models for mechanistic and translational diabetes research*. Theriogenology, 2016. **86**(1): p. 406-21.
21. Rydell-Törmänen, K. and J.R. Johnson, *The Applicability of Mouse Models to the Study of Human Disease*. Methods Mol Biol, 2019. **1940**: p. 3-22.
22. Bassols, A., C. Costa, P.D. Eckersall, J. Osada, J. Sabrià, and J. Tibau, *The pig as an animal model for human pathologies: A proteomics perspective*. Proteomics Clin Appl, 2014. **8**(9-10): p. 715-31.
23. Kleinert, M., C. Clemmensen, S.M. Hofmann, M.C. Moore, S. Renner, S.C. Woods, P. Huypens, J. Beckers, M.H. de Angelis, A. Schurmann, M. Bakhti, M. Klingenspor, M. Heiman, A.D. Cherrington, M. Ristow, H. Lickert, E. Wolf, P.J. Havel, T.D. Muller, and M.H. Tschop, *Animal models of obesity and diabetes mellitus*. Nat Rev Endocrinol, 2018. **14**(3): p. 140-162.
24. Schook, L.B., T.V. Collares, K.A. Darfour-Oduro, A.K. De, L.A. Rund, K.M. Schachtschneider, and F.K. Seixas, *Unraveling the swine genome: implications for human health*. Annu Rev Anim Biosci, 2015. **3**: p. 219-44.
25. Hou, N., X. Du, and S. Wu, *Advances in pig models of human diseases*. Animal Model Exp Med, 2022. **5**(2): p. 141-152.
26. Zettler, S., S. Renner, E. Kemter, A. Hinrichs, N. Klymiuk, M. Backman, E.O. Riedel, C. Mueller, E. Streckel, C. Braun-Reichhart, A.S. Martins, M. Kurome, B. Kessler, V. Zakhartchenko, F. Flenkenthaler, G.J. Arnold, T. Frohlich, H. Blum, A. Blutke, R. Wanke, and E. Wolf, *A decade of experience with genetically tailored pig models for diabetes and metabolic research*. Anim Reprod, 2020. **17**(3): p. e20200064.
27. Aigner, B., S. Renner, B. Kessler, N. Klymiuk, M. Kurome, A. Wunsch, and E. Wolf, *Transgenic pigs as models for translational biomedical research*. J Mol Med (Berl), 2010. **88**(7): p. 653-64.
28. Groenen, M.A., A.L. Archibald, H. Uenishi, C.K. Tuggle, Y. Takeuchi, M.F. Rothschild, C. Rogel-Gaillard, C. Park, D. Milan, H.J. Megens, S. Li, D.M. Larkin, H. Kim, L.A.

- Frantz, M. Caccamo, H. Ahn, B.L. Aken, A. Anselmo, C. Anthon, L. Auvil, B. Badaoui, C.W. Beattie, C. Bendixen, D. Berman, F. Blecha, J. Blomberg, L. Bolund, M. Bosse, S. Botti, Z. Bujie, M. Bystrom, B. Capitanu, D. Carvalho-Silva, P. Chardon, C. Chen, R. Cheng, S.H. Choi, W. Chow, R.C. Clark, C. Clee, R.P. Crooijmans, H.D. Dawson, P. Dehais, F. De Sapio, B. Dibbits, N. Drou, Z.Q. Du, K. Eversole, J. Fadista, S. Fairley, T. Faraut, G.J. Faulkner, K.E. Fowler, M. Fredholm, E. Fritz, J.G. Gilbert, E. Giuffra, J. Gorodkin, D.K. Griffin, J.L. Harrow, A. Hayward, K. Howe, Z.L. Hu, S.J. Humphray, T. Hunt, H. Hornshoj, J.T. Jeon, P. Jern, M. Jones, J. Jurka, H. Kanamori, R. Kapetanovic, J. Kim, J.H. Kim, K.W. Kim, T.H. Kim, G. Larson, K. Lee, K.T. Lee, R. Leggett, H.A. Lewin, Y. Li, W. Liu, J.E. Loveland, Y. Lu, J.K. Lunney, J. Ma, O. Madsen, K. Mann, L. Matthews, S. McLaren, T. Morozumi, M.P. Murtaugh, J. Narayan, D.T. Nguyen, P. Ni, S.J. Oh, S. Onteru, F. Panitz, E.W. Park, H.S. Park, G. Pascal, Y. Paudel, M. Perez-Enciso, R. Ramirez-Gonzalez, J.M. Reecy, S. Rodriguez-Zas, G.A. Rohrer, L. Rund, Y. Sang, K. Schachtschneider, J.G. Schraiber, J. Schwartz, L. Scobie, C. Scott, S. Searle, B. Servin, B.R. Southey, G. Sperber, P. Stadler, J.V. Sweedler, H. Tafer, B. Thomsen, R. Wali, J. Wang, J. Wang, S. White, X. Xu, M. Yerle, G. Zhang, J. Zhang, J. Zhang, S. Zhao, J. Rogers, C. Churcher and L.B. Schook, *Analyses of pig genomes provide insight into porcine demography and evolution*. Nature, 2012. **491**(7424): p. 393-8.
29. Schook, L.B., J.E. Beever, J. Rogers, S. Humphray, A. Archibald, P. Chardon, D. Milan, G. Rohrer, and K. Eversole, *Swine Genome Sequencing Consortium (SGSC): a strategic roadmap for sequencing the pig genome*. Comp Funct Genomics, 2005. **6**(4): p. 251-5.
30. Hammer, R.E., V.G. Pursel, C.E. Rexroad, R.J. Wall, D.J. Bolt, K.M. Ebert, R.D. Palmiter, and R.L. Brinster, *Production of transgenic rabbits, sheep and pigs by microinjection*. Nature, 1985. **315**(6021): p. 680-683.
31. Klymiuk, N., F. Seeliger, Y.M. Bohlooly, A. Blutke, D.G. Rudmann, and E. Wolf, *Tailored Pig Models for Preclinical Efficacy and Safety Testing of Targeted Therapies*. Toxicol Pathol, 2016. **44**(3): p. 346-57.
32. Lavitrano, M., R. Giovannoni, and M.G. Cerrito, *Methods for sperm-mediated gene transfer*. Methods Mol Biol, 2013. **927**: p. 519-29.
33. Springer, C., E. Wolf, and K. Simmet, *A New Toolbox in Experimental Embryology-Alternative Model Organisms for Studying Preimplantation Development*. J Dev Biol, 2021. **9**(2).
34. Liu, M., I. Hodish, L. Haataja, R. Lara-Lemus, G. Rajpal, J. Wright, and P. Arvan, *Proinsulin misfolding and diabetes: mutant INS gene-induced diabetes of youth*. Trends Endocrinol Metab, 2010. **21**(11): p. 652-9.
35. Sun, J., J. Cui, Q. He, Z. Chen, P. Arvan, and M. Liu, *Proinsulin misfolding and endoplasmic reticulum stress during the development and progression of diabetes*. Mol Aspects Med, 2015. **42**: p. 105-18.
36. Wright, J., J. Birk, L. Haataja, M. Liu, T. Ramming, M.A. Weiss, C. Appenzeller-Herzog, and P. Arvan, *Endoplasmic reticulum oxidoreductin-1alpha (Ero1alpha) improves folding and secretion of mutant proinsulin and limits mutant proinsulin-induced endoplasmic reticulum stress*. J Biol Chem, 2013. **288**(43): p. 31010-8.
37. Sprunger, M.L. and M.E. Jackrel, *Quality Control in the ER: Misfolded Prohormones Get a Checkup*. Mol Cell, 2019. **75**(3): p. 415-416.
38. Arunagiri, A., L. Haataja, C.N. Cunningham, N. Shrestha, B. Tsai, L. Qi, M. Liu, and P. Arvan, *Misfolded proinsulin in the endoplasmic reticulum during development of beta cell failure in diabetes*. Ann N Y Acad Sci, 2018. **1418**(1): p. 5-19.

39. Renner, S., A. Blutke, S. Clauss, C.A. Deeg, E. Kemter, D. Merkus, R. Wanke, and E. Wolf, *Porcine models for studying complications and organ crosstalk in diabetes mellitus*. Cell Tissue Res, 2020. **380**(2): p. 341-378.
40. Renner, S., C. Braun-Reichhart, A. Blutke, N. Herbach, D. Emrich, E. Streckel, A. Wunsch, B. Kessler, M. Kurome, A. Bahr, N. Klymiuk, S. Krebs, O. Puk, H. Nagashima, J. Graw, H. Blum, R. Wanke, and E. Wolf, *Permanent neonatal diabetes in INS(C94Y) transgenic pigs*. Diabetes, 2013. **62**(5): p. 1505-11.
41. Renner, S., A.S. Martins, E. Streckel, C. Braun-Reichhart, M. Backman, C. Prehn, N. Klymiuk, A. Bahr, A. Blutke, C. Landbrecht-Schessl, A. Wunsch, B. Kessler, M. Kurome, A. Hinrichs, S.J. Koopmans, S. Krebs, E. Kemter, B. Rathkolb, H. Nagashima, H. Blum, M. Ritzmann, R. Wanke, B. Aigner, J. Adamski, M. Hrabe de Angelis, and E. Wolf, *Mild maternal hyperglycemia in INS(C93S) transgenic pigs causes impaired glucose tolerance and metabolic alterations in neonatal offspring*. Dis Model Mech, 2019. **12**(8).
42. Blutke, A., S. Renner, F. Flenkenthaler, M. Backman, S. Haesner, E. Kemter, E. Landstrom, C. Braun-Reichhart, B. Albl, E. Streckel, B. Rathkolb, C. Prehn, A. Palladini, M. Grzybek, S. Krebs, S. Bauersachs, A. Bahr, A. Bruhschwein, C.A. Deeg, E. De Monte, M. Dmochewicz, C. Eberle, D. Emrich, R. Fux, F. Groth, S. Gumbert, A. Heitmann, A. Hinrichs, B. Kessler, M. Kurome, M. Leipzig-Rudolph, K. Matiassek, H. Ozturk, C. Otdorff, M. Reichenbach, H.D. Reichenbach, A. Rieger, B. Rieseberg, M. Rosati, M.N. Saucedo, A. Schleicher, M.R. Schneider, K. Simmet, J. Steinmetz, N. Ubel, P. Zehetmaier, A. Jung, J. Adamski, U. Coskun, M. Hrabe de Angelis, C. Simmet, M. Ritzmann, A. Meyer-Lindenberg, H. Blum, G.J. Arnold, T. Frohlich, R. Wanke, and E. Wolf, *The Munich MIDY Pig Biobank - A unique resource for studying organ crosstalk in diabetes*. Mol Metab, 2017. **6**(8): p. 931-940.
43. Hinkel, R., A. Howe, S. Renner, J. Ng, S. Lee, K. Klett, V. Kaczmarek, A. Moretti, K.L. Laugwitz, P. Skroblin, M. Mayr, H. Milting, A. Dendorfer, B. Reichart, E. Wolf, and C. Kupatt, *Diabetes Mellitus-Induced Microvascular Destabilization in the Myocardium*. J Am Coll Cardiol, 2017. **69**(2): p. 131-143.
44. Kleinwort, K.J.H., B. Amann, S.M. Hauck, S. Hirmer, A. Blutke, S. Renner, P.B. Uhl, K. Lutterberg, W. Sekundo, E. Wolf, and C.A. Deeg, *Retinopathy with central oedema in an INS (C94Y) transgenic pig model of long-term diabetes*. Diabetologia, 2017. **60**(8): p. 1541-1549.
45. Backman, M., F. Flenkenthaler, A. Blutke, M. Dahlhoff, E. Landstrom, S. Renner, J. Philippou-Massier, S. Krebs, B. Rathkolb, C. Prehn, M. Grzybek, U. Coskun, M. Rothe, J. Adamski, M.H. de Angelis, R. Wanke, T. Frohlich, G.J. Arnold, H. Blum, and E. Wolf, *Multi-omics insights into functional alterations of the liver in insulin-deficient diabetes mellitus*. Mol Metab, 2019. **26**: p. 30-44.
46. Flenkenthaler, F., E. Ländström, B. Shashikadze, M. Backman, A. Blutke, J. Philippou-Massier, S. Renner, M. Hrabe de Angelis, R. Wanke, H. Blum, G.J. Arnold, E. Wolf, and T. Fröhlich, *Differential Effects of Insulin-Deficient Diabetes Mellitus on Visceral vs. Subcutaneous Adipose Tissue-Multi-omics Insights From the Munich MIDY Pig Model*. Frontiers in medicine, 2021. **8**: p. 751277-751277.
47. Wolf, E., C. Braun-Reichhart, E. Streckel, and S. Renner, *Genetically engineered pig models for diabetes research*. Transgenic research, 2013. **23**.
48. Chang, A.S., A.N. Dale, and K.H. Moley, *Maternal diabetes adversely affects preovulatory oocyte maturation, development, and granulosa cell apoptosis*. Endocrinology, 2005. **146**(5): p. 2445-53.

49. Cerqueira, D.M., S.L. Hemker, A.J. Bodnar, D.M. Ortiz, F.O. Oladipupo, E. Mukherjee, Z. Gong, C. Appolonia, R. Muzumdar, S. Sims-Lucas, and J. Ho, *In utero exposure to maternal diabetes impairs nephron progenitor differentiation*. *Am J Physiol Renal Physiol*, 2019. **317**(5): p. F1318-F1330.
50. Grasemann, C., M.J. Devlin, P.A. Rzczkowska, R. Herrmann, B. Horsthemke, B.P. Hauffa, M. Grynopas, C. Alm, M.L. Bouxsein, and M.R. Palmert, *Parental diabetes: the Akita mouse as a model of the effects of maternal and paternal hyperglycemia in wildtype offspring*. *PLoS One*, 2012. **7**(11): p. e50210.
51. Lindegaard, M.L. and L.B. Nielsen, *Maternal diabetes causes coordinated down-regulation of genes involved with lipid metabolism in the murine fetal heart*. *Metabolism*, 2008. **57**(6): p. 766-73.
52. Litten-Brown, J.C., A.M. Corson, and L. Clarke, *Porcine models for the metabolic syndrome, digestive and bone disorders: a general overview*. *Animal*, 2010. **4**(6): p. 899-920.
53. Nykonenko, A., P. Vavra, and P. Zonca, *Anatomic Peculiarities of Pig and Human Liver*. *Exp Clin Transplant*, 2017. **15**(1): p. 21-26.
54. Ntonas, A., A. Katsourakis, N. Galanis, E. Filo, and G. Noussios, *Comparative Anatomical Study Between the Human and Swine Liver and Its Importance in Xenotransplantation*. *Cureus*, 2020. **12**(7): p. e9411.
55. Mameli, C., M. Ghezzi, A. Mari, G. Cammi, M. Macedoni, F.C. Redaelli, V. Calcaterra, G. Zuccotti, and E. D'Auria, *The Diabetic Lung: Insights into Pulmonary Changes in Children and Adolescents with Type 1 Diabetes*. *Metabolites*, 2021. **11**(2).
56. Rajasurya, V., K. Gunasekaran, and S. Surani, *Interstitial lung disease and diabetes*. *World J Diabetes*, 2020. **11**(8): p. 351-357.
57. Klein, O.L., J.A. Krishnan, S. Glick, and L.J. Smith, *Systematic review of the association between lung function and Type 2 diabetes mellitus*. *Diabet Med*, 2010. **27**(9): p. 977-87.
58. Schuyler, M.R., D.E. Niewoehner, S.R. Inkley, and R. Kohn, *Abnormal Lung Elasticity in Juvenile Diabetes Mellitus*. *American Review of Respiratory Disease*, 1976. **113**(1): p. 37-41.
59. Goldman, M.D., *Lung dysfunction in diabetes*. *Diabetes Care*, 2003. **26**(6): p. 1915-8.
60. Kolahian, S., V. Leiss, and B. Nurnberg, *Diabetic lung disease: fact or fiction?* *Rev Endocr Metab Disord*, 2019. **20**(3): p. 303-319.
61. Khateeb, J., E. Fuchs, and M. Khamaisi, *Diabetes and Lung Disease: A Neglected Relationship*. *The review of diabetic studies : RDS*, 2019. **15**: p. 1-15.
62. Zheng, H., J. Wu, Z. Jin, and L.J. Yan, *Potential Biochemical Mechanisms of Lung Injury in Diabetes*. *Aging Dis*, 2017. **8**(1): p. 7-16.
63. Khateeb, J., E. Fuchs, and M. Khamaisi, *Diabetes and Lung Disease: A Neglected Relationship*. *Rev Diabet Stud*, 2019. **15**: p. 1-15.
64. Klekotka, R., E. Mizgała, and W. Król, *The etiology of lower respiratory tract infections in people with diabetes*. *Advances in Respiratory Medicine*, 2015. **83**(5): p. 401-408.
65. Lim, S., J.H. Bae, H.-S. Kwon, and M.A. Nauck, *COVID-19 and diabetes mellitus: from pathophysiology to clinical management*. *Nature Reviews Endocrinology*, 2021. **17**(1): p. 11-30.
66. Hyldgaard, C., O. Hilberg, and E. Bendstrup, *How does comorbidity influence survival in idiopathic pulmonary fibrosis?* *Respir Med*, 2014. **108**(4): p. 647-53.

67. Ehrlich, S.F., C.P. Quesenberry, Jr., S.K. Van Den Eeden, J. Shan, and A. Ferrara, *Patients diagnosed with diabetes are at increased risk for asthma, chronic obstructive pulmonary disease, pulmonary fibrosis, and pneumonia but not lung cancer*. *Diabetes Care*, 2010. **33**(1): p. 55-60.
68. Becher, G., K. Winsel, E. Beck, G. Neubauer, and E. Stresemann, [*Breath condensate as a method of noninvasive assessment of inflammation mediators from the lower airways*]. *Pneumologie*, 1997. **51 Suppl 2**: p. 456-9.
69. Rogers, C.S., W.M. Abraham, K.A. Brogden, J.F. Engelhardt, J.T. Fisher, P.B. McCray, Jr., G. McLennan, D.K. Meyerholz, E. Namati, L.S. Ostedgaard, R.S. Prather, J.R. Sabater, D.A. Stoltz, J. Zabner, and M.J. Welsh, *The porcine lung as a potential model for cystic fibrosis*. *Am J Physiol Lung Cell Mol Physiol*, 2008. **295**(2): p. L240-63.
70. Glenny, R.W., S.L. Bernard, D.L. Luchtel, B. Neradilek, and N.L. Polissar, *The spatial-temporal redistribution of pulmonary blood flow with postnatal growth*. *J Appl Physiol* (1985), 2007. **102**(3): p. 1281-8.
71. Kubicki, N., C. Laird, L. Burdorf, R.N. Pierson, 3rd, and A.M. Azimzadeh, *Current status of pig lung xenotransplantation*. *Int J Surg*, 2015. **23**(Pt B): p. 247-254.
72. Brandler, M.D., S.C. Powell, D.M. Craig, G. Quick, T.J. McMahon, R.N. Goldberg, and J.S. Stamler, *A Novel Inhaled Organic Nitrate That Affects Pulmonary Vascular Tone in a Piglet Model of Hypoxia-Induced Pulmonary Hypertension*. *Pediatric Research*, 2005. **58**(3): p. 531-536.
73. Sen, P., B. Shashikadze, F. Flenkenthaler, E. Van de Kamp, S. Tian, C. Meng, M. Gigl, T. Fröhlich, and D. Merkus, *Proteomics- and Metabolomics-Based Analysis of Metabolic Changes in a Swine Model of Pulmonary Hypertension*. *International Journal of Molecular Sciences*, 2023. **24**(5): p. 4870.
74. Canning, B.J. and Y. Chou, *Using guinea pigs in studies relevant to asthma and COPD*. *Pulm Pharmacol Ther*, 2008. **21**(5): p. 702-20.
75. Rodriguez-Pineiro, A., F. Jaudas, N. Klymiuk, A. Bähr, G. Hansson, and A. Ermund, *Proteome of airway surface liquid and mucus in newborn wildtype and cystic fibrosis piglets*. *Respiratory Research*, 2023. **24**.
76. Judge, E.P., J.M. Hughes, J.J. Egan, M. Maguire, E.L. Molloy, and S. O'Dea, *Anatomy and bronchoscopy of the porcine lung. A model for translational respiratory medicine*. *Am J Respir Cell Mol Biol*, 2014. **51**(3): p. 334-43.
77. Mclaughlin, R.F., W.S. Tyler, and R.O. Canada, *A study of the subgross pulmonary anatomy in various mammals*. *American Journal of Anatomy*, 1961. **108**: p. 149-165.
78. Horter, D.C., K.J. Yoon, and J.J. Zimmerman, *A review of porcine tonsils in immunity and disease*. *Anim Health Res Rev*, 2003. **4**(2): p. 143-55.
79. Meurens, F., A. Summerfield, H. Nauwynck, L. Saif, and V. Gerdtts, *The pig: a model for human infectious diseases*. *Trends Microbiol*, 2012. **20**(1): p. 50-7.